An Investigation of the Gas Phase Thermolysis of Hexaborane(10) by Quantitative Mass Spectrometry

Graham Jump

Submitted in fulfilment of the requirements for the degree of Doctor of Philosophy

The University of Leeds

Department of Inorganic and Structural Chemistry

June 1984

ABSTRACT

A method has been developed, after extensive evaluation of several different types of experimental system, which allows a gaseous reaction mixture to be sampled by a mass spectrometer. Samples from the reaction mixture flow into the spectrometer under a regime of viscous flow in an excess background of helium. This technique preserves the composition of the sample as it passes from the reaction vessel into the source of the mass spectrometer. Analysis of the resultant mass spectrum gives the composition of the mixture.

The gas phase thermolysis of hexaborane(10) has been studied by this method for pressures in the range 1-10 mmHg, and at temperatures between 75 and 153°C. Hexaborane(10) is found to decompose by a second order process having an activation energy of 79 ± 5 kJ mol^{-1} and a pre-exponential factor of $\sim 10^{7}$ m^{3} mol^{-1} s^{-1}. The main products are hydrogen and a non-volatile solid, though small amounts of pentaborane(9) and decaborane(14) are also produced. In addition there is evidence for a B_{12} intermediate, and octaborane(12) is observed in trace amounts during the early stages of the thermolysis in the lower temperature runs. Some preliminary work on the effects of deuterium on the reaction is also described. Additionally, studies of a red glassy solid obtained from the room temperature, liquid phase decomposition of hexaborane(10) suggest that this reaction may be related to that in the gas phase.

The overall results are consistent with a mechanism involving polymerization via a reactive B_{12} intermediate formed in a bimolecular reaction between two hexaborane(10) molecules. The pentaborane(9) and decaborane(14) are considered to be products of a relatively minor side reaction. Possible mechanisms are proposed and discussed.

To my mother and father

ACKNOWLEDGEMENTS

The work described in this Thesis was supported by the U.S. Government through its U.S. Army Research and Standardization Group (Europe). The author thanks this Group for a Maintenance Grant and for other financial support.

I would like to thank my supervisor, Professor Norman Greenwood, for his contributions in all aspects of this work, both academic and administrative, and for putting me under the wing of Dr. Bob Greatrex.

For Bob, my special thanks. His enthusiasm and professionalism influenced me throughout, and he gave me great encouragement when it was needed.

Many thanks to Darshan Singh for his maintenance of the spectrometer in superb condition over the course of this work.

Thanks also to co-worker Chris Potter who allowed me more than my fair share of spectrometer time, and for help in the preparation of boranes and maintenance of the vacuum line.

Towards the end of the work, Dr. Ann Woollins undertook repetitive preparations of hexaborane(10), and I am extremely grateful to her.

Others who deserve thanks include: Peter Halford-Maw of the Department of Physical Chemistry for much time and effort on the installation of our computer link to the University mainframe, and Lou Bailey of the Department of Chemical Engineering for advice on this matter; Dr. Keith Bartle, Dr. Don Baulch, Dr. Tony Clifford and Dr. Norman Taylor, all of the Department of Physical Chemistry, for advice and discussion on various aspects of the work; the School of Chemistry glassblowers, and the electronic and mechanical workshops.

Elaine Goodrich did the typing and gave advice on presentation and layout, many thanks.

Finally, I would like to thank my wife Allison for her very real support and encouragement throughout this work.

CONTENTS

		Page
CHAPTER 1 - Introduction		1
1.1	Historical	1
1.2	Thermolysis: mono-, di- and triboranes	1
1.3	The mechanism of production of higher boranes	6
1.4	Aims of this work	9
1.4.1	Chemical objectives	9
1.4.2	Experimental development	12
CHAPTER 2 - Experimental		14
2.1	Mass spectrometer and data acquisition system	14
2.1.1	Single beam, low resolution mode	17
2.1.2	Single beam, high resolution mode	19
2.1.3	Double beam mode	19
2.2	The data acquisition system	21
2.3	Reaction vessel and vacuum line	22
2.4	Sampling system	26
2.4.1	Original method	28
2.4.2	Molecular flow sampling	34
2.4.3	Modified viscous flow sampling	41
CHAPTER 3 - Calibration Procedure and Data Analysis		51
3.1	Calibration	51
3.2	Computational analysis of reaction mixtures	60
3.3	Experimental accuracy	64
CHAPTER 4 - Results		68
4.1	Initial observations	68
4.2	Investigation of reaction order	69

Page

4.3 Activation energy 83

4.4 Stoichiometry 96

4.5 Effect of added hydrogen 101

4.6 Other species present in the gas phase 105

4.6.1 Pentaborane(9) and decaborane(14) 105

4.6.2 A species containing 12 boron atoms 107

4.6.3 An octaborane species 114

4.7 The solid residue 114

4.8 Room temperature "polymerization" of hexaborane(10) 120

4.9 Preliminary work with deuterium 125

CHAPTER 5 - Discussion 133

5.1 Background 133

5.2 Experimental method 134

5.2.1 Discussion of method; its strengths and limitations 135

5.2.2 Possible development of experimental method 136

5.3 Discussion of experimental results 137

5.3.1 $B_{12}H_x$: product, intermediate or secondary ion? 138

5.3.2 Observations on the polymeric materials 141

5.3.3 Deuteration work 142

5.3.4 Possible mechanisms of thermolysis 143

5.3.5 Future work 148

APPENDIX A - Calibration Data and Standard Spectra 151

APPENDIX B - Tables of Thermolysis Data 158

APPENDIX C - Preparation of Hexaborane(10) 186

REFERENCES 190

CHAPTER ONE

Introduction

1.1 Historical

The boranes constitute a fascinating series of binary compounds of boron and hydrogen. Since Alfred Stock undertook the first systematic study starting in 1912 [1] they have been the subject of considerable and growing research effort to the present day. Great impetus was given to their study after the Second World War when their properties as possible high energy fuels attracted the interest of various government departments in the U.S.A. [2].

The work described in this thesis is concerned with the gas phase thermolysis of hexaborane(10). Accordingly, this introduction gives a brief discussion of the thermolysis of boranes in general before the detailed aims of the work are discussed in the next chapter. It must be said however that the great bulk of research on the boranes is not in the field of simple boron-hydrogen compounds. Borane chemistry has developed rapidly and has had influence in many areas of chemistry. The concept of the three-centre two-electron bond, leading to the multi-centre two-electron bond, is now routinely taught to undergraduates and had its roots in borane research [3]. The rules which were originally developed to describe clusters of boron atoms can be applied to clusters of metal atoms [4], and the wide variety of tailored reducing agents available from borane derivatives has great usage in organic chemistry.

1.2 Thermolysis: mono-, di- and triboranes

In the thermolysis of the boranes, diborane(6) is the starting compound in a series of reactions leading to the formation of decaborane(14). Planned syntheses of higher boranes are of great interest, certainly high

yields of pentaborane(9) and decaborane(14) and their derivatives were desirable in the high energy fuel programmes. Pertinent to the question of planned syntheses is the problem of the actual mechanisms and intermediates involved in the conversion of diborane(6) to decaborane(14).

Many neutral boranes up to and beyond decaborane(14) have been prepared or observed. Discounting conjuncto-boranes which consist of simpler boranes linked together, the more stable neutral boranes comprise B_2H_6, B_4H_{10}, B_5H_9, B_5H_{11}, B_6H_{10}, B_6H_{12}, B_8H_{12}, B_8H_{14}, B_9H_{13}, $n\text{-}B_9H_{15}$, $i\text{-}B_9H_{15}$, and $B_{10}H_{14}$ [5]. B_8H_{16} has also been reported but no structural information has been obtained [6]. Several unstable intermediates have also been postulated and identified, namely $\{BH_3\}$ [7], $\{B_3H_7\}$ [8], $\{B_3H_9\}$ [8,9] and $\{B_4H_8\}$ [8], although of course the properties of stability and isolability are continuous so the distinction is somewhat arbitrary. No neutral borane containing seven boron atoms has yet been identified, and heptaboranes reported in the literature were later identified as ethyl pentaboranes [10-13].

In the thermolysis of diborane(6) even the first step has been the subject of disagreement. It is generally accepted that the kinetics of diborane(6) thermolysis is three-halves order with an overall activation energy of about 112 kJ mol^{-1}. Some of the available data are shown in Table 1 [14-20]. Discounting immediately Fehlner's proposed mechanism [21] which starts

$$B_2H_6 \rightleftharpoons \{BH_2\} + \{BH_4\}$$

and which was later withdrawn [22], there are two slightly different mechanisms proposed for the initial steps of the thermolysis of diborane(6). The earlier of the two is as follows [14,15,23]:

$$B_2H_6 \rightleftharpoons 2\{BH_3\}$$

Table 1: Activation energy data for diborane(6) thermolysis

Date	Activation Energy/kJ mol^{-1}	Reaction Order	Reference
1951	114.6, 106.7	3/2	[14]
1951	108.8	5/2	[15]
1953	85.4, 91.2	3/2	[16]
1960	113.4	3/2-5/2	[17]
1960	121.3	3/2	[18]
1970	108.8	1/2*	[19]
1973	42.7, 96.2	3/2	[20]

* Surface mechanism

$$\{BH_3\} + B_2H_6 \rightleftharpoons \{B_3H_9\}$$

$$\{B_3H_9\} \rightleftharpoons B_3H_7 + H_2 \quad .$$

In 1969 Long put forward the following [8]:

$$2B_2H_6 \rightleftharpoons \{BH_3\} + \{B_3H_9\}$$

$$\{BH_3\} + B_2H_6 \rightleftharpoons \{B_3H_9\}$$

$$\{B_3H_9\} \rightleftharpoons \{B_3H_7\} + H_2 \quad .$$

In both cases the rate determining step is the last one given. Both these mechanisms are consistent with an order of reaction of three-halves if it is accepted that a steady-state equilibrium is established, i.e. for both mechanisms the "overall initial" stoichiometry is

$$3B_2H_6 \rightleftharpoons 2\{B_3H_9\}$$

and so therefore

$$[\{B_3H_9\}] = K[B_2H_6]^{3/2}$$

where K is constant.

Long objected to the reversibility of the step

$$B_2H_6 \rightleftharpoons 2\{BH_3\}$$

and cited two particular pieces of evidence supporting his view that the step

$$\{BH_3\} + \{BH_3\} \longrightarrow B_2H_6$$

could not occur. The first was that in studies of diborane(6) thermolysis at pressures too low for intermolecular collisions to be significant, the temperature needed to effect 50% decomposition of the diborane(6) was 750 K, and that under these conditions triboranes were absent. However, at higher pressures the temperature required for 50% decomposition was only 525 K, and triboranes were present [24]. Long interpreted the high temperature required at low pressures as supporting his suggestion that

$$B_2H_6 + B_2H_6 \rightleftharpoons \{BH_3\} + \{B_3H_9\}$$

would occur more readily at higher pressures. But his interpretation is not the only one possible, as the reaction

$$B_2H_6 \rightleftharpoons 2\{BH_3\}$$

must require molecular collisions to activate the diborane(6), i.e.

$$B_2H_6 + M \rightleftharpoons 2\{BH_3\} + M$$

where M can of course be diborane(6). Furthermore, the second step of the first mechanism, i.e.

$$\{BH_3\} + B_2H_6 \rightleftharpoons \{B_3H_9\}$$

could not occur at pressures too low for intermolecular collisions and hence one would not expect the triborane species to be observed. The second piece of evidence used by Long to support his mechanism was an estimation of the activation energy of the reaction

$$B_2H_6 \rightleftharpoons 2\{BH_3\} \quad .$$

The value used by Long (though now thought incorrect) was 247 kJ mol^{-1} [25], and he inferred from this that two combining $\{BH_3\}$ molecules would have a final excess energy of at least 247 kJ mol^{-1} to dissipate and that this would destroy the newly formed diborane(6) molecule immediately, so preventing the equilibrium. This reasoning has been dealt with by Fehlner in chapter four of reference [7] where he utilizes widely accepted termolecular deactivation to account for any excess energy after recombination:

$$\{BH_3\} + \{BH_3\} \rightleftharpoons B_2H_6^*$$

$$B_2H_6^* + M \rightleftharpoons B_2H_6 + M^* \quad .$$

An introduction to this type of mechanism can be found in [26]. With due fairness to Long, Fehlner's work was carried out after Long wrote his review, but it is also true to say that lower estimates of the activation energy of the reaction

$$B_2H_6 \rightleftharpoons 2\{BH_3\}$$

have been made. These estimates were obtained when the activation energy of the reverse step was considered to be small, so that the activation energy of the forward step becomes equal to the bond dissociation energy of $(BH_3\text{-}BH_3)$, measured to be about 150 kJ mol^{-1} by Fehlner [27,28]; others have also estimated this value [29,30].

Thus the story starts. Only after some 25-30 years of study of the thermolysis of diborane(6) did the mechanism begin to enjoy some form of acceptance. Indeed a paper was published as recently as 1977 claiming to present "the first unambiguous evidence" that borane(3) was produced from thermolyzed diborane(6) [31].

1.3 The mechanism of production of higher boranes

What then of steps subsequent to the rate determining step? Many workers have presented reaction schemes up to and beyond decaborane(14) [8,15,32-34]. Some of the postulated steps had their entire basis in chemical intuition, admittedly a powerful tool in the right hands, but none of the reported mechanisms had experimental support for every postulated step. More kinetic data are required before some of the proposed steps can be justified.

Apart from diborane(6) and decaborane(14), the two most abundant isolable species in the pyrolysis of diborane(6) are initially tetraborane(10) and pentaborane(11). Later, as the reaction proceeds, pentaborane(9) appears. The question of whether tetraborane(10) or pentaborane(11) was formed first was in dispute at one time [18,35] but the observation that, up to pentaborane(11) at least, the borane-species appear in ascending order of boron content (i.e. B_2, B_3, B_4, B_5) is now generally accepted, and supports Schaeffer's view [24,35]. Given the presence of diborane(6), monoborane(3) and triborane(7), the tetraborane(10) probably arises chiefly by the route

$$B_2H_6 + \{B_3H_7\} \rightleftharpoons \{BH_3\} + B_4H_{10} \quad .$$

Experimental evidence for this step is furnished by work in which isotopically labelled tetraborane(10) was prepared from sodium octahydrotriborate and diborane(6) [36]:

$$\{^{11}B_3H_7\} + {}^{10}B_2H_6 \longrightarrow {}^{10}B^{11}B_3H_{10} + \{^{10}BH_3\} .$$

Pentaborane(11) is subsequently formed from tetraborane(10). An equilibrium exists which is perturbed by slow decomposition to pentaborane(9) and decaborane(14). The equilibrium is

$$2B_4H_{10} + B_2H_6 \rightleftharpoons 2B_5H_{11} + 2H_2 ,$$

which has been observed by several workers [34,35,37,38]. Possible reactions which might form pentaborane(11) are:

$$B_4H_{10} + \{B_3H_7\} \longrightarrow B_5H_{11} + B_2H_6$$

$$\{B_4H_8\} + \{BH_3\} \longrightarrow B_5H_{11}$$

and $$\{B_4H_8\} + B_2H_6 \longrightarrow B_5H_{11} + \{BH_3\}$$

where $\{B_4H_8\}$ is formed in the reaction

$$B_4H_{10} \longrightarrow \{B_4H_8\} + H_2 .$$

Long writes [8]

$$B_4H_{10} + \{B_3H_9\} \longrightarrow B_5H_{11} + B_2H_6 + H_2$$

but since the rate determining step of the entire process is

$$\{B_3H_9\} \longrightarrow \{B_3H_7\} + H_2$$

it is more probable that triborane(7) is the active triborane species. Steps of the type

$$\{B_3H_7\} + B_2H_6 \longrightarrow B_5H_{11} + H_2$$

are not consistent with the observation that the boranes appear in order of boron content [24]. Pentaborane(9) is not thought to appear until

after pentaborane(11) [14,39]. The step

$$B_5H_{11} \longrightarrow B_5H_9 + H_2$$

does not occur, the favoured mechanism being

$$B_5H_{11} \longrightarrow \{B_4H_8\} + BH_3$$

$$\{B_4H_8\} + \{B_3H_7\} \longrightarrow B_5H_9 + B_2H_6 \quad ,$$

although Schaeffer suggested that

$$B_4H_{10} + B_5H_{11} \longrightarrow B_5H_9 + 2B_2H_6 \quad .$$

After the appearance of the pentaboranes, decaborane(14) appears rapidly, and nonaborane(15) and octaborane(12) are implicated [13,40]. Any stepwise mechanism of build-up to decaborane(14) from the pentaboranes must stop at the hexaboranes anyway, as heptaboranes have not yet been demonstrated (they may, of course, be extremely unstable). Rather than a stepwise mechanism, the final part of the route to decaborane(14) has been proposed as the following [8,13]:

$$B_5H_{11} + \{B_4H_8\} \longrightarrow n\text{-}B_9H_{15} + 2H_2$$

$$n\text{-}B_9H_{15} \rightleftharpoons B_8H_{12} + \{BH_3\}$$

$$B_8H_{12} + \{B_3H_7\} \longrightarrow B_9H_{13} + B_2H_6$$

$$B_9H_{13} + \{B_3H_7\} \longrightarrow B_{10}H_{14} + B_2H_6 \quad .$$

Thus a plausible mechanism from diborane(6) to decaborane(14) has been assembled since the pioneering work of Stock [1]. However, by no means have all the reactions described above been proven, and much work remains to be done on this fascinating system.

Our work in Leeds has been concerned with developing a technique

which will enable us to observe the thermolysis of boranes quantitatively and provide kinetic and stoichiometric data in specific areas of the field. In the following section the aims of the present work will be described in detail.

1.4 Aims of this work

1.4.1 Chemical objectives

The initial aims of any research program can only comprise a more or less broad description of the area of work concerned and the objectives considered desirable at the time. In research, by definition, one cannot know what will be found, so any statement of intent must be limited. This introduction, however, is written with the benefit of hindsight.

The work described in this thesis is concerned with an intensive study of the gas phase thermolysis of hexaborane(10), undertaken to identify the importance or otherwise of this compound in the thermolysis of diborane(6). In this reaction, boranes containing six, seven, eight or nine boron atoms are not nearly as abundant as their smaller counterparts; indeed heptaboranes are unknown [13]. The abundance of tri-, tetra- and pentaboranes as products or reactive intermediates and the stepwise appearance of these, together with the scarcity or non-appearance of hexa-, hepta-, octa- and nonaboranes in the thermolysis of diborane(6) raises questions as to the nature of the mechanism of further conversion of pentaboranes to decaborane(14). Hexaborane(10) is an obvious candidate for investigation if this problem is to be solved.

Hexaborane(10) is interesting in a number of other ways. Commonly the boranes behave as acids, sometimes as protic acids but more usually as Lewis acids, and this characteristic can be rationalized if one recalls that the boranes are members of the class of so-called electron

deficient compounds. For example, hexaborane(10) can form adducts with phosphines in the way that other boranes do, thus:

$$B_6H_{10} + 2L \longrightarrow B_6H_{10}\cdot 2L \quad .$$

In this type of reaction the borane is clearly acting as a Lewis acid [41]. However, an interesting feature of hexaborane(10) is its ability to act not only as an acid but also as a base. The basic properties of hexaborane(10) have been demonstrated by several workers [42-45]. Schaeffer in particular has studied its properties as a Lewis base [46-49]. The single two-centre two-electron bond in the base of the hexaborane(10) pyramid is obviously the focus of both this Brønsted and Lewis base behaviour (the structure of hexaborane(10) is shown in Figure 1.1, data from reference [50]). The Lewis base character of hexaborane(10) may lead to some interesting consequences for its role in the gas phase thermolysis of other boranes [51]. Apart from these aspects of the chemistry of hexaborane(10), little work has been done on this compound, and this may be explained in part by the fact that hexaborane(10) was for many years the most difficult borane to prepare [52], although that was before the development of a reasonable yield process by Shore and co-workers [53,54].

In summary, hexaborane(10) exhibits a chemistry which can be either basic or acidic, and its involvement in the overall mechanism of the thermolysis of diborane(6) to decaborane(14) remains unknown. Indeed, the published schemes devised to explain the formation of decaborane(14) from diborane(6) do not require hexaboranes as intermediates [8]. This thesis presents the results of investigations into the gas phase thermolysis of hexaborane(10).

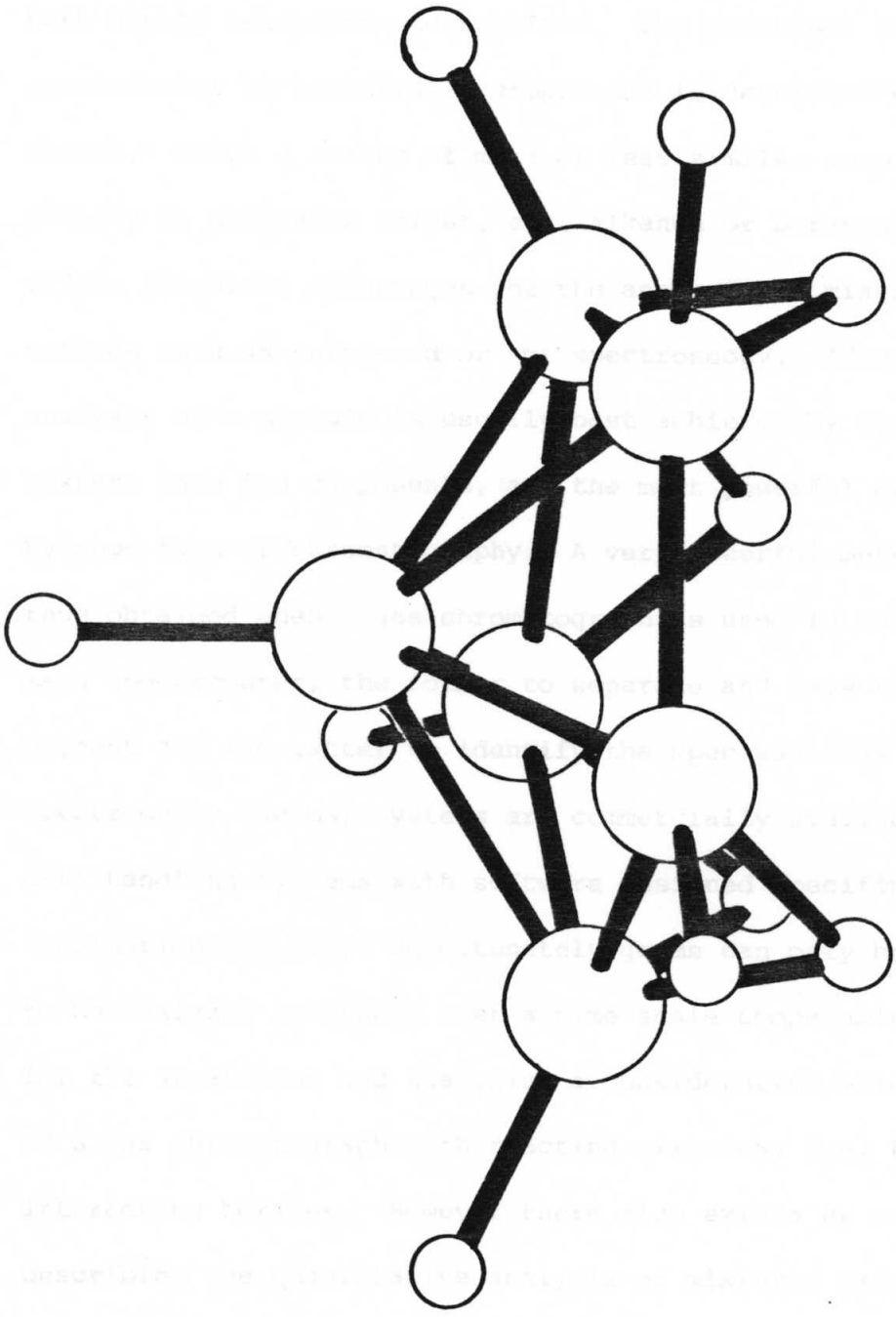

Figure 1.1. ORTEP drawing of B_6H_{10}

1.4.2 Experimental development

The instrument used for detection and measurement of the various borane species in this work was a Kratos MS3074 double-beam mass spectrometer. The mass spectrometer is a powerful analytical instrument and is both highly sensitive and specific. The principal of operation of a mass spectrometer is essentially simple and is described elsewhere in this thesis. Given a series of more or less similar compounds differing chiefly in molecular weight, e.g. alkanes or boranes, mass spectrometry offers immediate advantages for the analysis of mixtures over other methods such as infra-red or nmr spectroscopy. Ideally quantitative analysis of a mixture is usually best achieved by first separating the mixture into its components, and the most powerful method of doing this is by some form of chromatography. A very powerful method of analysis is thus obtained when a gas chromatograph is used in conjunction with a mass spectrometer, the former to separate and measure the quantities present and the latter to identify the species. Gas chromatograph/mass spectrometry (gc/ms) systems are commercially available together with data handling systems with software designed specifically for the gc/ms combination [55,56]. Unfortunately gc/ms can only be used if the mixture to be analyzed is stable over a time scale comparable to that required for the separation and analysis, a consideration which precludes the use of a gas chromatograph with reacting mixtures, i.e. thermolyzing and interacting boranes. However there also exists an extensive literature describing the quantitative analysis of mixtures using a mass spectrometer only [57-61]. The use of a mass spectrometer for quantitative analysis is very demanding of the instrument and requires a great deal of development and improvisation to obtain a system suited to the requirements of the work being undertaken.

When this work was being planned, it was thought that a method had been developed which would allow a systematic quantitative study of the gas phase thermolysis of several boron hydrides to be carried out [62]. This was to entail investigation of the volatile boron hydrides both singly and in mixtures, under varying conditions of temperature and pressure. In this way it was hoped to build up a fund of knowledge which could then be used in conjunction with the literature to establish more certainly the mechanism of interconversion of the boranes. However it rapidly became apparent that the experimental method as inherited was not sufficiently quantitative to permit meaningful analyses of simple mixtures and certainly inadequate for more complex mixtures. It was therefore necessary to re-appraise the experimental method so that the work could proceed from a firm quantitative starting point. A large part of this thesis will be devoted to a description of the development of the quantitative mass spectrometric method used in this work. So far as is known, the method as it stands is unique, and so a complete description will be valuable in itself. This is given in the following two chapters which describe the development of the experimental technique and the method of data analysis. This is then followed by a presentation of the results obtained and a discussion of their significance.

CHAPTER TWO

Experimental

2.1 Mass spectrometer and data acquisition system

The first mass spectrometer was built in 1910 by J.J. Thomson, and the power and wide applicability of the method led to the development of many variations. Mass spectrometers became commercially available in the early 1940s [63] and today many companies offer very powerful models, usually under mini-computer control.

The mode of operation of a mass spectrometer is essentially quite straightforward, Figure 2.1. Their primary use is in establishing the identity of samples introduced into the mass spectrometer. The sample is usually volatile enough to provide an adequate pressure of sample in the source (10^{-6} mmHg), although specialized sources and inlet procedures are available for non-volatile samples [64]. The volatilized sample is bombarded by a beam of electrons at an energy of 70 eV (this energy is usually variable) and the result is the production of mainly singly charged ions of the sample molecules, the so called parent ion, i.e.

$$X \longrightarrow X^{+} + e^{-} \quad .$$

Usually these ions are not stable and they decompose into singly charged fragment ions and neutral species (although some sources are designed to produce negative ions [64]).

The whole source is subject to a potential of the order of 10^{3} volts which accelerates the positive ions from the source region. They pass into a radial electric field having acquired from the accelerating potential a kinetic energy given by the expression

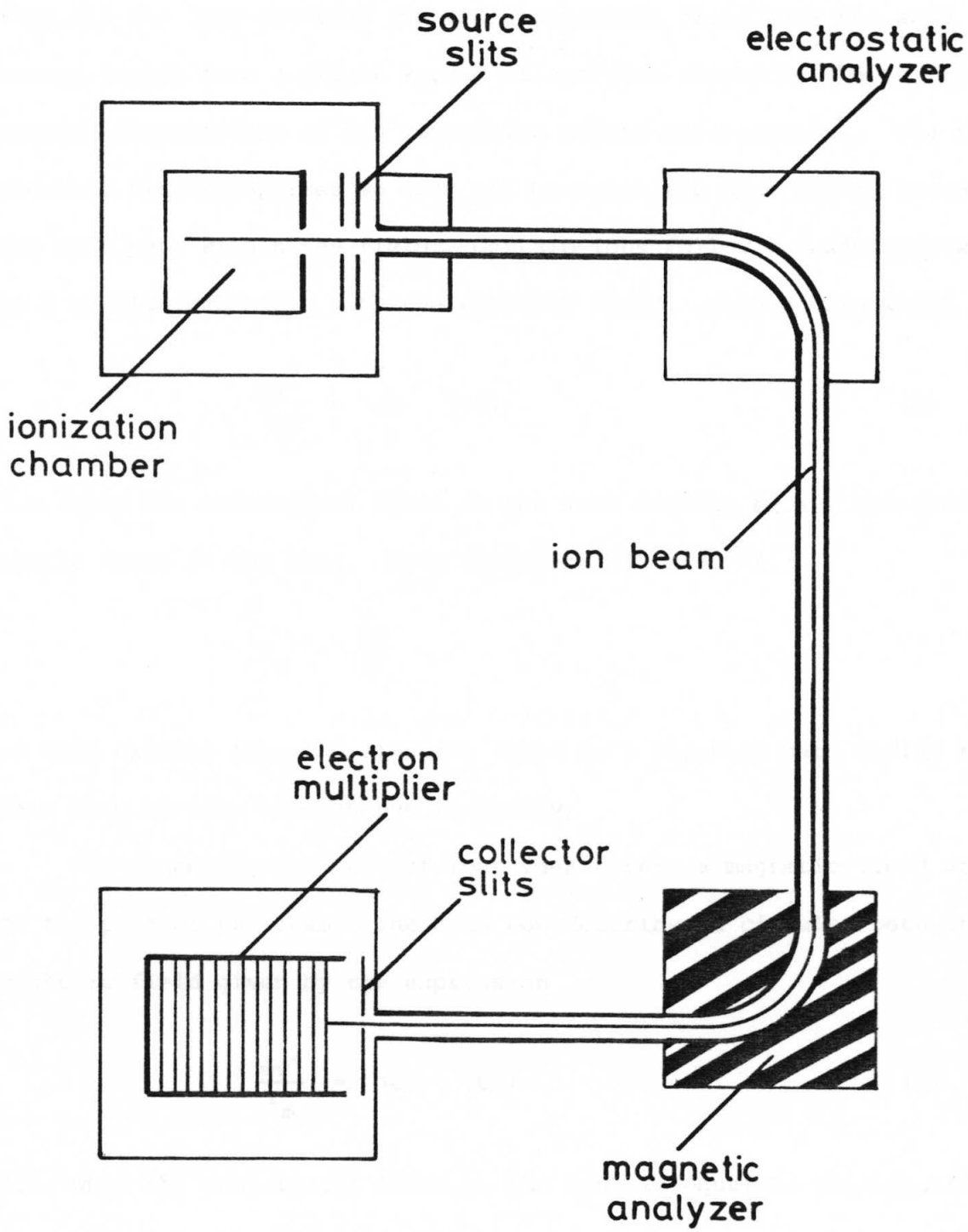

Figure 2.1. Schematic view of MS 30 (second beam omitted for clarity)

$$\frac{mv^2}{2} = eV \quad [63] \quad . \qquad (1)$$

Thus all the ions entering the radial electric field have the same energy (apart from a slight spread of energies caused by the initial thermal distribution of ion velocities before acceleration). The radial electric field disperses so that all ions with the same energy traverse the same path within the field. Certain ions follow a trajectory which is a circle concentric with the electric field. This occurs where

$$\frac{mv^2}{r_e} = eE \quad [63] \qquad (2)$$

i.e. when the centripetal force on the ions exactly equals the electrostatic force on the ions. From equations (1) and (2),

$$r_e = \frac{2V}{E}$$

so that exiting from the electric field on a circular path radius r_e will be a beam of ions homogeneous in energy.

The monoenergetic beam of ions then enters a magnetic field at 90° to the path of the beam. The beam now describes a circular path in the magnetic field given by the expression

$$\frac{mv^2}{r_m} = Bev \quad [63] \qquad (3)$$

i.e. when the centripetal force on the ions is equal to the magnetic force on them. Rearranging (3),

$$\frac{m}{e} = \frac{Br_m}{v} \qquad (4)$$

and substituting from (1)

$$\frac{m}{e} = \frac{B^2 r_m^2}{2V}$$

i.e. for a given V (accelerating voltage) and a given B (magnetic field strength), ions of a particular m/e value exit from the magnetic field at r_m. Thus the energy dispersing property of the electric field and the mass dispersing property of the magnetic field serve as a system capable of producing a mass spectrum, either by changing the accelerating voltage V or the magnetic field B. The electric field can be thought of as an energy prism, i.e. a means of separating energies, and the magnetic field can be thought of as a mass prism. In addition the electric field acts as a direction lens in that it has properties enabling it to focus monoenergetic beams having slight angular divergence [63]. The magnetic field acts both as a direction lens and as a velocity lens, i.e. monoenergetic beams presented to it with angular divergence and a velocity spread are focussed in both these respects.

Thus the sample in the source has been ionized and the ions separated according to their mass to charge ratios. They are detected by electron multipliers, giving good sensitivity, and the signal from the electron multipliers can be used to drive a chart recorder pen or can be digitized by a computerized data acquisition system.

Two mass spectrometers were used in this work. The main one was a Kratos model MS3074. This is a double focussing instrument of the type just described and is also a double beam instrument. This spectrometer was used for borane analysis, and it was under computer control. The other spectrometer was a small A.E.I. model MS10, a very simple instrument which was used for hydrogen analysis, Figure 2.2.

The double beam MS3074 could be used in several modes.

2.1.1 Single beam, low resolution mode

This is the mode used most frequently in thermolysis work. In this mode, only one of the mass spectrometer beams is used. Resolution is determined by the width of the analyzer slits; in low resolution

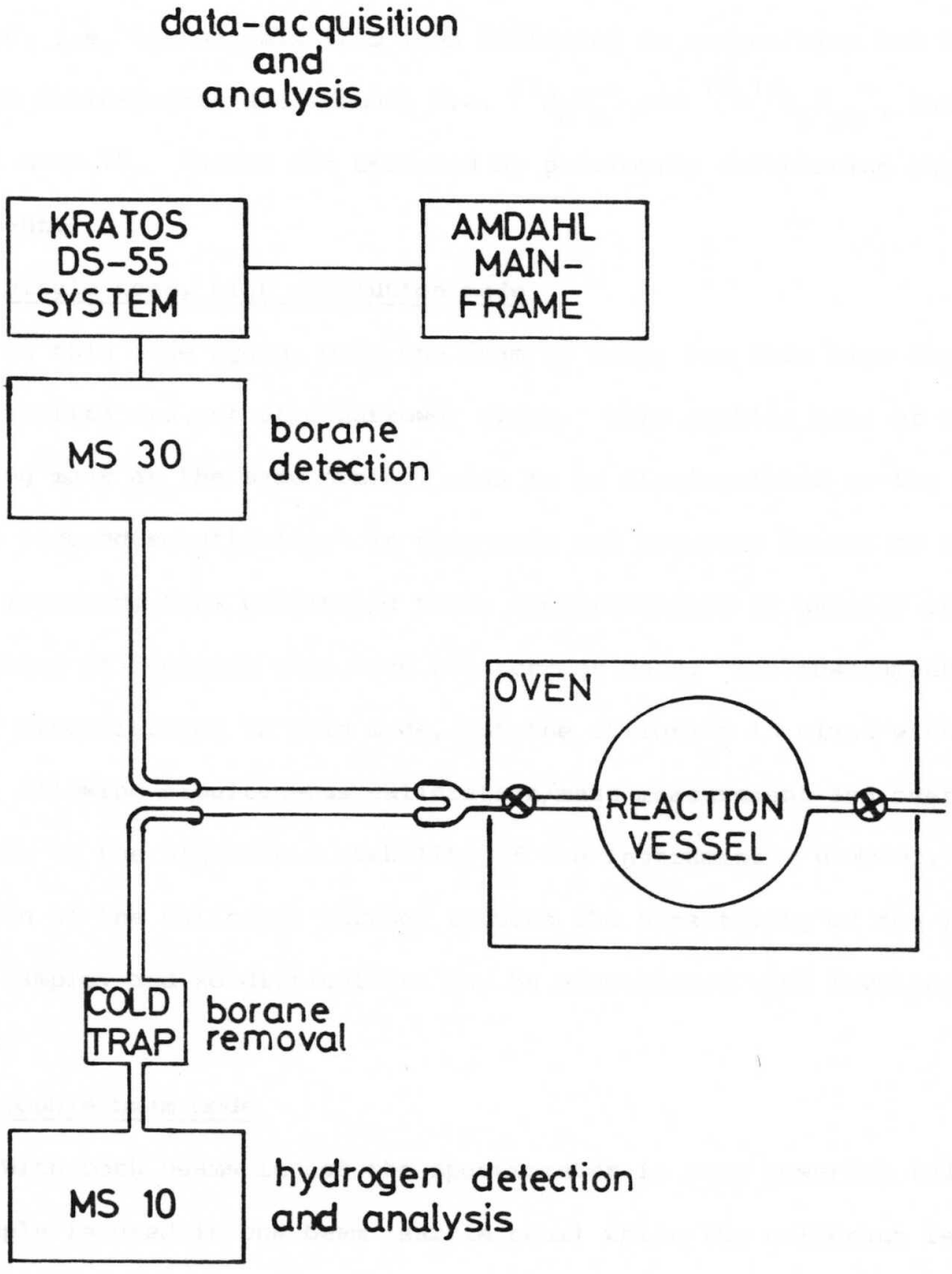

Figure 2.2. Diagram showing relationship of reaction vessel and mass spectrometers

these slits are at their widest, thus ions of slightly differing mass are not differentiated, but the sensitivity of the instrument is at its highest. Because of the low resolution, only a *unit-mass* spectrum is obtained, i.e. the signals from ions differing in composition but having the same nominal mass are summed, i.e. $^{11}B_6H_9^+$ and $^{10}B^{11}B_5H_{10}^+$, both nominal mass 75. Masses are measured by previously calibrating the instrument.

2.1.2 Single beam, high resolution mode

In this mode again, only one beam is used, but this time the analyzer slits are set at a narrower width. This enables ions of slightly differing mass at the same nominal mass to be distinguished at the expense of much reduced sensitivity. In this mode the accurate masses of ions may be measured, thus permitting their identification as usually only one combination of isotopes will have the correct mass. The instrument is not usually precalibrated in this mode, but the calibrant is mixed with the sample, allowing simultaneous calibration/mass measurement and overcoming any drift in the electronic stability of the instrument. However, inclusion of the calibrant further reduces the sensitivity of the instrument to the sample, and so difficulties may be encountered with involatile samples.

2.1.3 Double beam mode

With both beams in use the spectrometer is very powerful indeed. The sample is used in one beam (sample beam) while the calibrant is used in the other beam (reference beam). This mode thus allows simultaneous calibration and mass measurement, thus eliminating the loss of sensitivity incurred by using the calibrant in the sample beam. Furthermore, accurate masses may be obtained even using low resolution, so sensitivity is further enhanced. High resolution is not necessary for accurate mass measurement, a fact illustrated in Figure 2.3. In practice the number

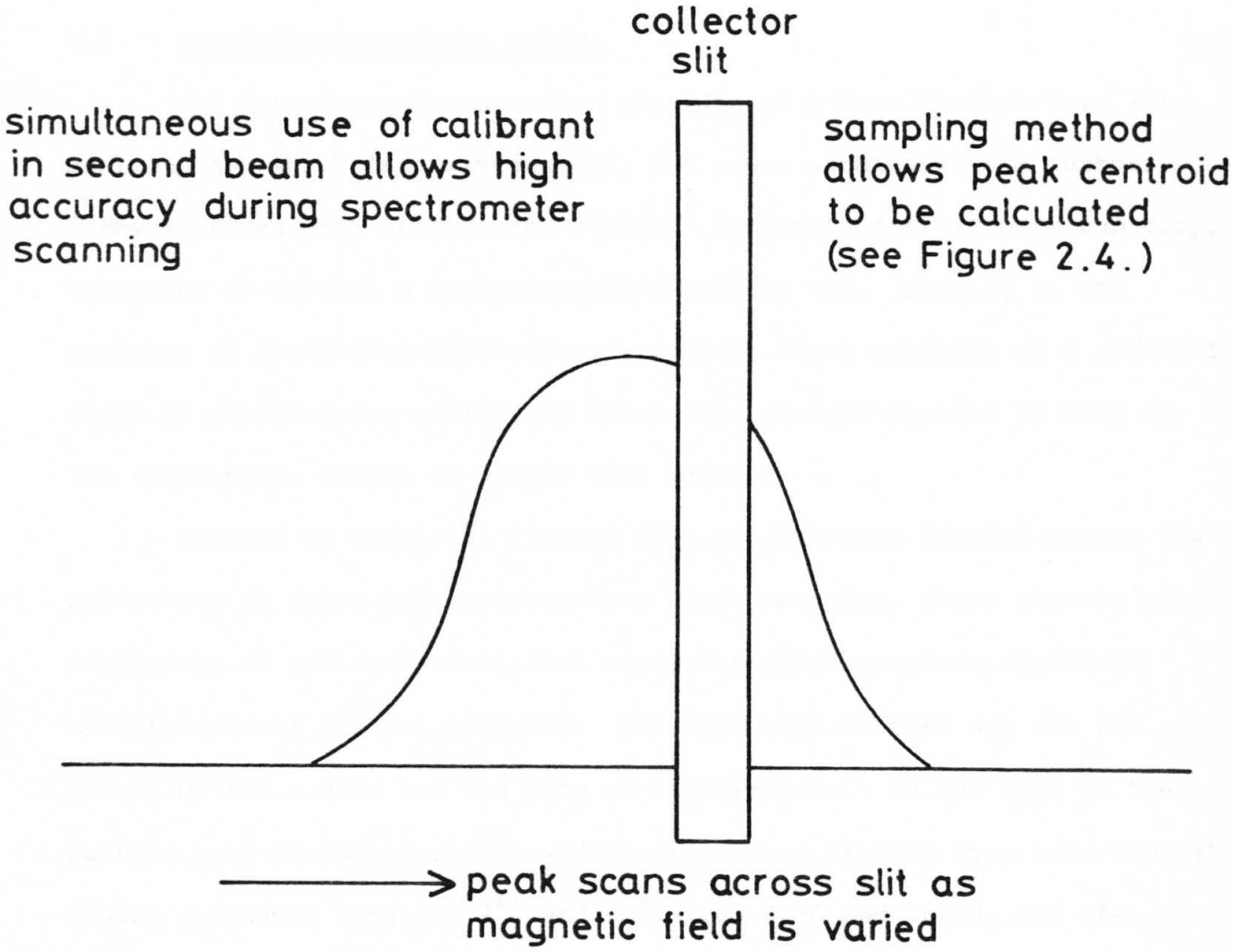

Figure 2.3. Accurate mass in double-beam low resolution mode

of unresolved peaks seen as a single peak will be few, and one will often predominate, so the information gained is meaningful. The spectrometer can be considered to be at its most powerful when in double-beam high resolution mode, when the fast data handling capacity of the data-acquisition system is indispensible. The next section briefly describes the data-acquisition system.

2.2 The data-acquisition system

The data-acquisition system consists of a Data General Nova III minicomputer which is a sixteen bit, 32K core machine with a further 5 Mbyte fixed disk storage and 5 Mbyte removable disk storage capacity. Operation is through a Hewlett-Packard HP2623A vdu. Running on the computer is the Kratos DS55 software package which consists of a powerful suite of programs for collecting and analyzing mass spectra in high or low resolution, double or single beam mode.

Instead of using the signals from the electron multipliers in the collectors to drive galvanometers in a chart recorder, these signals are sampled by an analogue-to-digital converter which provides digitized measurements of the ion currents. Two important factors are the bit widths of the a.d.c. and the rate of digitization. In the case of the machine used in this work the widths were 12 and 14 bits (two beam boards) giving a dynamic range of 2^{12} and 2^{14}, i.e. 4096 and 16384, and the digitization rate was 50 kHz, i.e. every 20 microseconds.

Thus the analogue signal produced by the spectrometer is recorded by the computer as a digital signal. The computer can identify peaks above the baseline (zero or threshold) and can distinguish real peaks from noise peaks on the basis of user definable parameters. What the software normally does is to identify the centre of gravity of each peak

and record the time after the scan start that this centroid occurred, along with the intensity of the peak (its area) [63], Figure 2.4. The usual procedure is for the peak retention times to be automatically converted to masses by comparison with a previously obtained calibrated reference file. This file normally contains peak retention time data recorded for a sample of PFK (perfluorokerosene), a high molecular weight fluorinated carbon compound which has been adopted for use as a mass spectrometer calibrant, although others are available. Its mass spectrum is well known, both in terms of accurate masses and fragment intensities, and can be used for calibration up to about 1000 a.m.u. Indeed the computer is pre-programmed with the PFK spectrum which it uses to calibrate itself once the time data have been recorded.

In low resolution, single beam, nominal mass work, a single calibration may remain valid for several months for masses up to about 200 a.m.u. if the spectrometer is not disturbed. The data acquisition system thus records spectra in terms of the mass measurements of peaks and their associated intensities. This data can be processed in several ways by a suite of powerful programs. Series of spectra can be compared to locate the most intense, or they can be averaged, or backgrounds can be subtracted. In high resolution and double beam work, other methods of data treatment can be invoked. In all cases the operator has very great control over all data processing parameters. Finally, the mass spectra can be output in tabular or pictorial form, or stored for further processing.

2.3 Reaction vessel and vacuum line

A great deal of the work involved in this research has concerned learning, adapting and developing the methods and principles of quantitative mass spectrometry as applied to the analysis of gaseous

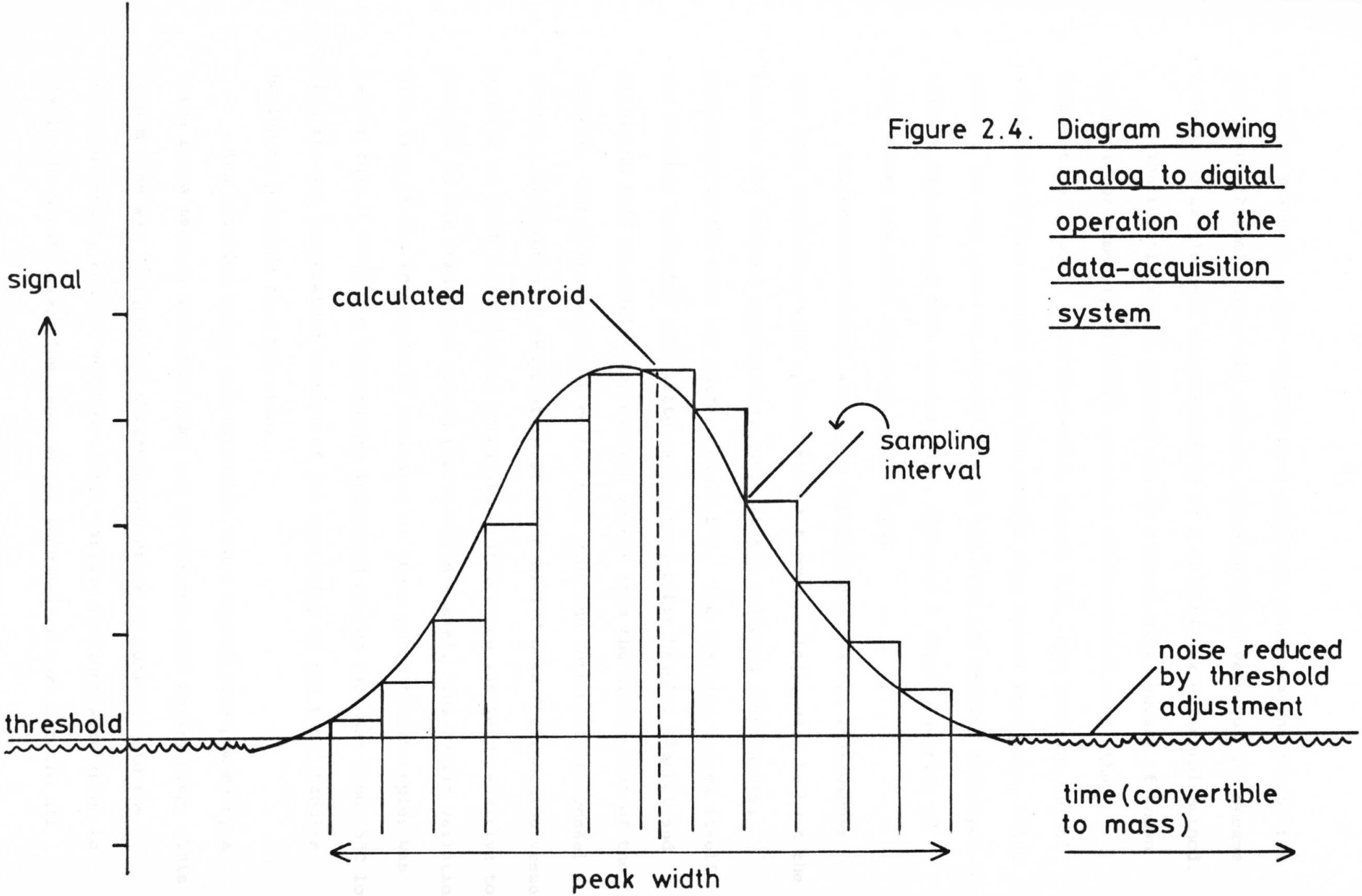

Figure 2.4. Diagram showing analog to digital operation of the data-acquisition system

reaction mixtures. What started as a proposed broad examination of the gas phase thermolysis of the neutral boron hydrides very quickly became a detailed development and assessment of a suitable experimental method.

The reactions were carried out in a pyrex glass vessel of known volume (approximately 1000 cm^3) inside a thermostatted oven, the temperature of which could be varied, Figure 2.5. The reaction vessel was sealed by two Young's glass and teflon long barrel type taps, which enabled the tap seals to be well inside the oven and reduced cold-spot effects experienced with shorter taps, although a slight lowering of temperature was still observed at the taps.

Temperature control was via a sophisticated Oxford Instruments type DTC2 controller with a three kilowatt power output, used to heat the oven to the desired temperature. Once at the selected temperature, variation in the oven was better than 0.5°C. The reaction vessel itself was further insulated with Triton Refractory Fibre Needled Blanket and aluminium foil to shield the reaction vessel from the direct heat of the element. Patch thermocouples on the top, side and bottom of the vessel showed a difference in temperature at 130°C of 1°C over the reaction vessel and 2°C at 150°C, though this temperature difference was very sensitive to changes in the insulation around the reaction vessel. The cyclic variation with time of the temperatures indicated on these patch thermocouples was better than 0.2°C. The temperature indicated on the taps was about 5°C lower than the set temperature because of the necessity of the taps' handles having to protrude from the oven.

The reaction vessel was evacuable via a vacuum line pumped by a three stage mercury diffusion pump and an Edwards ED50 rotary pump. This vacuum line was designed for mixing gases prior to admission to the reaction vessel, and the volumes of its various sections were known to ∿1% in the worst case. The taps on the vacuum line were Rotaflo all

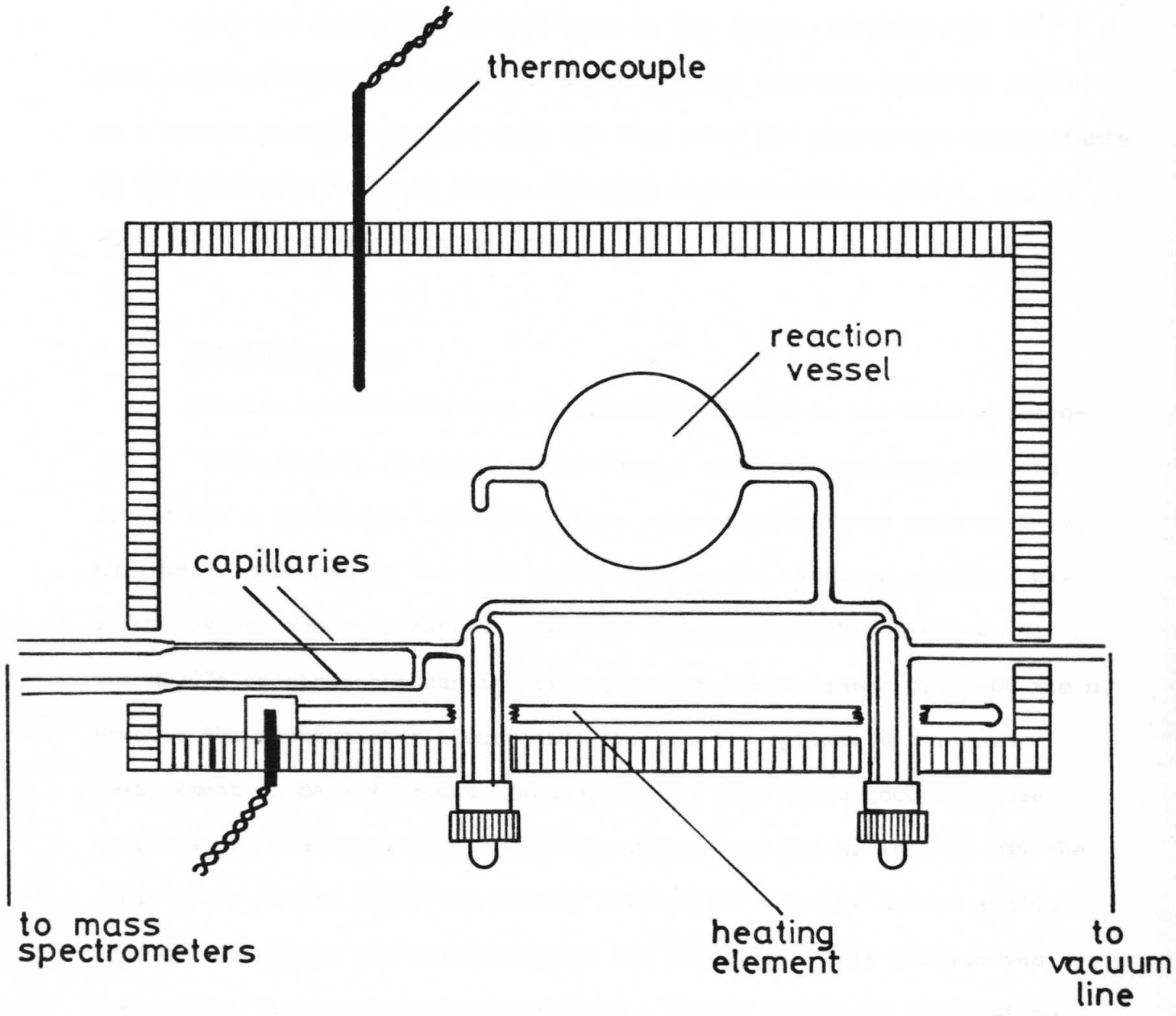

Figure 2.5. Detail of reaction vessel in oven (not to scale)

teflon type in the part of the line where boranes were mixed, and greased (Apiezon L) elsewhere. Pressure measurement was by mercury manometer and was accurate to ±0.4 mmHg. For this reason gases were usually measured to high pressure by using suitably small volumes, thus minimizing any errors of pressure measurement.

With the whole vacuum line open to the pumps, pressures of 10^{-3} mmHg could routinely be attained, while smaller sections could be pumped to a better vacuum. Leakage into the line when not pumped was undetectable on the manometer after 24 hours, and also undetectable in the N_2 and O_2 signals in the mass spectrometer.

2.4 Sampling system

Samples must be led from the reaction vessel to the mass spectrometer. This is done by allowing the sample to bleed directly into the source via a capillary. As stated, two mass spectrometers were used in this work. The use of the MS10 spectrometer for hydrogen analysis was started by Dr. Robert Greatrex, a senior co-worker on this project. The MS3074 spectrometer can in principle scan a mass range of 0-600 a.m.u. However the spectrometer electronics are usually optimized for mass measurement on mass 40 a.m.u. (argon), which then gives good response over most of the mass range. Unfortunately, when set up in this way the sensitivity of the MS3074 is greatly reduced at very low masses and so hydrogen detection and measurement is not possible. This problem was overcome by Dr. Greatrex by introducing a second capillary parallel to the capillary leading to the MS3074, Figure 2.2. This second capillary led directly to the MS10 spectrometer which was used exclusively for hydrogen detection and measurement. It was found that boranes reaching the MS10 would seriously impair its sensitivity to hydrogen and so a cold glass spiral trap was introduced between the capillary and the MS10

spectrometer. The MS10 was under manual control throughout the work, using the Kratos solid state MS10S control unit.

All arguments presented concerning flow in capillaries and calibration techniques are generally applicable to both the MS3074 and MS10. The calibrating gas used in the final method to correct the hydrogen response on the MS10 was helium, as opposed to argon for borane correction in the MS3074.

As stated, samples are bled directly into the spectrometer sources through capillaries. The sample flow can be interrupted by a tap. Two conditions must be met:

1. The sample reaching the mass spectrometer source must be representative of the reaction mixture [55].
2. The act of sampling must not alter the composition of the reaction mixture.

Two distinct types of flow can occur in a capillary:

1. Molecular flow. Here the mean free path of the flowing molecules is much greater than the diameter of the capillary. Therefore molecules effectively collide only with the walls of the capillary and not with each other.
2. Viscous flow. Here the mean free path of the flowing molecules is smaller than the diameter of the capillary, and the molecules collide with each other and the walls. There is a velocity gradient normal to the direction of flow, i.e. molecules flow more slowly near the wall than in the centre of the capillary [65].

Intermediate between these two forms of flow is transitional flow, which can be described by a combination of viscous and molecular flow terms. It will not be further discussed here.

Both viscous and molecular flow can be precisely described. For viscous flow [65]:

$$G = \frac{1}{\eta} \cdot \frac{\pi}{8} \left(1 + \frac{4\eta}{\varepsilon r} \right) \frac{M}{RT} \cdot \frac{r^4}{l} \cdot (P_1 - P_2) P$$

For molecular flow [55]:

$$G = \frac{4}{3} \sqrt{2\pi} \sqrt{\frac{M}{RT}} \frac{r^3}{l} (P_1 - P_2)$$

where G = flow rate through capillary/kg s^{-1}

η = viscosity/poise

ε = a constant of the walls and the gas

P_1 = upstream pressure/pascals

P_2 = downstream pressure/pascals

P = average pressure/pascals

The response of the mass spectrometer to a particular component is a function of two variables:

1. The pressure of the component in the source.
2. The sensitivity of the spectrometer to that component.

The latter can be considered as fixed for the purposes of the argument to be developed here, whereas the pressure of the component in the source is obviously a function of the flow rate of the sample into the source. In order to obtain quantitative results, careful thought must be given to the flow conditions in the capillary.

It was rapidly realized that the method as inherited was unsatisfactory. There follows a brief description of that method and its shortcomings [62].

2.4.1 Original method

No attempt was made to calculate directly the response of the mass spectrometer to particular component pressures in the reaction vessel; rather the spectrometer was calibrated against a range of component pressures in the reaction vessel. The responses of the mass spectrometer

to measured pressures of a particular borane were measured and plotted to give the calibration curve for that borane. The pressure range over which the calibration curves were measured was ∿0-20 mmHg, and the capillary diameter was 0.1 mm, so the flow in the capillary was viscous. Thus calibration curves were of the form IC (ion current) $\propto P^2$, Figure 2.6. Calibration curves were obtained for each borane, and for argon. A known partial pressure of the inert gas argon was included in every reaction mixture to act as a standard so that correction could be made for changes in spectrometer performance. In a typical experiment, the ion current due to the argon was measured and compared with its expected value. Invariably the two were not equal. This led to a factor F_1.

$$\frac{\text{Expected argon ion current}}{\text{Observed argon ion current}} = F_1$$

This factor was then applied to the observed ion current for the boranes, thus correcting for changes in performance of the mass spectrometer. However, for test mixtures containing known pressures of boranes and argon, it was found that multiplication by F_1 failed to correct the borane ion currents to their expected values. It was asserted that a further factor F_2, obtained

$$\frac{\text{Expected borane ion current}}{\text{Observed borane ion current} \times F_1} = F_2$$

by observing the ion current of a borane at t = 0, was sufficient to correct the ion currents of all the boranes in the mixture, when applied with F_1. Although the magnitude of F_1 cannot be predicted, there does seem to be a rational basis for this factor. F_2 is another matter. It was asserted that F_2 was independent of the number and partial pressures of boranes present in the mixture, but that it was dependent on the partial

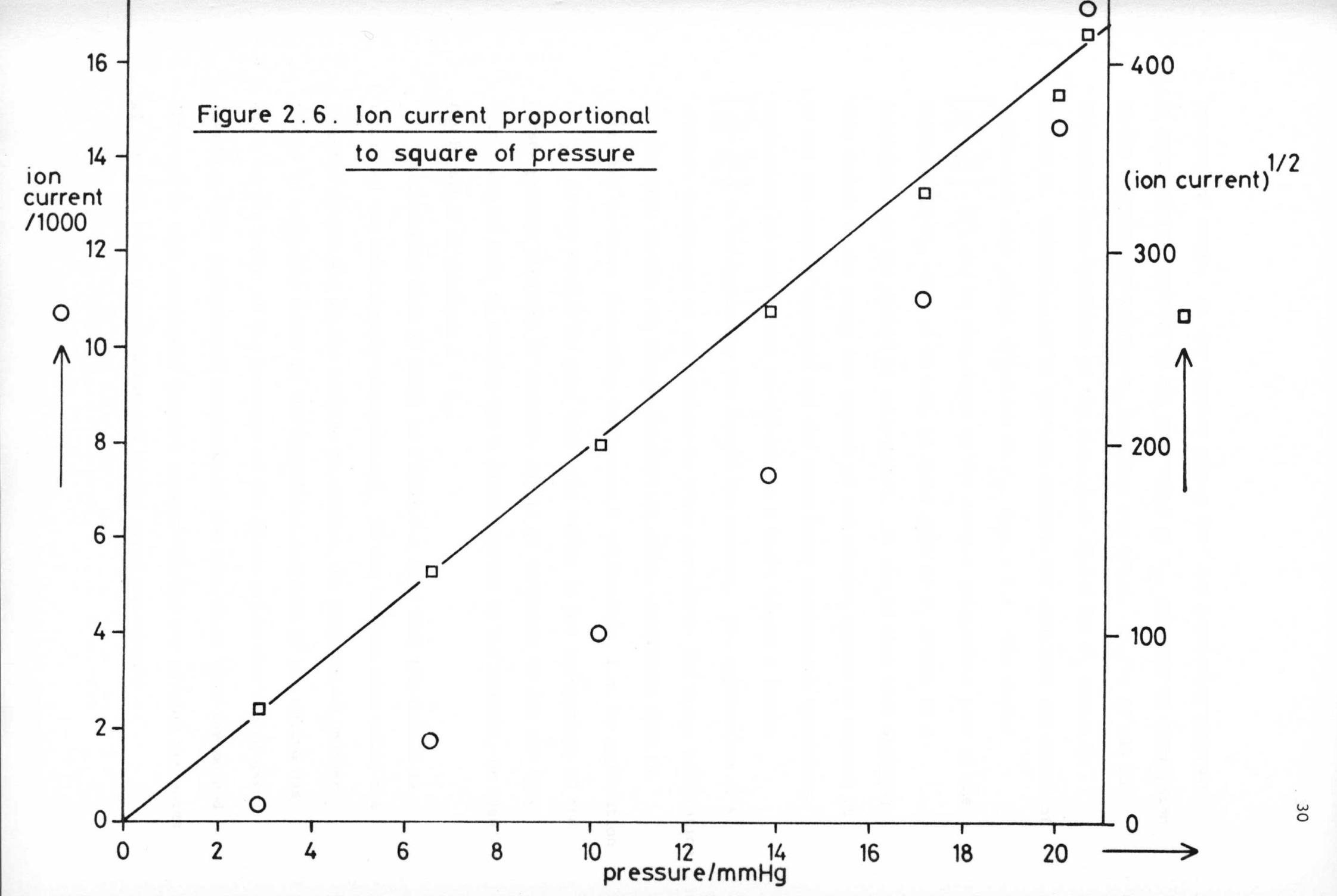
Figure 2.6. Ion current proportional to square of pressure
ion current /1000
(ion current)^1/2
pressure/mmHg
0
2
4
6
8
10
12
14
16
18
20
100
200
300
400

(1) pure Ar; pressure = P_a, viscosity = η_a

$$\text{ion current} \propto \text{flow rate} \propto \left[\frac{P_a^2}{\eta_a}\right] \qquad \text{I}$$

(2) mixture of Ar and borane b; pressure = $P_a + P_b = P_{mix}$

viscosity = η_{mix}

$\therefore$ ion current due to Ar $\propto$ flow rate $\times$ partial pressure Ar

$$\left[\frac{P_{mix}^2}{\eta_{mix}} \cdot \frac{P_a}{P_{mix}}\right] = \left[\frac{P_{mix} \cdot P_a}{\eta_{mix}}\right] \qquad \text{II}$$

$\therefore$ ratio of I to II = $\left[\frac{P_a}{P_{mix}} \cdot \frac{\eta_{mix}}{\eta_a}\right]$ = factor F_1'

(3) for the same mixture; ion current due to borane b

$\propto$ flow rate $\times$ partial pressure b

$$\left[\frac{P_{mix}^2}{\eta_{mix}} \cdot \frac{P_b}{P_{mix}}\right] = \left[\frac{P_{mix} \cdot P_b}{\eta_{mix}}\right] \qquad \text{III}$$

applying factor F_1' to III gives $\left[\frac{P_a \cdot P_b}{\eta_a}\right]$

but the expected value is $\left[\frac{P_b^2}{\eta_b}\right]$ (from consideration of the pure borane case)

so a further factor is required, $\left[\frac{P_b \cdot \eta_a}{P_a \ \eta_b}\right]$ = factor F_2

Figure 2.7. Hypothetical derivation of flow factors

pressure of argon. It was further stated that any particular pressure of argon always resulted in the same value of F_2, although no description of the relationship between F_2 and p(Ar) was given. As far as can be determined from notebooks of the time, such claims for F_2 cannot be justified. Consideration of the flow through the capillary and method of calibration also raises objection to F_2, Figure 2.7. The factor $\left[\frac{P_A}{P_M} \cdot \frac{\eta_M}{\eta_A}\right]$, F_1', can be considered as the machine independent part of the argon factor F_1, that is to say, at least part of F_1 arises as a consequence of the method of calibration. It can be seen that applying this factor to the argon ion current of the mixture serves to correct it to the ion current expected for the argon under calibration conditions. Application of this factor to the borane B still leaves a factor $\left[\frac{P_B}{P_A} \cdot \frac{\eta_A}{\eta_B}\right]$ to be applied to the borane ion current. So, application of F_1 corrects conditions in the mixture to those pertaining for argon calibration. But in order to use the borane calibration curve, conditions must be corrected to those pertaining for borane B calibration, i.e. by application of F_2. It can readily be seen that this factor is not independent of the borane partial pressure as claimed, and it is difficult to see how this factor can be used to correct for a second borane in the mixture, or even for borane B at pressure $P \neq P_B$.

Calculations such as those in Figure 2.8 show that the method as inherited was considerably misconceived. It can be seen that using the response of one gas in the mixture to correct the response of another causes an automatic error in the calculated response of the second gas equal to the ratio of the pressure of the first gas to the second gas (evidence from experimental notebooks of the time shows that the method appeared to give reasonably correct answers because the partial pressures of the test gases were similar and so the error was missed).

mixture; argon pressure = 5 mmHg
borane b pressure = 1 mmHg
borane c pressure = 10 mmHg
} total = 16mmHg

neglecting viscosity effects,

argon ion current = $16^2 \times \frac{5}{16} = 80$

1) pure argon ion current = $5^2 = 25$

$\therefore F_1' = 25/80 = 5/16$

2) borane b ion current = $16^2 \times \frac{1}{16} = 16$

applying F_1'; $5/16 \times 16 = 5$

pure b, expected ion current = $1^2 = 1$

$\therefore F_2 = 1/5$

3) borane c ion current = $16^2 \times \frac{10}{16} = 160$

applying F_1' and F_2; $5/16 \times 1/5 \times 160 = 10$

pure c, expected ion current = $10^2 = 100$

note that the calculated value is in error by a factor of 10, i.e. equal to the ratio of the pressures of borane c and borane b.

Figure 2.8. Calculation of systematic error

Early work [62] made two specific claims about the original method of calibration/correction. Firstly, it claimed that the factor F_2 was not required unless boranes were present in the mixture, and secondly that when the boranes *were* present, F_2 (as determined from one borane) served to correct all the borane pressures satisfactorily. Both these claims can be explained. In the test mixture containing no borane, *all the gases in the mixture were present at the same partial pressure*, so the factor F_2' becomes equal to 1. In the test mixture containing boranes, the two boranes were present at equal partial pressures *while the argon was present at a different partial pressure*. Hence F_2 was not equal to 1 as the argon and borane pressures were unequal, but the F_2 so obtained *did* correct for both boranes as their pressures were equal.

2.4.2 Molecular flow sampling

Consideration of the literature [57-61,66] in the light of our thoughts on the method suggested that good quantitative data could be obtained by developing the system so that molecular flow would occur in the capillaries. Under such conditions the ion current of each component would be proportional to its partial pressure and the gases would flow independently of each other, thus eliminating the troublesome effects described above.

The mean free path of a gas is given by the expression

$$\lambda = \frac{1}{\sqrt{2}.\sigma} \cdot \frac{kT}{P}$$

where λ = mean free path/m

σ = collison cross section/m^2

k = Boltzmann constant/J K^{-1}

T = temperature/K

P = pressure/pascals

So for a capillary of diameter 10^{-4} m, Table 2.1 shows the pressure at which the mean free path of molecules of various sizes becomes equal to the capillary diameter.

Table 2.1. Pressure when $\lambda = 10^{-4}$ m at different molecular diameters

Molecule	10^{10} x collision diameter/m	Pressure (when $\lambda = 10^{-4}$ m)/mmHg
H_2	2.36	1.23
Ar	2.87	0.83
B_5H_9	∿6	0.19
Hypothetical	10	0.07

Now in order to obtain molecular flow the mean free path of the molecules must be much greater than the capillary diameter so it was decided that sample pressures of 0.01 mmHg would be low enough to give an adequate margin for molecules of large size likely to be encountered in this work, e.g. decaborane(14). Since reaction pressures were likely to be of the order of 10 mmHg, a thousand-fold reduction in pressure was required, though this needed to be only approximate.

The pressure reduction was achieved by expanding a small sample from the reaction vessel into an expansion vessel of suitable dimension, Figure 2.9.

Calibration curves for argon and hydrogen using the new system gave absolutely straight lines, and admixtures of argon in the hydrogen calibrations did not alter the form of the calibration curve, i.e. there was no suppression effect, Figure 2.10. It was envisaged that only the argon factor F_1 need be retained (to correct for machine effects). A drawback of molecular flow is mass discrimination, since light molecules

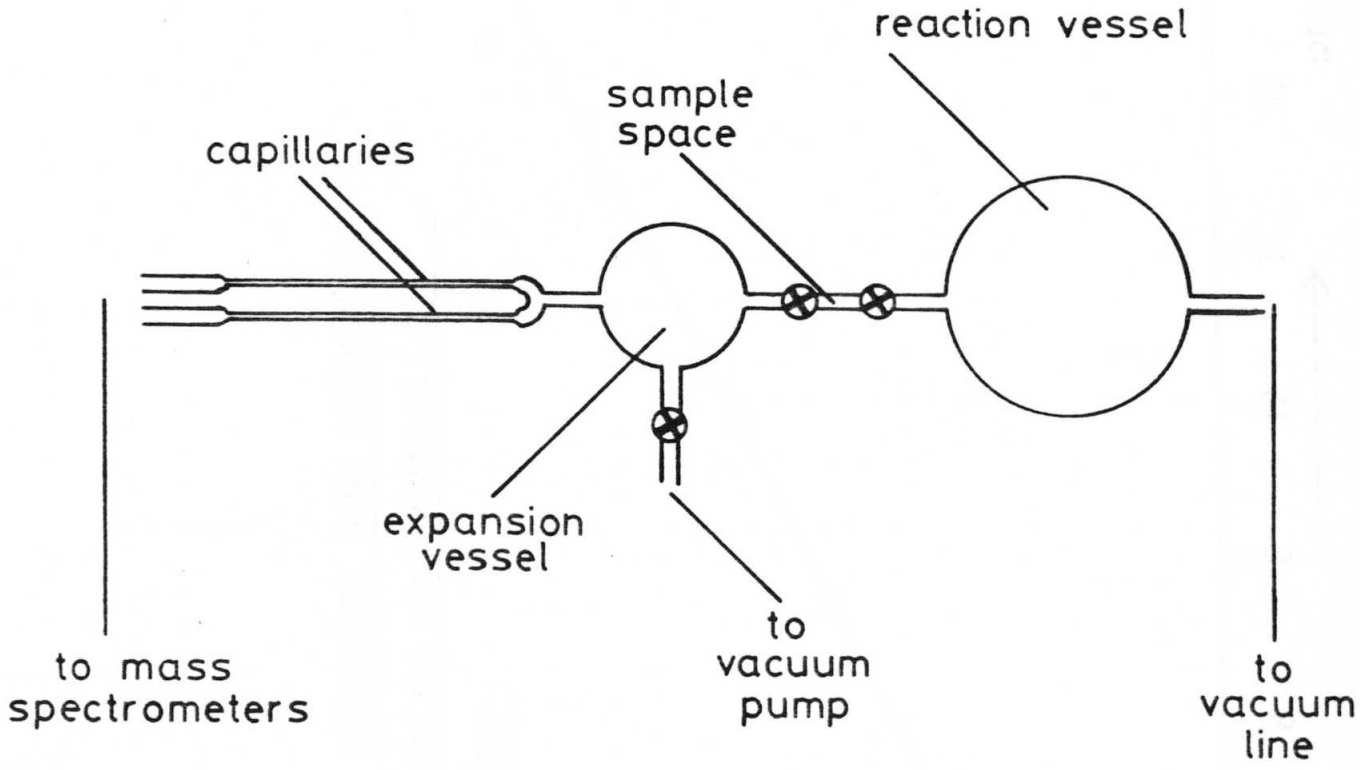

Figure 2.9. Molecular flow reaction vessel with expansion vessel

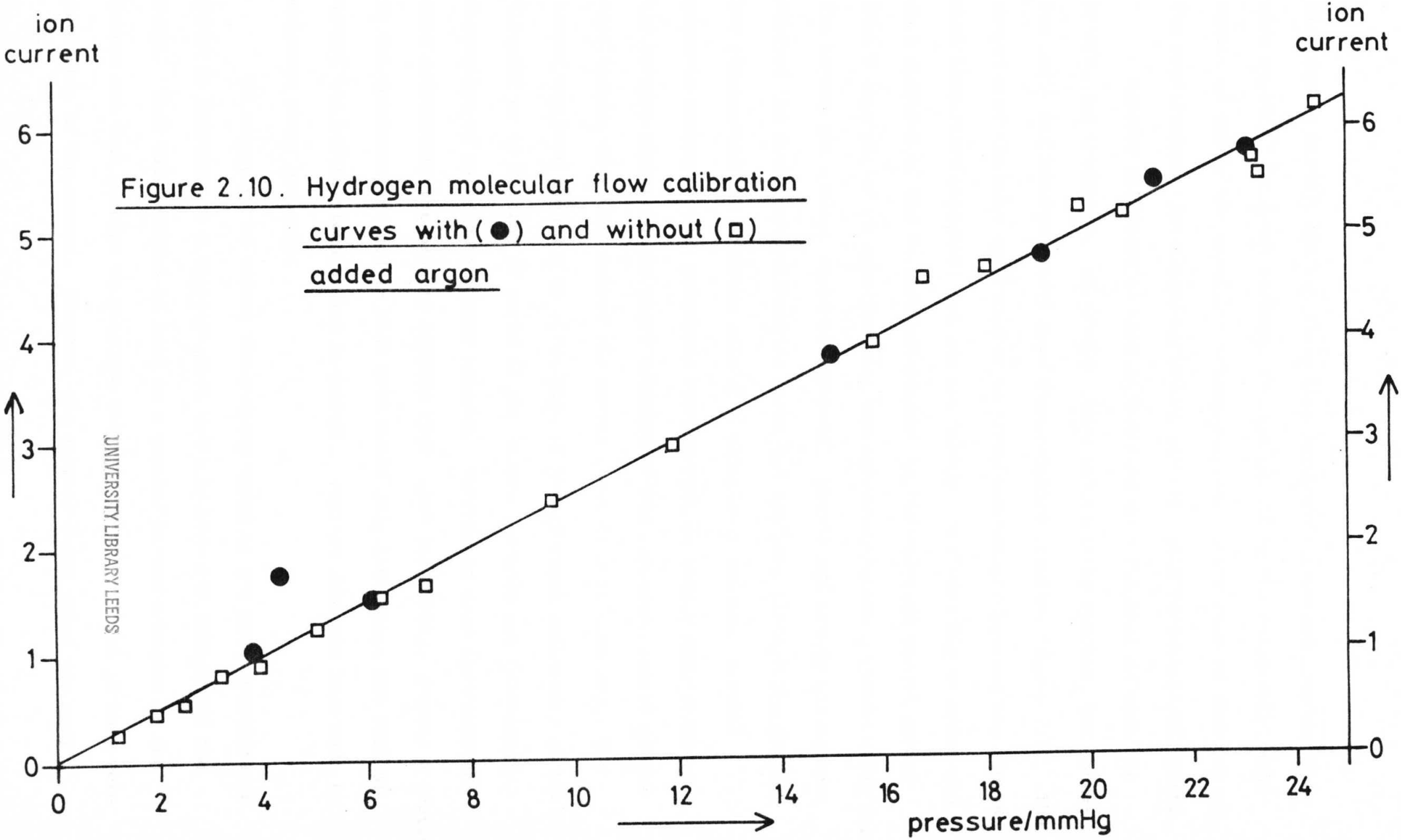

Figure 2.10. Hydrogen molecular flow calibration curves with (●) and without (□) added argon

flow faster through the capillary than heavy molecules and thus deplete more rapidly. This was overcome in this method by the relatively large amount of gas in the expansion vessel compared to the rate of flow out of the capillaries. The expansion vessel was evacuated between measurements.

However difficulties were encountered when calibration with the boranes was attempted. Diborane(6) gave satisfactory results, but pentaborane(9) and hexaborane(10) gave disappointing results, Figure 2.11. The response of the mass spectrometer to these two heavier boranes was always much lower than expected, and was not steady. Successively scanning the mass spectrum of the calibration mixture in the reaction vessel showed that a long period of equilibration was necessary before a steady value for the borane ion current could be obtained. When these steady values were plotted the resultant calibration curve did not pass through the origin, but intersected the pressure axis at a positive pressure. Several possible causes of this behaviour were suspected, namely adsorption of the boranes either on the glass surfaces of the expansion vessel or the capillaries, or alteration of the source conditions in some way. The latter may have been due to alteration of the electron emissivity of the filament or to coating of parts of the source (boranes are notoriously disruptive of mass spectrometer sources. Sources in mass spectrometers used exclusively for organic samples might last for months, whereas a source in the spectrometer used in this work would only last about one week of normal use before cleaning was required). Various attempts were made to overcome these problems.

We attempted to reduce the pumping speed of the mass spectrometer pumps by introducing a quarter-swing valve between the source and the pumps. This was intended to lead to a greater borane pressure in the source and thus perhaps to overcome the adsorption problems if they were occurring in the source. However, the quarter-swing valve was very

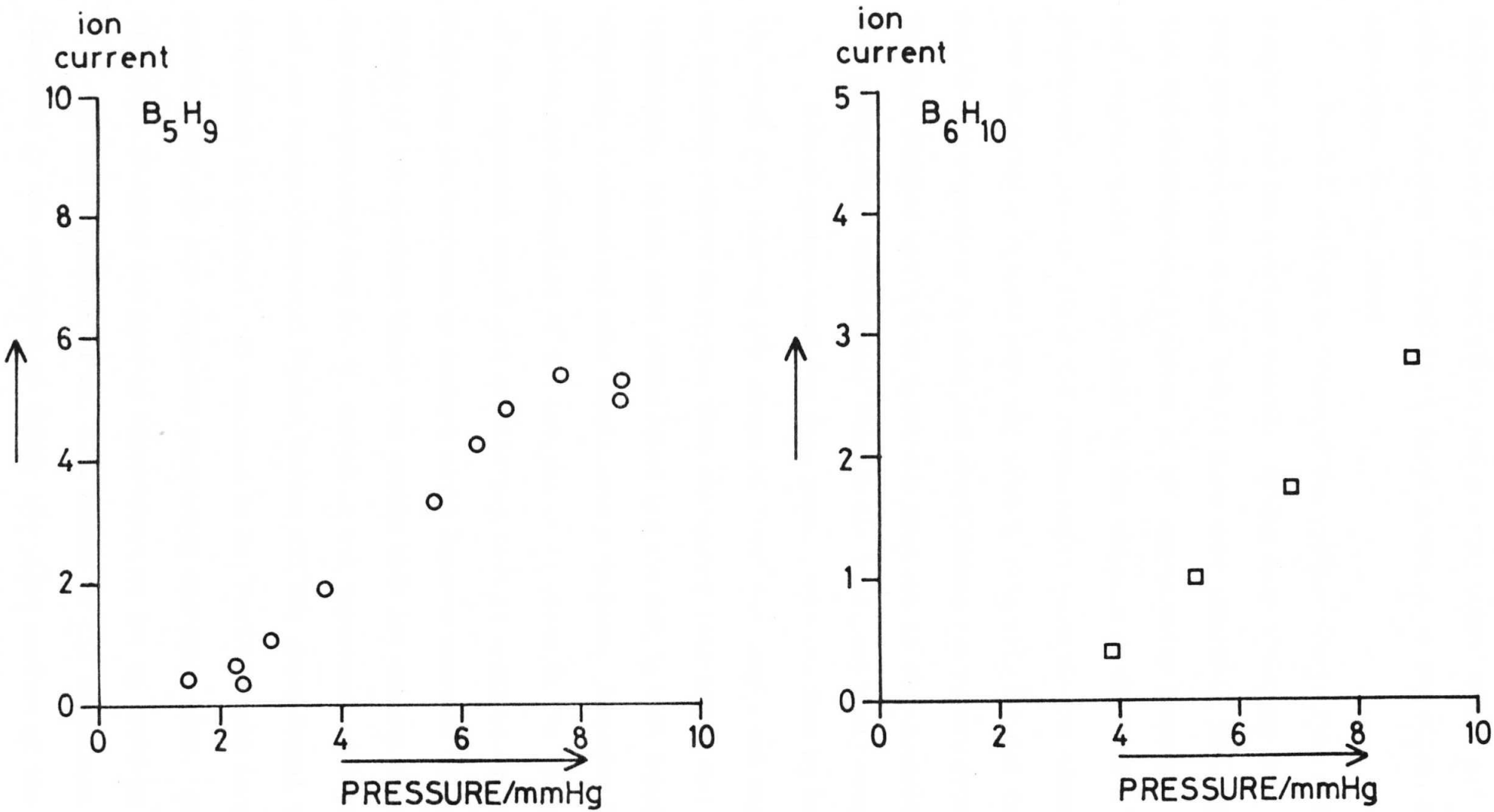

Figure 2.11. Pentaborane(9) and hexaborane(10) molecular flow calibration curves

difficult to use in controlling the pumping speed, nearly all of its effect occurring over the final small movement of the valve, and no improvement was obtained.

Another attempt to overcome the problem was to take multiple samples from the reaction vessel. Rather than admitting just one sample into the expansion vessel, two or more were admitted. The expectation was that the difference in response of the spectrometer between n samples and n-1 samples would be equivalent to the response to one sample were there no adsorption, i.e. the first n-1 sample would saturate the adsorption sites. Some encouraging results were obtained in this way, but not consistently and at the expense of slowing and complicating the experimental procedure. Too many samples would also raise the pressure in the expansion vessel to a point where transitional flow in the capillary would occur.

Source pretreatment was attempted. This was done by sampling in the usual way, allowing the source to "see" the sample and any coating or filament effects to occur, then discarding that sample and rapidly resampling. Again, some encouraging results but, as with cumulative sampling, a slower and more complicated procedure. Assuming that the problem was adsorption of the boranes on to glass in the low pressure region of the expansion vessel and capillaries then it would be expected that modifying the surfaces by coating might improve matters. Firstly, the inside of the reaction vessel was coated with polytetrafluoroethylene. This was borrowed from Dr. D. Baulch of the Department of Physical Chemistry and was Dupont Industrial Finish Teflon 852-201 Clear Enamel (12% suspension in toluene). It was used in Dr. Baulch's work to render glassware suitable for use with reactions generating hydrogen atoms. However it was difficult to apply and gave no improvement as far as could be seen.

At the suggestion of Dr. K.D. Bartle of the Department of Physical Chemistry it was attempted to modify the glass surface of the expansion vessel by silylation. Silylation is a common practice in gas chromato-

graphic work and it entails deactivation of the glass chromatography columns towards polar molecules by binding hydroxyl groups on the glass surface to trimethylsilyl groups. Using the method of Lee and co-workers [67] with a 5:1 mixture of hexamethyldisilazane:chlorotrimethylsilane, the internal surface of the expansion vessel was silylated. Unfortunately no improvement was obtained.

Finally the tempting simplicity of a molecular flow system had to be abandoned, mainly because the amounts of borane used were far too small and were being "lost" in the system due to adsorption. Some confirmation of this was obtained by packing a 500 cm^3 expansion vessel with 40 cm^3 of pyrex glass spirals. This new expansion vessel then had a volume comparable to the old one (460 cm^3 c.f. 400 cm^3) but a greatly increased surface area. An argon calibration curve measured with this vessel was reasonable, but attempts to obtain a measurement for B_6H_{10} with this vessel gave extremely slow response times, and cumulative sampling gave worse responses than with the previous unpacked expansion vessel.

It was concluded that this molecular flow method was not practicable and that larger pressures of boranes were needed before progress could be made.

2.4.3 Modified viscous flow sampling

The need to use larger pressures of the boranes meant resorting to viscous flow of course. As described earlier, consideration of the effect of changes in partial pressure and viscosity on flow through the capillaries showed that simple viscous flow would not give quantitative results. Quite apart from the pressure effects shown in the hypothetical calculations, the changes in viscosity between a calibration experiment and a thermolysis experiment would cause a change in flow rate through the capillary. Such effects would be exacerbated in reactions in which

hydrogen was produced, as the low viscosity and low molecular weight of hydrogen enhance its effects on the viscosity of the gas mixture.

Ideally, if the flow rate into the source of every component in the reaction vessel was determined by the *same* pressure and the *same* viscosity, all the effects previously described would vanish and the components in the mixture would not interfere with each other. This objective could be achieved by making up all gas mixtures (for quantitative purposes) in a "background" or "diluant" pressure of an inert gas. One of the factors which led to this line of thought was some evidence obtained by Dr. Robert Greatrex, suggesting that the argon factor F_1 tended towards a fixed value with increasing argon pressure.

Methods exist for estimating the viscosities of gaseous mixtures. In order to select a sufficient background pressure of inert gas, calculations were made of the viscosity of hypothetical gas mixtures.

The viscosity of a mixture of gases can be approximated by the equations [68]:

$$\eta_m = \sum_{i=1}^{n} \frac{y_i \eta_i}{\sum_{j=1}^{n} y_i \phi_{ij}}$$

where η_m = viscosity of mixture/poise

η_i = viscosity of pure component i/poise

y_i = mole fraction of pure component i/poise

ϕ_{ij} = a function of the viscosities and molecular weights of pure components i and j

$$\phi_{ij} = \frac{[1 + (\eta_i/\eta_j)^{\frac{1}{2}}(M_j/M_i)\ ]^2}{[8(1 + M_i/M_j)]^{\frac{1}{2}}}$$

Consider calculations of viscosity for various hypothetical mixtures of helium, argon and pentaborane(9). Table 2.2 shows the viscosities of these gases at 20°C and 1 atm.

Table 2.2. Viscosities of helium, argon and pentaborane(9) at 20°C and 1 atmosphere pressure

	He	Ar	B_5H_9
η/micropoise	194	222	70
M/a.m.u.	4	40	64

The value of 70 μpoise for the viscosity of pentaborane(9) was estimated from the density of pentaborane(9) at its boiling point [69] and its dipole moment [70] using the empirical formulae from reference [68], i.e.

$$\eta = 26.69 \frac{\sqrt{MT}}{\sigma^2 \Omega_{V(STOCK)}}$$

$$\Omega_{V(STOCK)} = \Omega_{V(L-J)} + 0.2 \frac{\delta^2}{T^*}$$

$$\delta = \frac{1.94 \times 10^3 \mu_p^2}{V_b T_b}$$

$$\sigma = \left(\frac{1.585 V_b}{1 + 1.3 \delta^2} \right)^{1/3}$$

$$T^* = \frac{kT}{\varepsilon}$$

$$\frac{k}{\varepsilon} = [1.18(1 + 1.3\delta^2) T_b]^{-1}$$

where η = viscosity/micropoise

M = molecular weight/a.m.u.

σ = collision diameter/Å

$\Omega_{V(STOCK)}$ = Stockmayer collision integral

$\Omega_{V(L-J)}$ = Lennard-Jones collision integral

δ = a polar parameter (dimensionless)

V_b = specific molar volume at boiling point/cm^3 mol^{-1}

T_b = boiling point/K

ε = energy minimum in intermolecular potential curve/ joules

Letting He = gas 1, Ar = gas 2, and B_5H_9 = gas 3 the ϕ function can be calculated for the six possible pairs of gases:

ϕ_{12} (He/Ar) = 2.3893

ϕ_{21} (Ar/He) = 0.2734

ϕ_{13} (He/B_5H_9) = 6.4296

ϕ_{31} (B_5H_9/He) = 0.1450

ϕ_{23} (Ar/B_5H_9) = 2.5011

ϕ_{32} (B_5H_9/Ar) = 0.4928

Table 2.3: He/Ar mixture

	mole fraction				
He	1.00	0.75	0.50	0.25	0.00
Ar	0.00	0.25	0.50	0.75	1.00
η_m/micropoise	194	230	232	227	222

Table 2.4: Ar/B_5H_9 mixture

	mole fraction				
Ar	1.00	0.75	0.50	0.25	0.00
B_5H_9	0.00	0.25	0.50	0.75	1.00
η_m/micropoise	222	149	110	86	70

Table 2.5: $He/Ar/B_5H_9$ mixture

	mole fraction				
He	0.900	0.900	0.900	0.900	0.900
Ar	0.100	0.075	0.050	0.025	0.000
B_5H_9	0.000	0.025	0.050	0.075	0.100
η_m/micropoise	217	193	174	157	144

These calculations on the viscosities of mixtures show a smooth change in viscosity for a binary mixture from that of one pure component to the other, Figure 2.12, Table 2.3. If the viscosities of the two components differ widely, the change in viscosity as the mixture composition changes is also wide, Figure 2.13, Table 2.4. Addition of a third component in excess greatly reduces the change in viscosity, Figure 2.14, Table 2.5. Argon would have been particularly good as the excess gas as its mass is comparable to the masses of the boranes, but it could not be used both as the excess gas and the internal calibrant (as its ion current in the spectrometer would be saturated), so it was decided to use helium instead. As can be seen from the form of the

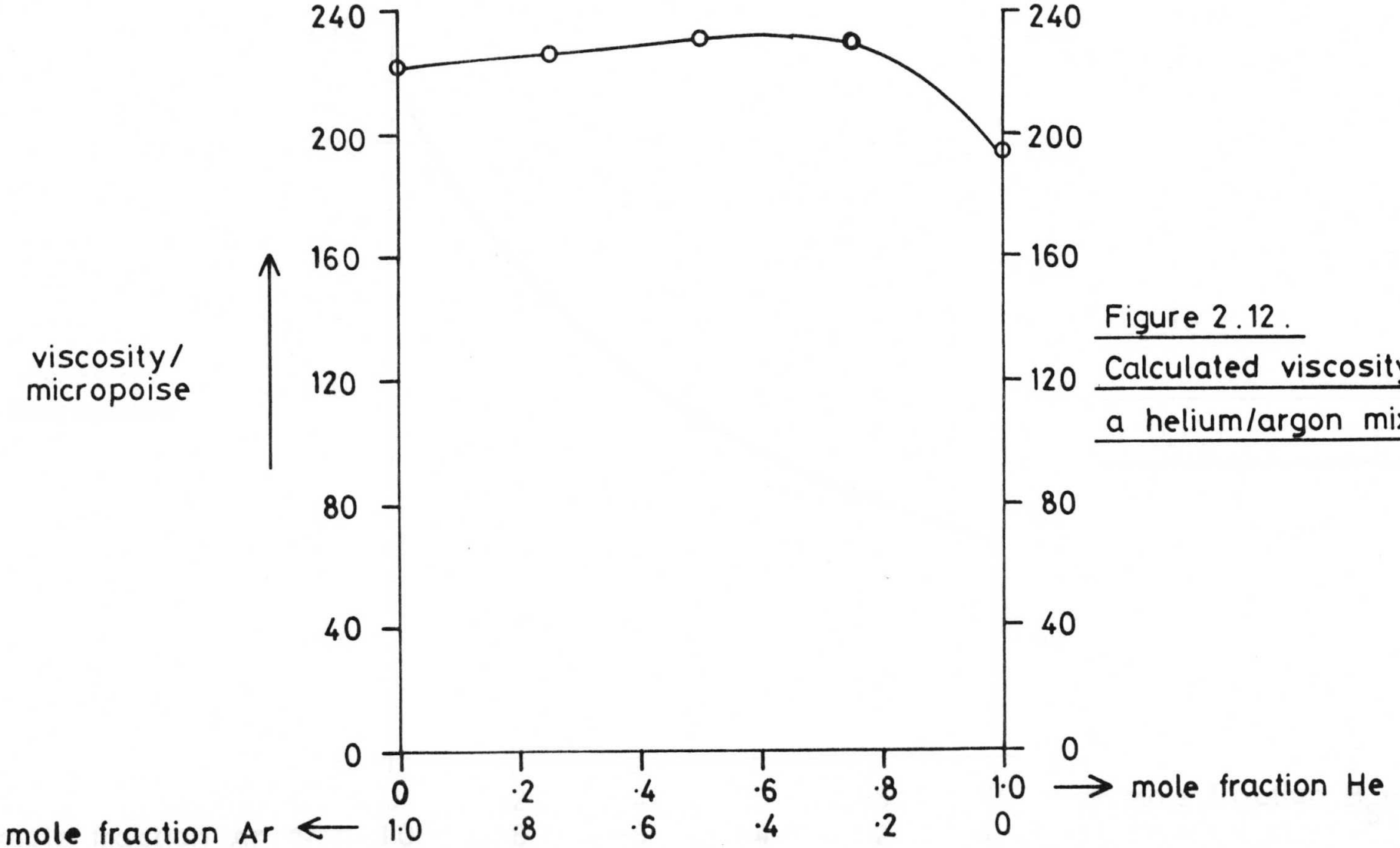

Figure 2.12.
Calculated viscosity of a helium/argon mixture

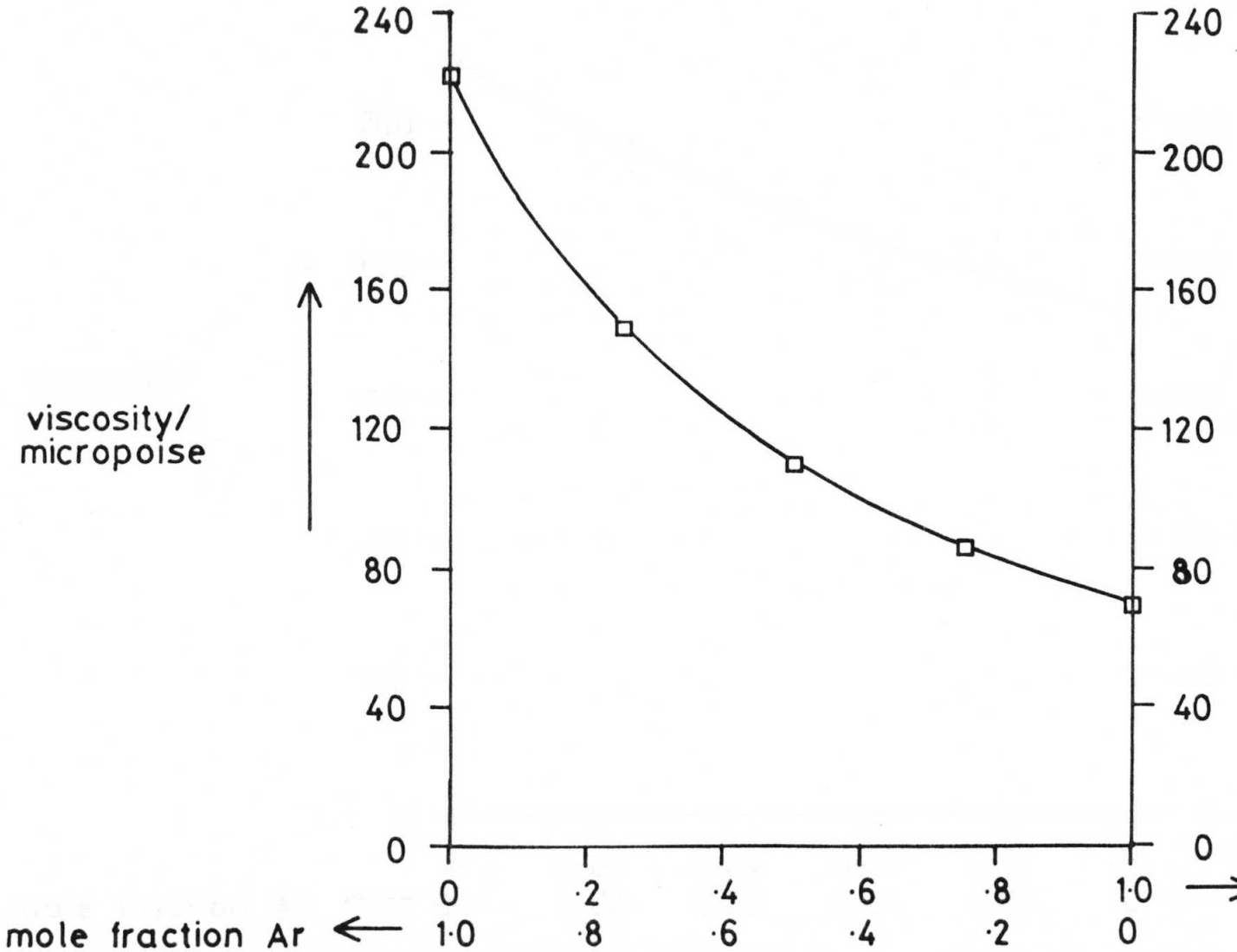

Figure 2.13.
Calculated viscosity of a B_5H_9/argon mixture

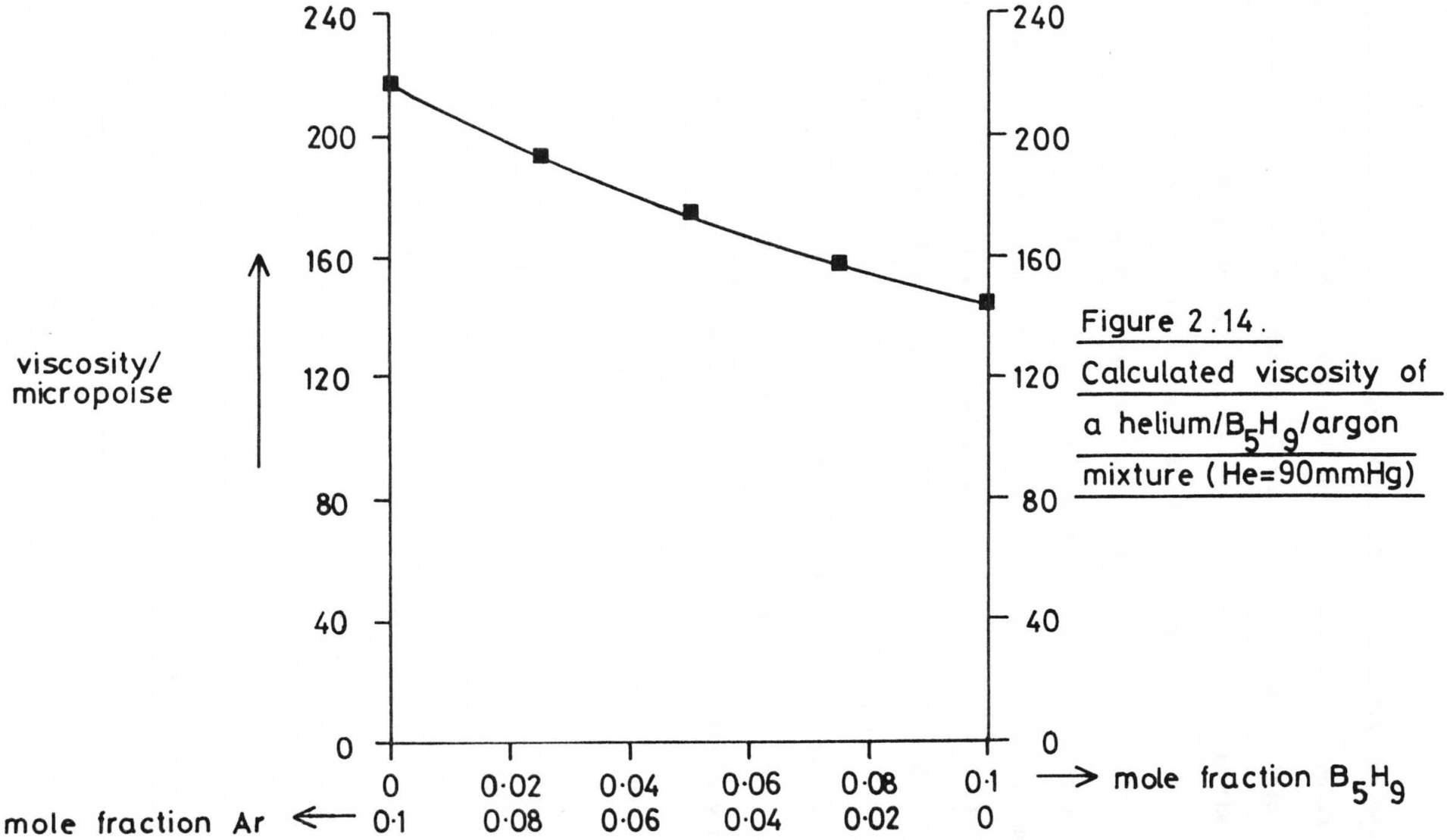

Figure 2.14.
Calculated viscosity of a helium/B_5H_9/argon mixture (He=90mmHg)

equations used in the estimation of the mixture viscosities, the low mass of helium compared to the boranes makes it less efficient than argon in keeping the viscosity at a constant value, but other advantages helped to offset this consideration, i.e. its use as a calibrant for H_2 in the MS10 spectrometer and its low efficiency as a kinetic third body.

So the introduction of an excess background of an inert gas reduces the variability of viscosity in the reaction mixtures. It can also be shown by calculations similar to those in Section 2.4.1 (Figures 2.7 and 2.8) that effects due to changes in total pressure (because of reaction) will be much reduced compared to the original method, and negligible compared with the probable overall experimental error, Figure 2.15. Indeed the argon correction factor F_1 is now seen to have only a small component arising from pressure changes, its chief remaining function being to correct for changes in instrument sensitivity.

mixture; helium pressure = 100 mmHg
argon pressure = 5 mmHg
borane b pressure = 1 mmHg
borane c pressure = 10 mmHg
} total = 116 mmHg

neglecting viscosity effects,

$$\text{argon ion current} = 116^2 \times \frac{5}{116} = 580$$

1) $$\text{pure argon ion current} = 105^2 \times \frac{5}{105} = 525$$

$$\therefore \underline{F_1' = 525/580 = 105/116}$$

2) $$\text{borane b ion current} = 116^2 \times \frac{1}{116} = 116$$

applying F_1'; $105/116 \times 116 = 105$

pure b*, expected ion current $= 101^2 \times \frac{1}{101} = 101$

$$\therefore \underline{F_2 = 101/105}$$

3) $$\text{borane c ion current} = 116^2 \times \frac{10}{116} = 1160$$

applying F_1' and F_2; $105/116 \times 101/105 \times 1160 = 1010$

pure c*, expected ion current $= 110^2 \times \frac{10}{110} = 1100$

note that the final error is again equal to the ratio of the pressures of borane c* and borane b*, but the error is reduced by the excess helium.

* including 100mmHg helium

Figure 2.15. Flow calculations with helium background

CHAPTER 3

Calibration Procedure and Data Analysis

Having established the how and why of a suitable experimental method, it remained only to calibrate the system before using the apparatus to attack the question of the thermolysis of hexaborane(10). Two types of information were required in order to analyse the spectrum of a mixture. Firstly, calibrations of spectrometer response to reaction vessel pressure were necessary and the measurement of these is described in section 3.1. Secondly, a "standard mass spectrum" was required for each of the boranes, enabling recognition of the boranes during analysis. The use of these standard spectra is discussed in section 3.2.

3.1 Calibration

The spectrometer was calibrated for a particular borane by introducing a series of mixtures of that borane, helium and argon into the reaction vessel and measuring the response of the mass spectrometer to the borane and the argon. The series of mixtures varied only in the borane content, the helium and argon partial pressures being always 100 mmHg and 5 mmHg respectively.

The calibration mixtures were prepared using the vacuum line described in section 2.3. Very careful thought had to be given to the way in which the gases were mixed to ensure efficient mixing. Gas pressures were measured with a mercury manometer and the simple gas laws were used to calculate the pressures and expansions required. Mixtures which had been prepared by quite complex series of expansions gave final measured pressures which agreed with the calculated pressures to the order of 2%.

The response of the mass spectrometer to the argon is simply the ion current of its mass spectrum, which consists of a single peak at m/z value

40. However reliance was not placed on a single measurement of the mass spectrum of the mixture. The powerful software on the data-acquisition system enabled a series of successive scans to be compared. If the spectrometer response was found to be stable in this comparison, a number of the scans could then be averaged. It was the normal practice to follow this procedure for every measurement on the MS3074, usually taking an average of 5-10 scans. The averaged scan was taken as the mass spectrum of the sample in question. Scan averaging was performed in all aspects of the work, i.e. standard spectra, argon and borane calibration and in the measurement of the mass spectra of mixtures.

Argon was chosen as the calibrant for the boranes because none of the stable boranes have significant peaks in their mass spectra at m/z = 40. The spectra of the boranes consist of course of many peaks, and the response of the spectrometer to a particular borane is obtained by summing the ion currents of all the peaks in the spectrum of that borane, Figure 3.1.

The argon correction factor for each mixture was then obtained from the simple relationship

$$F_1 = \frac{\text{expected argon response}}{\text{observed argon response}}$$

(the expected argon response was that obtained from an argon calibration curve made with a series of argon/helium mixtures). This factor was then applied to the borane response of that mixture. After repeating this procedure for each mixture, a table of borane pressures versus responses could be constructed from which the calibration curve could be obtained, Table 3.1

Calibration curves were obtained for hexaborane(10), pentaborane(9) and hydrogen (in an analogous manner on the MS10, using chart recorder peak heights instead of digitized ion currents). The hexaborane(10) and hydrogen calibration curves were required immediately for the thermolysis

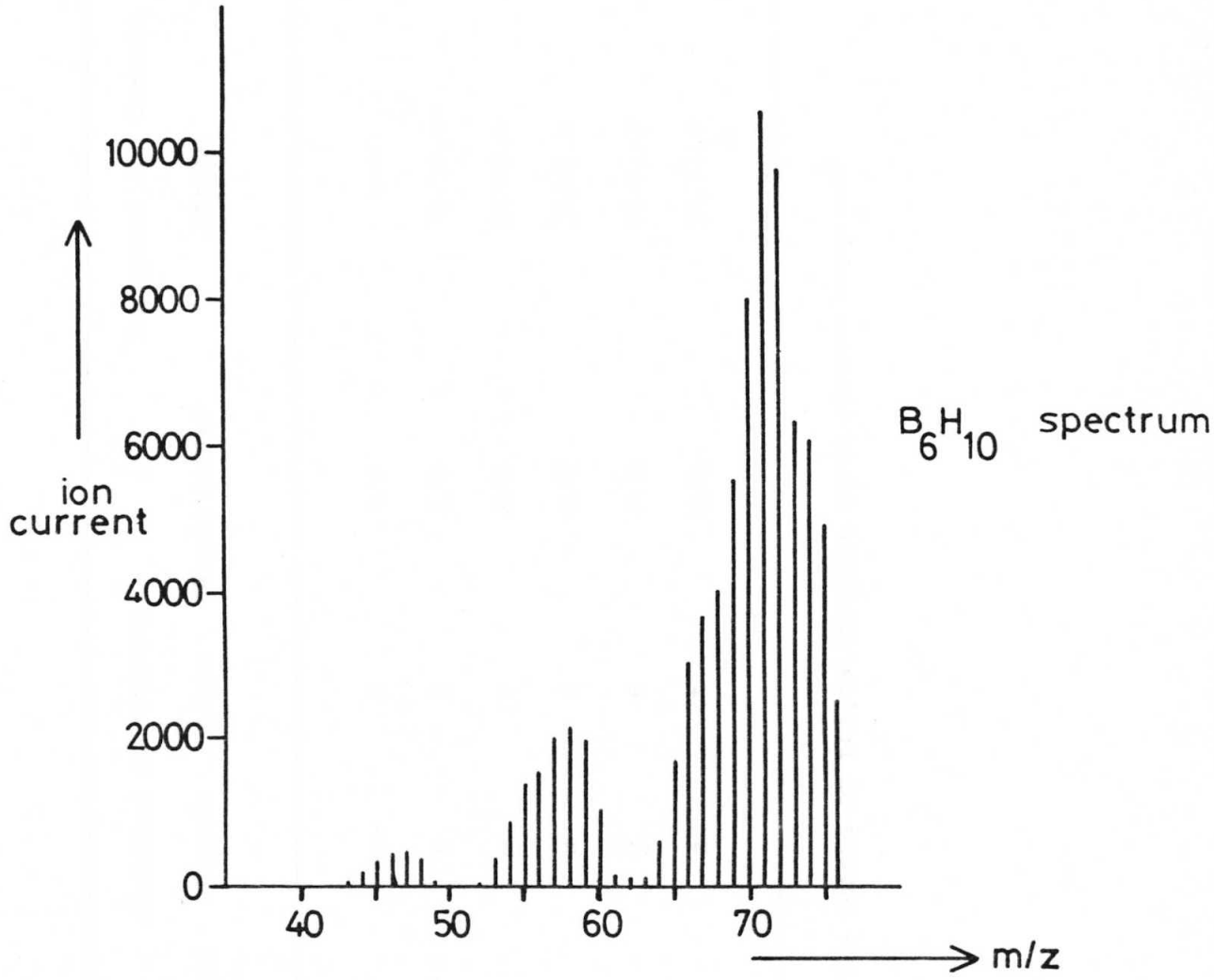

m/e	ion current
65	1692
66	3054
67	3672
68	4025
69	5539
70	8028
71	10570
72	9746
73	6318
74	6029
75	3918
76	2532
	65123 = measured response

Figure 3.1. Summing of borane peaks to obtain spectrometer response

Table 3.1. Construction of calibration curves

Mixture Composition*		Observed Ion Current			Corrected Ion Current
Borane partial pressure /mmHg	Argon partial pressure /mmHg	Borane	Argon	Argon factor	Borane
0	5	---	A	A/A	---
2	5	v	b	A/b	(A/b).v
4	5	w	c	A/c	(A/c).w
6	5	x	d	A/d	(A/d).x
8	5	y	e	A/e	(A.e).y
10	5	z	f	A/f	(A/f).z

These columns give the points of the calibration curve

* All in a background of 100 mmHg helium

work while the pentaborane(9) curve was measured as part of a programme to calibrate the apparatus for as many boranes as possible. Christopher Potter, a colleague working on other aspects of borane thermolysis has measured calibration curves for diborane(6) and tetraborane(10). During the early part of the work presented in this thesis, a decaborane(14) calibration curve was not measured as this borane was only a minor component of the reaction mixtures resulting from the thermolysis of hexaborane(10). In these early stages, decaborane(14) pressures were estimated using the hexaborane(10) calibration curve. As work progressed however, better estimates of the decaborane(14) partial pressures were required. Mixing accurate pressures of decaborane(14), helium and argon was exceedingly difficult due to the low volatility of decaborane(14). To obtain accurate pressures of decaborane(14), the decaborane(14) was weighed so that complete vaporization would give the required pressure in a vessel of known volume. The decaborane(14) calibration curve was finally obtained by using a specially designed reaction vessel which permitted quantitative transfer of a known weight of decaborane(14) into the vessel followed by complete vaporization in the necessary background of 100 mmHg helium and 5 mmHg argon. Decaborane(14) will not vaporize and mix efficiently against a pressure of gas if it is in a constricted space and the design of the vessel avoided this, Figure 3.2. Care was taken not to attempt to exceed the reported vapour pressure of decaborane(14) at the temperature used (393 K), although literature reports of the vapour pressure of decaborane(14) are confused [71-73].

Once the necessary calibration data were obtained for a borane, the calibration curve could be generated in a form suitable for incorporation into the computer programs for data analysis, section 3.2. This was done using a standard numerical analysis routine from the NAG (Numerical Algorithms Group) Library. The NAG Library is widely available, and

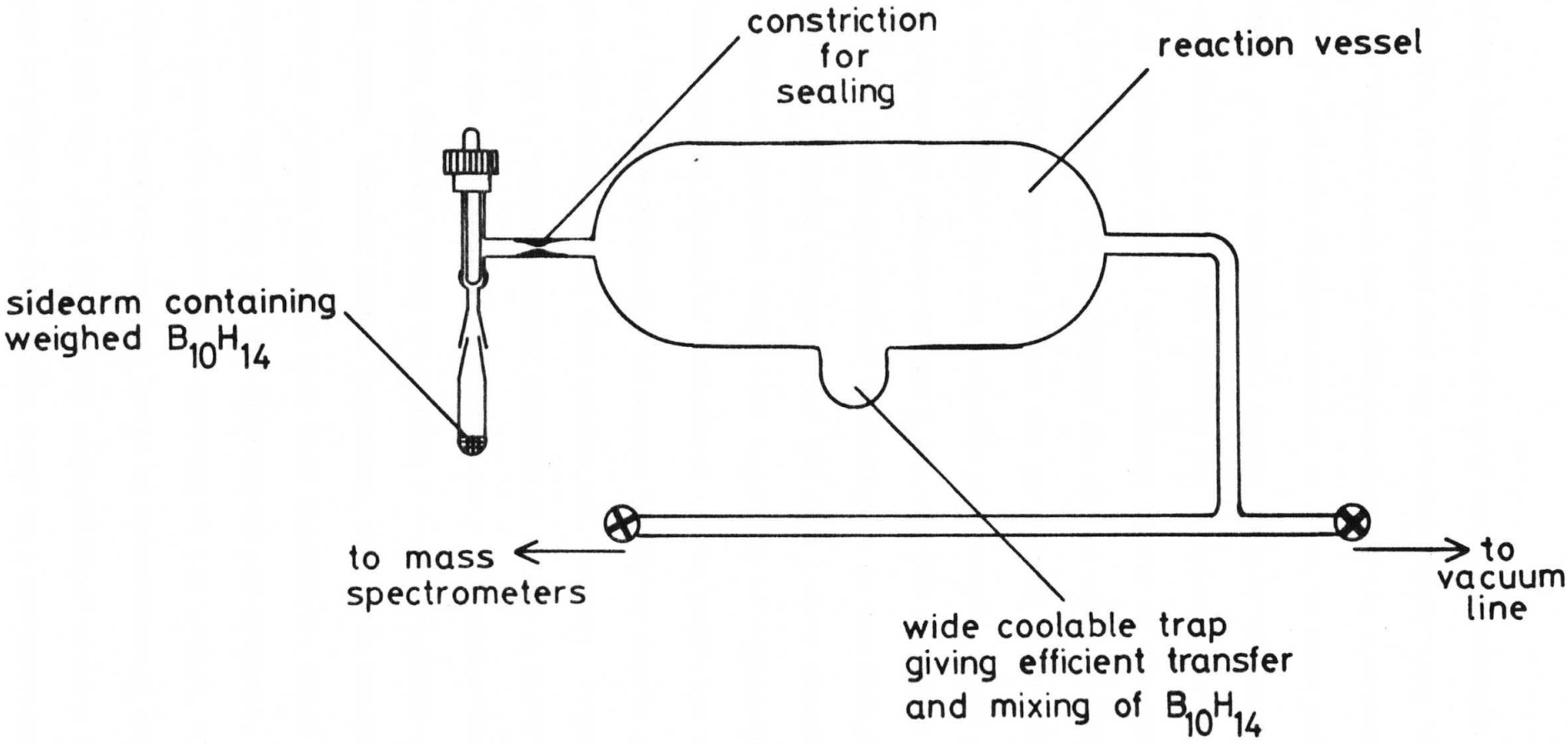

Figure 3.2. $B_{10}H_{14}$ calibration vessel

provides expertly developed routines for many kinds of problems in numerical analysis. The routine used was routine E02ADF (the 'F' stands for FORTRAN, the Library also has ALGOL versions of its routines). The routine computes a polynomial approximation to a set of data points which can be weighted. It uses the Chebyshev series of polynomials $T_0(x)$, $T_1(x)$ etc., the forms of which are outside the scope of this thesis but can be found in reference [74]. The closeness of fit of the curve is controlled by the operator by specifying the degree of the polynomial to be used. Specifying degree 0 causes the routine to fit a curve to the points using only the first of the Chebyshev polynomials, $T_o(x)$, whereas degree 7 would allow the routine to use $T_o(x)....T_7(x)$. Figure 3.3 shows how the form of the fitted polynomial approximates to the data points as the degree changes. Visual inspection of the data points showed that the form of the calibration curves would most logically be represented by smooth functions with no points of inflection. This condition was satisfied by a Chebyshev polynomial of degree 2, higher degree polynomials giving curves which followed the data points too closely. These higher degree curves have a 'fine structure' determined by the scatter in the data points and are thus physically meaningless. All curves were 'forced' through the point (0,0) by giving that point a large weighting when computing the curve. Without such a weighting, the curve usually intersected the axes at a point slightly away from the origin, which gave distorted pressures from very low ion currents during analysis, Figure 3.4.

Of course, given the experimental accuracy of the method, a curve of equally justifiable form and accuracy could be drawn through the data points by hand and eye. The use of this sophisticated routine was necessary only to obtain the calibration curve in a mathematical form which could be incorporated into the analytical programs for interpretation by a further routine, see section 3.2.

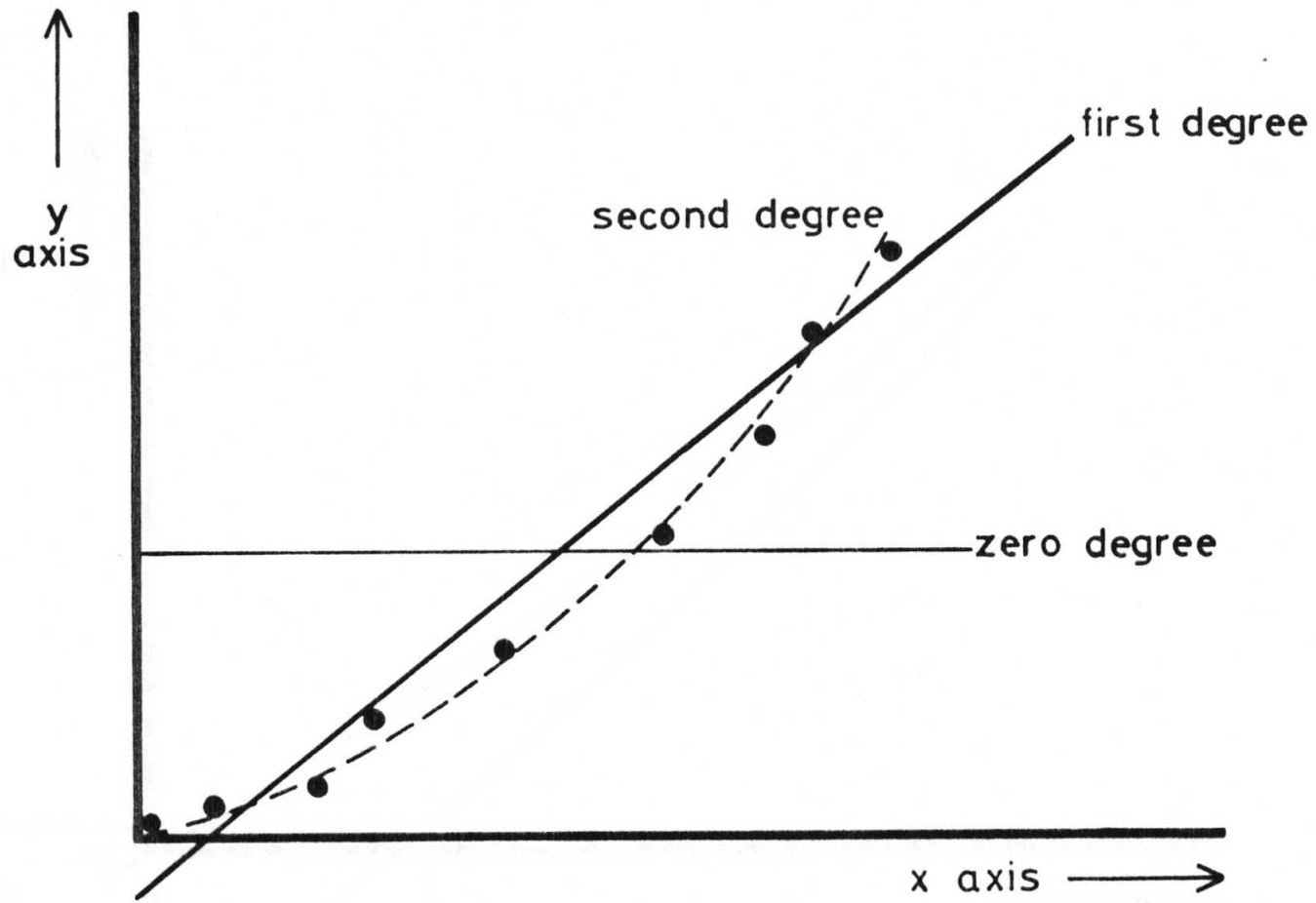

Figure 3.3. Effect of degree on shape of fitted Chebyshev polynomial

Figure 3.4. Systematic error if curve is not forced through origin

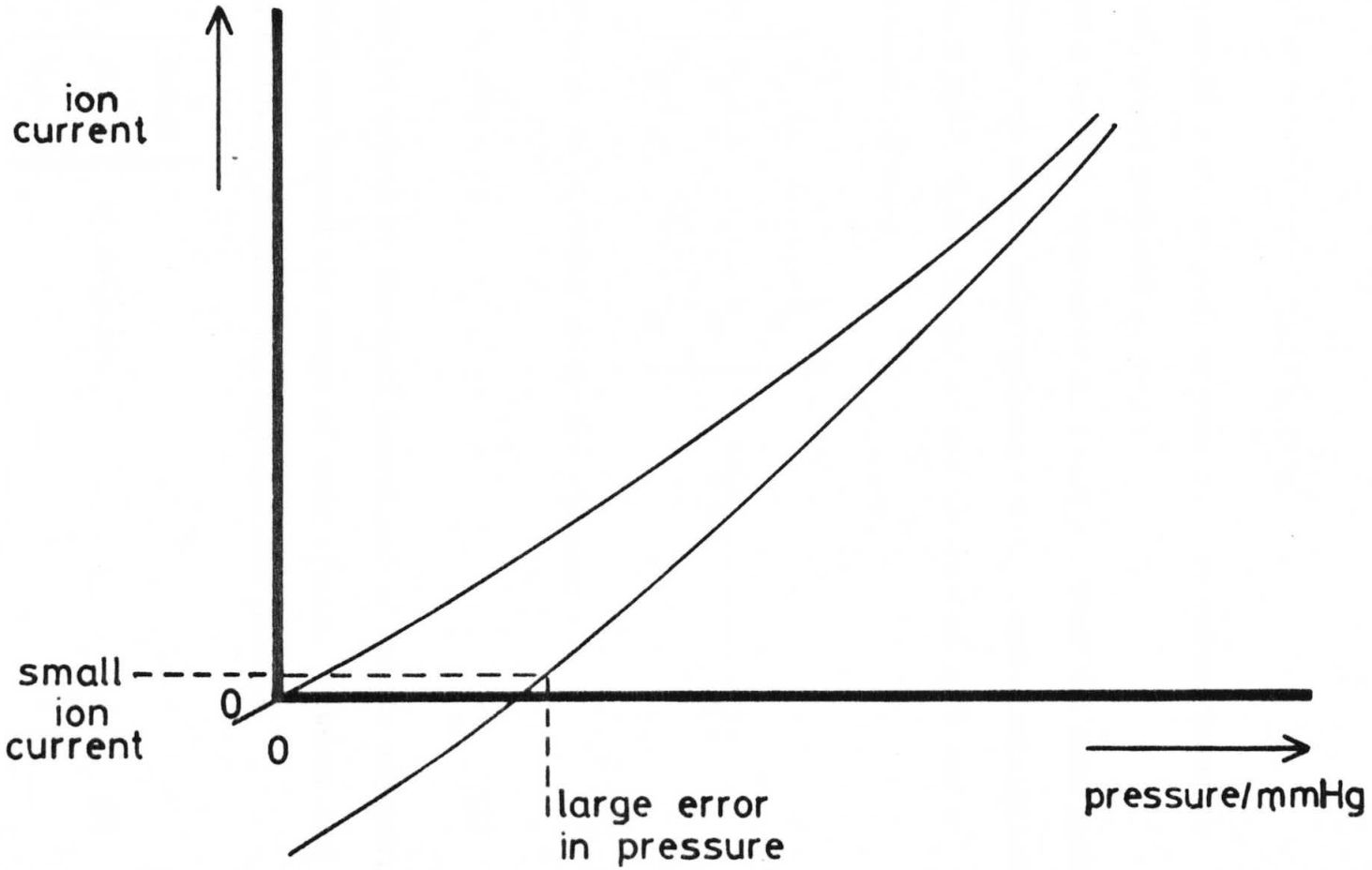

3.2 Computational analysis of reaction mixtures

The mass spectrum of a substance can be represented as a one dimensional matrix containing the intensities of the positively charged fragments of the substance, summed at each particular unit mass number, i.e.

$$(i_1, i_2, i_3, \ldots\ldots\ldots\ldots, i_{m-2}, i_{m-1}, i_m)$$

where i_x is the intensity of the peak at mass x. The values taken by the intensities are either positive or zero.

Let a mixture m contain components a, b and c. Then the mass spectrum of m will be a simple sum of the mass spectra of a, b and c multiplied by coefficients A, B and C which depend on the amounts of a, b and c present in the mixture. Thus

$$(A,B,C) \begin{pmatrix} a_1, a_2, \ldots\ldots, a_m \\ b_1, b_2, \ldots\ldots, b_m \\ c_1, c_2, \ldots\ldots, c_m \end{pmatrix} = (m_1 m_2, \ldots\ldots, m_m)$$

which can be written as an equation in matrix algebra:

$$(X)(x) = (m) \quad . \tag{1}$$

This expression can be solved by standard techniques of matrix algebra, the details of which are beyond the scope of this thesis. However the essentials are as follows. Consider the hypothetical problem

$$(X,Y,Z) \begin{pmatrix} a,b,c \\ d,e,f \\ g,h,i \end{pmatrix} = (r,s,t) \quad . \tag{2}$$

A matrix (Q) can be found such that

$$(Q)\begin{pmatrix} a,b,c \\ d,e,f \\ g,h,i \end{pmatrix} = \begin{pmatrix} a,b,c \\ o,e,f \\ o,o,i \end{pmatrix}$$

(Q) is applied to both sides of equation (2) thus

$$(Q)\ (r,s,t) = (r',s',t')$$

and so

$$(X,Y,Z)\begin{pmatrix} a,b,c \\ o,e,f \\ o,o,i \end{pmatrix} = (r',s',t') \quad . \qquad (3)$$

It follows immediately from (3) that

$$Xa = r'$$

$$Xb + Ye = s'$$

$$Xc + Yf + Zi = t'$$

and hence X, Y and Z are solved. The matrix (Q) is called a Householder transformation and its effect is to produce the so-called upper right triangular matrix

$$\begin{pmatrix} a,b,c \\ o,e,f \\ o,o,i \end{pmatrix} \quad .$$

This method of solution is general and thus applicable to the problem in mass spectrometric form, equation (1). The matrices (m) and (x) are known; (m) contains the mass spectrum of the mixture and (x) contains the standard mass spectra of the possible component boranes. (X) is the solution matrix sought. Fuller treatment of the mathematics can be found in reference [75].

All the calculations were performed using a suite of computer programs developed originally by Dr. T.C. Gibb of the Department of Inorganic and Structural Chemistry for Derek Taylorson and Dr. T. Spalding who were the original workers on this project. The programs have been altered to suit the requirements of the experimental method developed since that time, see section 2.4.3.

The addition of the computerized data-acquisition system to the mass spectrometer allowed the development of a direct line between the data-acquisition computer (Data General Nova III) and the University's mainframe (Amdahl VM/470) on which the analysis programs ran. Software was written for the Nova III enabling it to transmit data directly to the Amdahl for subsequent analysis. Assistance with the development of the direct line software was given by Mr. Peter Halford-Maw of the Department of Physical Chemistry who wrote the assembler sections. The addition of the direct line to the data-acquisition system permitted a vast increase in the amount of data which could be generated and processed compared to the original and laborious method of measuring individual peak heights manually and entering the data into the Amdahl through a terminal.

In essence the Nova III produces the mass spectrum of a mixture in tabular form, which it then transmits through the direct line to the Amdahl. There the table is edited and the mass spectrum is resolved into its components and their partial pressures.

The matrix algebra is performed in the calculations by another NAG Library routine, F04AMA, which gives the least mean square solution matrix (X) in the expression

$$(X)(x) = (m)$$

which was derived earlier in this section. The method of solution employed by the routine is essentially that of reducing matrix (x) to upper right

triangular form as described earlier, but it produces an approximate solution which it refines by a least-squares method and repeated correction until full machine accuracy is obtained.

The program is flexible in the way in which it solves the composition of the mixtures. The manner of solution is determined by the operator, who selects the "mass cut-offs" to be used in the solution. Mass cut-offs are unit mass numbers between which the least mean squares solution is obtained. For instance, if the mass cut-offs supplied by the operator are 10 and 124 then the solution is calculated in one pass of the routine over the mass range 10-124 for all specified components. Alternatively the operator may specify mass cut-offs 10, 76 and 124. In this case the solution is obtained between the two higher cut-offs, i.e. 76-124. Of course the composition given by this solution will have a contribution to the spectrum in the range 10-76. This calculated contribution is subtracted from the mixture spectrum in the range 10-76, followed by a reapplication of the routine to obtain the least mean squares solution in that region of the spectrum. The real composition of the mixture is then given by the sum of the compositions obtained for the two parts of the spectrum. In practice the mass cut-offs are used in such a way as to cause the contribution to the mixture spectrum from the heaviest component to be "stripped" out, followed by the next heaviest component and so on.

Each method (the single-pass or stripping method) has its advantages and disadvantages depending on the composition of the mixture to be analyzed. The single-pass method was used most frequently in this work, where most of the mixtures were fairly simply composed of hexaborane(10) as the major component and decaborane(14) and pentaborane(9) as minor components (hydrogen does not affect the solution for the boranes). The second method was found to give essentially identical solutions.

The solution returned by routine F04AMA does not contain the partial pressures of the components in the mixture but rather gives the spectrum of the mixture broken down into the standard mass spectra of its components and their abundances, i.e. matrix (X) in the expression

$$(X)(x) = (m) \quad .$$

The standard spectra of the components are not the same as the calibration curves of the components. The calibration curves give the relationship between the total ion current produced in the spectrometer and the pressure of the component in the reaction vessel, section 3.1. The total ion current is an extensive property of the substance under consideration but the standard spectrum is an intensive property of the substance. The standard spectra are recorded on the spectrometer under conditions identical to those used for mixture analysis and are all collected in a file on the Amdahl called MASTER DATA to which the analysis programs have access. The fraction of the total ion current of the mixture due to each component is thus accessible and is converted to an absolute ion current due to each component. Another NAG Library routine, E02AEA, then converts these ion currents to partial pressures using the Chebyshev polynomials calculated for each component, described in section 3.1. Figure 3.5 summarizes the operation of the analytical programs. A detailed description of the software used in this work is beyond the scope of this thesis but the programs are available for inspection from Dr. R. Greatrex.

3.3 Experimental accuracy

A thesis such as this, in which heavy reliance has been placed on the measurement of physical quantities, cannot purport to be complete without some declaration by the author of his confidence in the data.

Generally speaking, hydrogen data (obtained with the MS10) showed

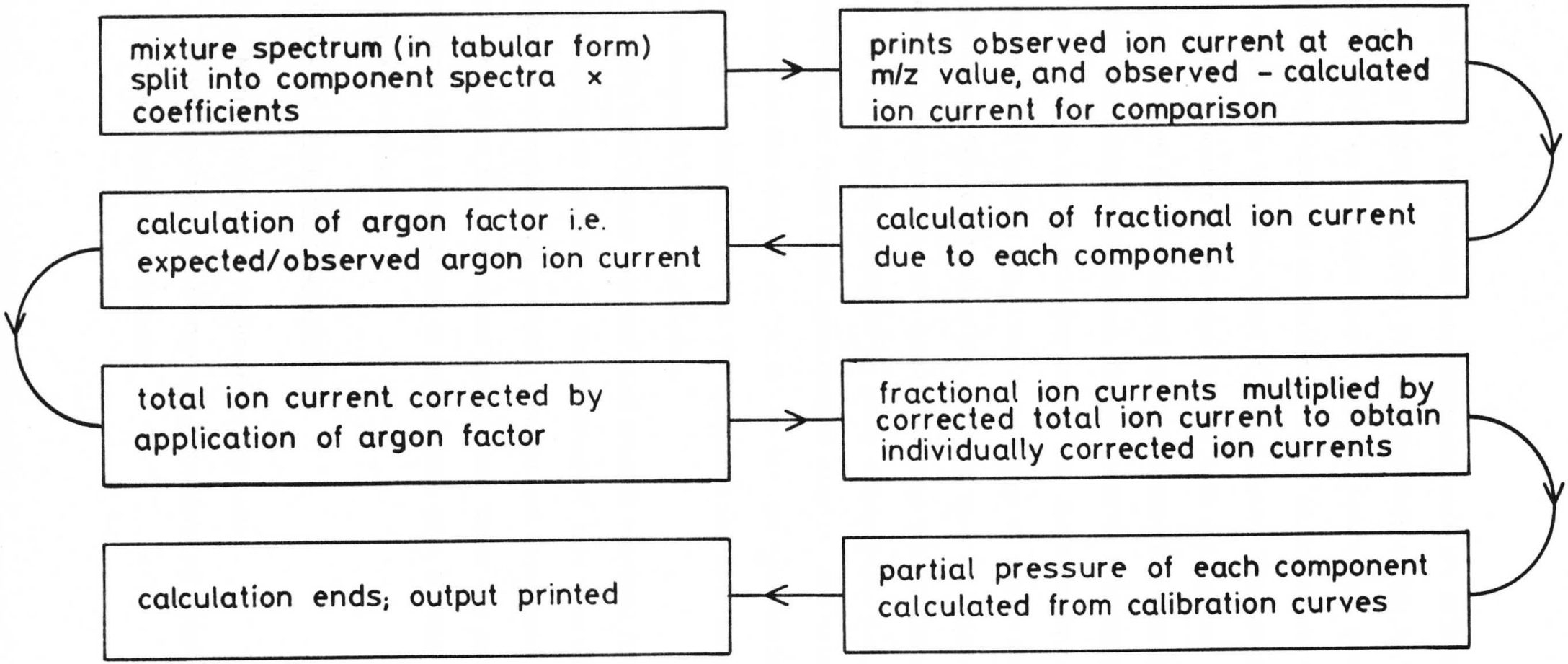

Figure 3.5. Scheme of operation of analysis programs

less scatter than borane data (obtained with the MS3074). This was extremely irritating given the relative cost of the two machines but was unavoidable as the major source of this problem was probably the deleterious effect of the boranes on the source of the MS3074. Within this context there were two types of borane data. The first type occurred in perhaps a quarter of the experiments; this data showed far too much scatter to be useful, leaving only hydrogen data from which to evaluate those particular experiments. The poorness of this type of borane data was assumed to be due to malfunctions of the spectrometer, e.g. an electron source about to burn out. The second type of borane data displayed less scatter and was usable from the point of view of attempting to calculate mixture compositions. The quality of this type of data usually decreased in the experiments conducted at lower temperature, i.e. at high temperatures, reaction was rapid hence spectrometer samples were taken at short intervals, minimizing the chances of 'drift' in the spectrometer electronics, whereas at lower temperatures, when the reactions may have taken more than ten days, the chance of 'drift' increased.

The best borane data was thus usually obtained from the faster reactions. An estimate of the accuracy of this data can be made by taking into consideration the possible sources and magnitudes of the errors at all stages of the measurement procedure. These are presented here in the sequence they occur during an experiment, with a brief explanation of how they were estimated.

Source of Error/*Brief Explanation*	Estimated Magnitude
1. Mixing reaction mixtures in vacuum line *From knowledge of volumes and comparison of final with calculated pressures*	<2%

Source of Error/*Brief Explanation (continued)*	Estimated Magnitude
2. Viscous flow into spectrometer *From calculations in section 2.4.3 and Figure 2.15.*	5%
3. Errors inherent in standard spectra *Complex effect depending on composition of mixture.*	---
4. Error caused by routine FO4AMA *Many more equations than unknowns means problem is overdetermined.*	probably negligible
5. Error inherent in argon calibration curve *From scatter of points about fitted curve.*	5%
6. Error inherent in borane calibration curve *From scatter of points about fitted curve.*	5%

These errors can be combined to give an estimate of the overall error in the final borane pressures returned by the computer programs after analysis. Assuming randomness in the errors the overall error can be estimated as the square root of the sum of the squares of the component errors, thus

$$\text{overall error} = \sqrt{2^2 + 5^2 + 5^2 + 5^2}$$

$$\approx 9\%$$

This estimate of the overall error compares well with the error observed between the calculated intial hexaborane(10) pressure and the expected hexaborane(10) pressure for the well behaved activation energy experiments. The observed discrepancy was $\sim$10%.

CHAPTER 4

Results

4.1 Initial observations

An examination of the gas phase thermolysis of hexaborane(10) was undertaken using the equipment and techniques described in the preceding chapter. The overall qualitative features were quickly established.

At the initial temperature and pressures of hexaborane(10) used (393 K and ∿1-10 mmHg respectively) the reaction was extremely slow, hexaborane(10) still being observed in the mass spectrum of the mixture after about two weeks (∿20,000 minutes). At 348 K no reaction was discernible after 24 hours.

The initial work was carried out, as stated, at 393 K and at this temperature the hexaborane(10) slowly disappeared while a pressure of hydrogen built up in the reaction vessel. The only other species observed in the gas phase were pentaborane(9) and decaborane(14) both of which appeared gradually and to a small extent as the reaction proceeded. In later experiments in which the spectrometer was operated at very high sensitivity settings, other species were observed and these will be discussed later in the chapter. At this early stage, estimates of the partial pressures of the pentaborane(9) and decaborane(14) suggested that they did not account for more than 10% of the hexaborane(10) consumed. On the other hand, the amount of hydrogen generated was comparable to the hexaborane(10) loss throughout the reactions. When the oven was dismantled to reveal the glass reaction vessel after experiments, a thin film was always observed on the inside surface of the vessel. It was believed that this film accounted for approximately 90% of the boron content of the hexaborane(10), though at this stage nothing was known of the nature of the film, except that it was completely involatile.

These then were the gross characteristics of the gas phase thermolysis of hexaborane(10). The remainder of this chapter describes the detailed quantitative work on the system, and in Chapter 5 the results will be discussed with reference to other related work.

4.2 Investigation of reaction order

The first aspect of the gas phase thermolysis of hexaborane(10) to be tackled in detail was that of the dependence of the rate of reaction on the concentration of hexaborane(10). The form of this dependence would lead to the order of the reaction.

Given the generalized reaction

$$aA + bB + cC \ldots \longrightarrow nN + oO + pP \ldots$$

(where A, B, C ... are reactants with a, b, c ... their stoichiometric coeffcients and N, O, P ... are products with n, o, p ... their coefficients) then the rate of the reaction can be expressed as the rate of change of concentration of the products and reactants thus:

$$-\frac{1}{a}\frac{d[A]}{dt} = -\frac{1}{b}\frac{d[B]}{dt} = -\frac{1}{c}\frac{d[C]}{dt} \ldots$$

$$= \frac{1}{n}\frac{d[N]}{dt} = \frac{1}{o}\frac{d[O]}{dt} = \frac{1}{p}\frac{d[P]}{dt} \ldots$$

When the concentrations of reactants are varied, the rate of reaction usually changes according to some well defined function of the reactant concentration. If doubling the concentration of a reactant doubles the rate of reaction then

$$-\frac{1}{a}\frac{d[A]}{dt} = k[A]$$

where k is the rate constant, and the reaction is said to be first order with respect to the concentration of A. Similarly, if doubling the concentration causes the reaction rate to be quadrupled then

$$-\frac{1}{a}\frac{d[A]}{dt} = k[A]^2$$

and the reaction is second order in A. If changing the concentration has no effect then the reaction is zero order in A. The order of a reaction is a consequence of its mechanism so a full knowledge of the reaction mechanism enables the order of reaction to be predicted. However, knowledge of the reaction order does not of itself permit prediction of the mechanism, but is one of the most powerful pieces of evidence required in attempting to establish the mechanism.

The order of reaction of hexaborane(10) thermolysis in the gas phase was investigated by following the reaction at a fixed temprature (393 K) over a range of hexaborane(10) concentrations. The only reactant was hexaborane(10) and the major products were gaseous hydrogen and a solid film deposited on the wall of the reaction vessel. Several other minor products will be discussed later in this chapter. The reaction was followed by observing the disappearance of hexaborane(10) and the appearance of hydrogen. Figures 4.1-4.8 show plots of the hexaborane(10) and hydrogen pressures versus time for the eight experiments in this series. The experiments were named PYR, 2PYR, 3PYR, 4PYR, 5PYR, 6PYR, 7PYR and 8PYR. The data are shown graphically in Figures 4.1-4.8 and also tabulated in Appendix B, Tables B.1-B.8.

Having followed the thermolysis of hexaborane(10) at several different starting pressures the order of the reaction was then established. If the order of a reaction is unknown then:

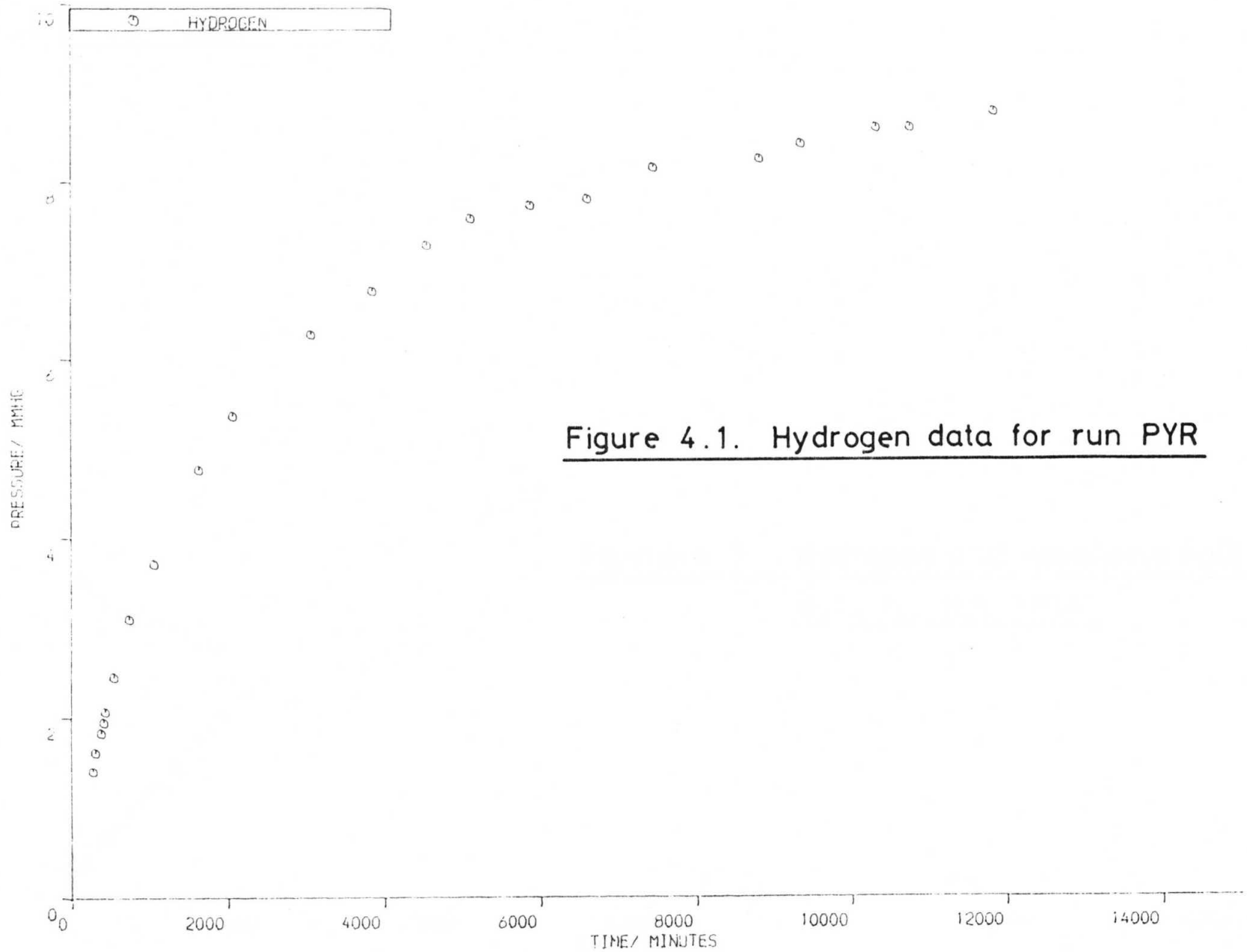

Figure 4.1. Hydrogen data for run PYR

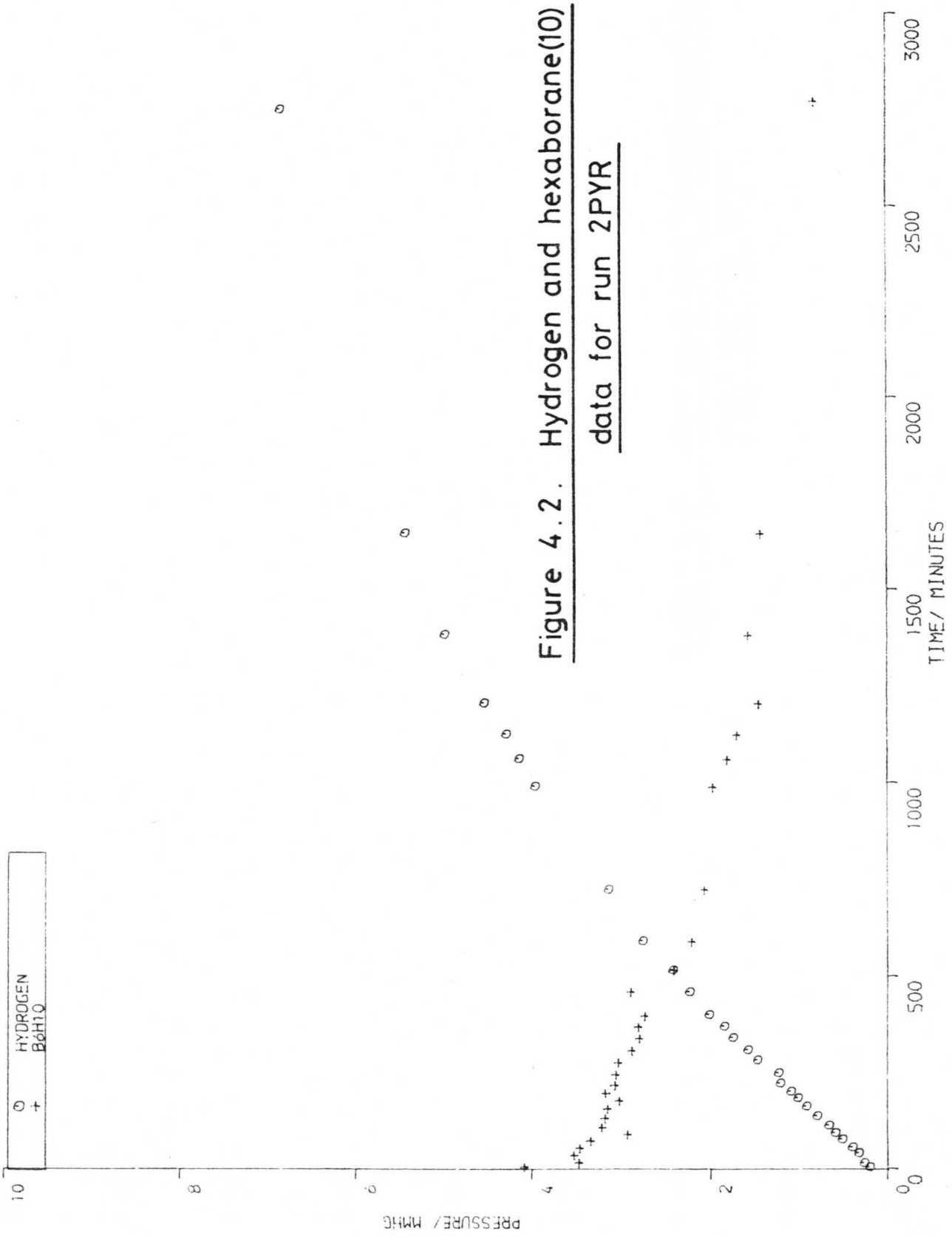

Figure 4.2. Hydrogen and hexaborane(10) data for run 2PYR

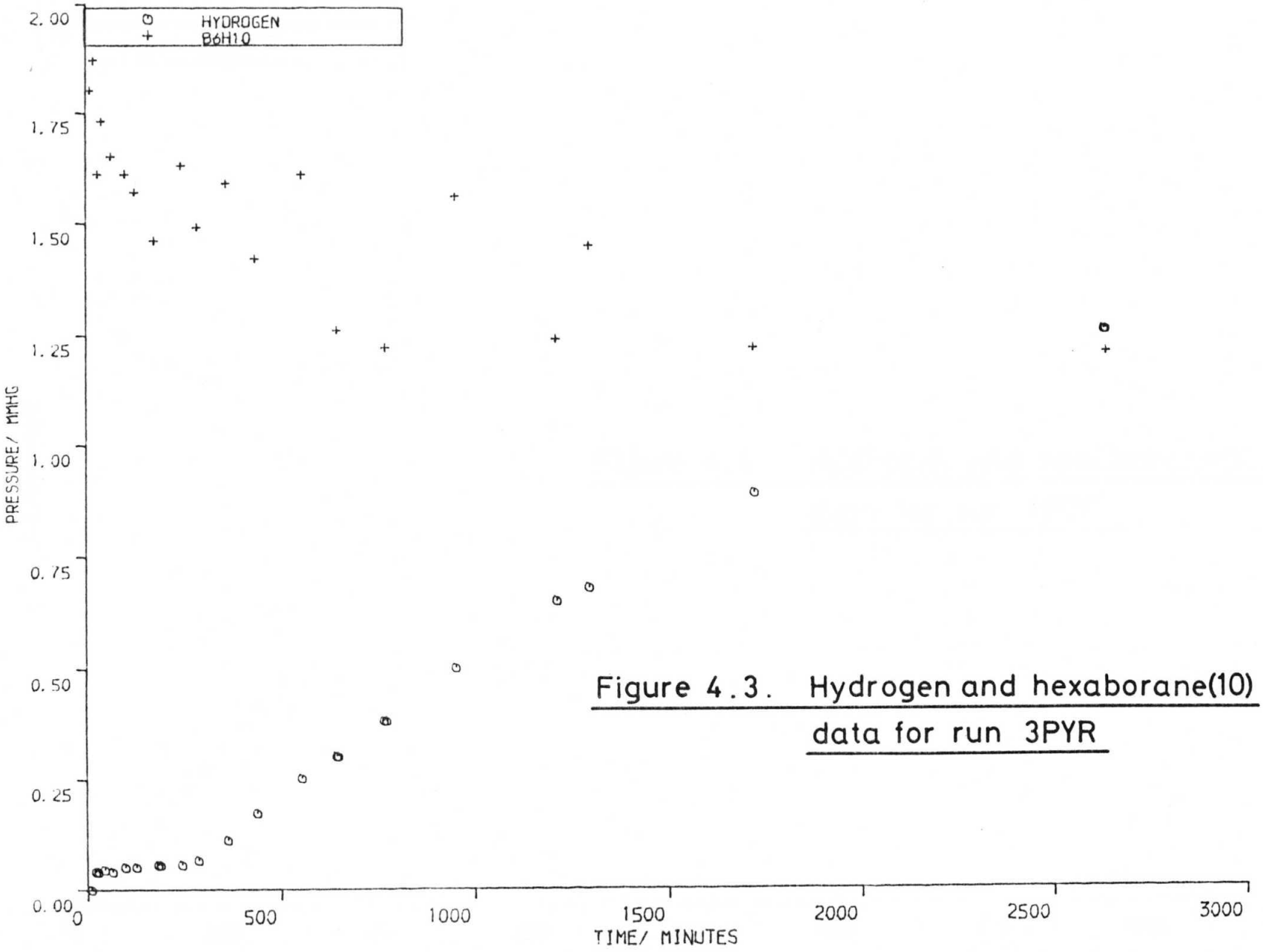

Figure 4.3. Hydrogen and hexaborane(10) data for run 3PYR

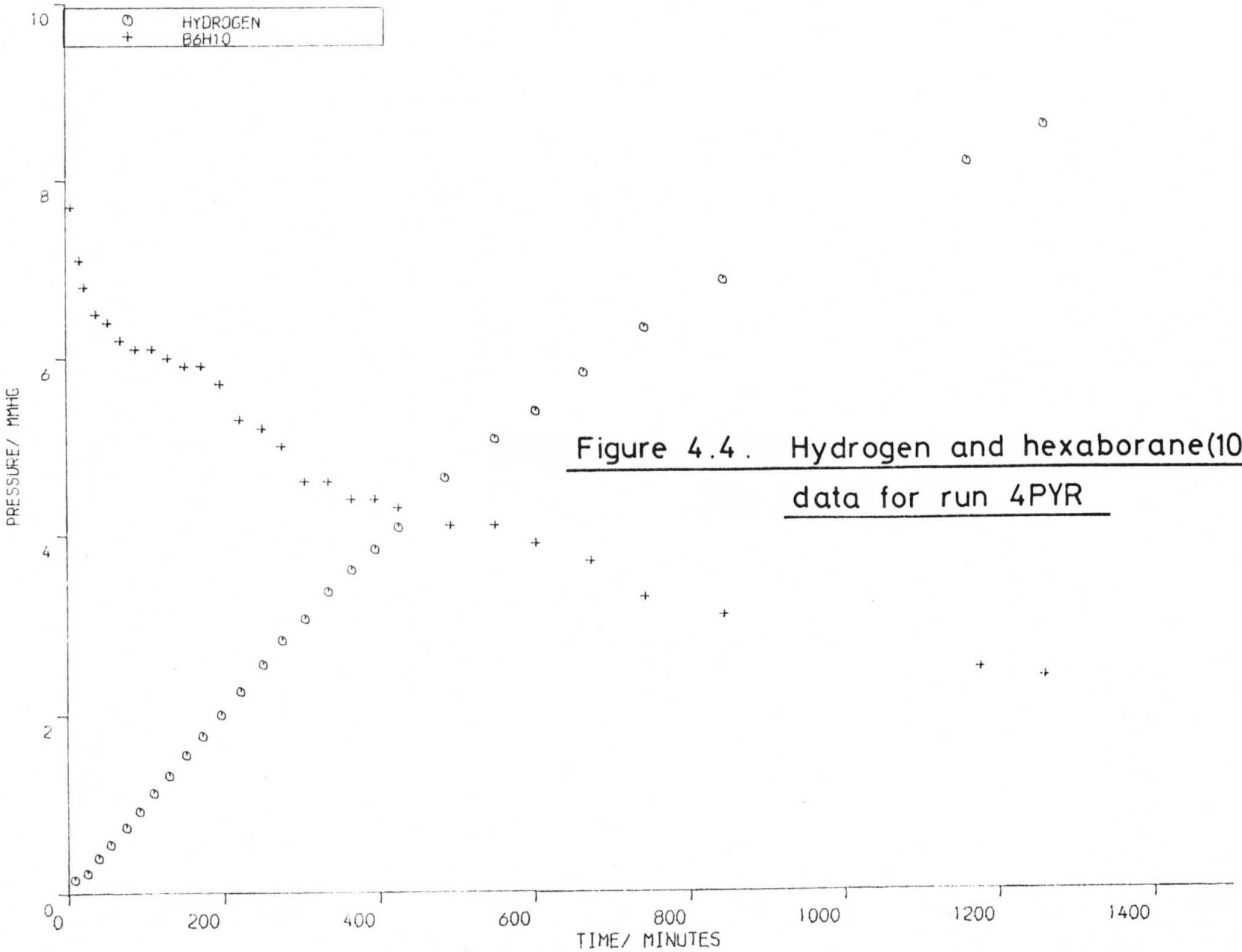

Figure 4.4. Hydrogen and hexaborane(10) data for run 4PYR

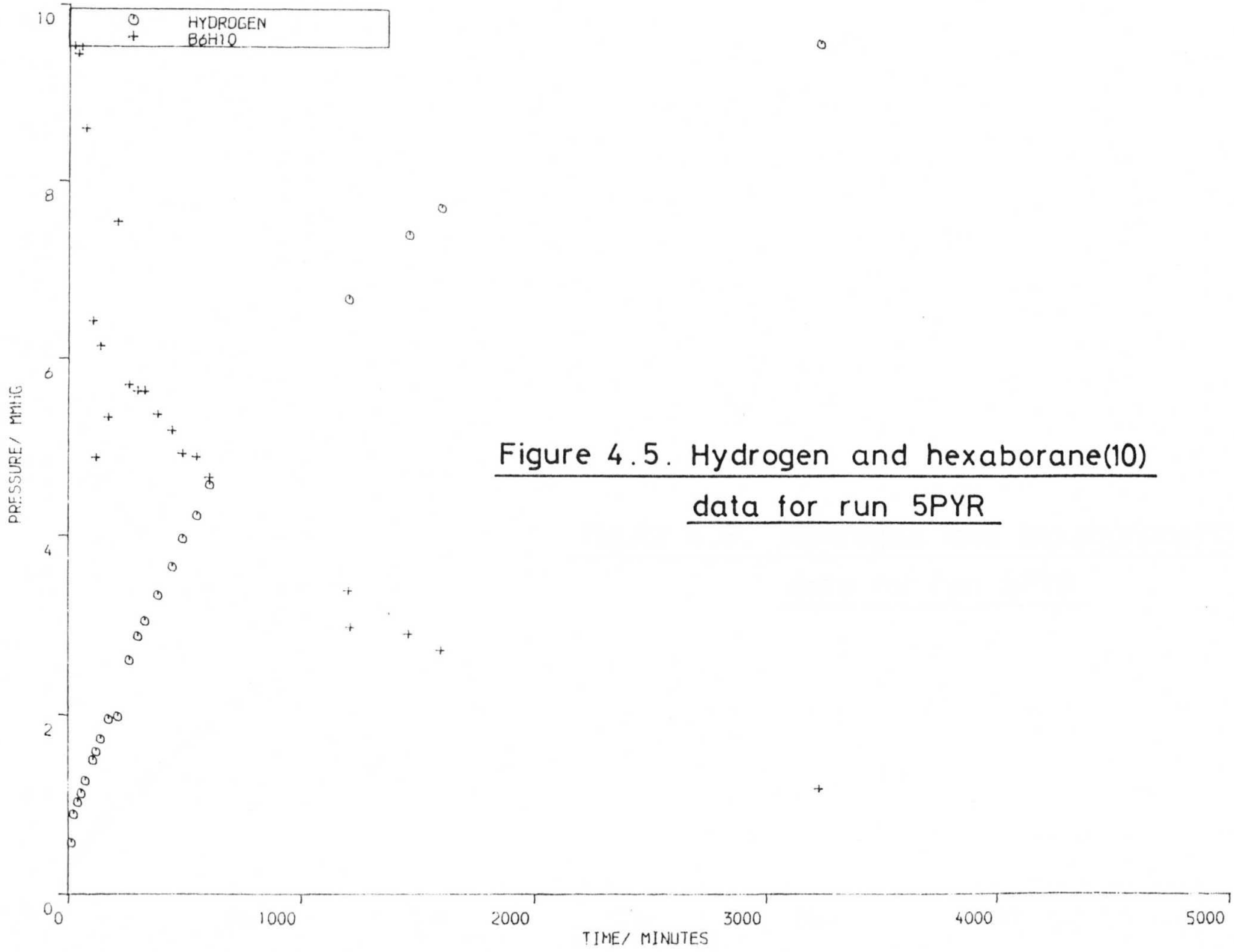

Figure 4.5. Hydrogen and hexaborane(10) data for run 5PYR

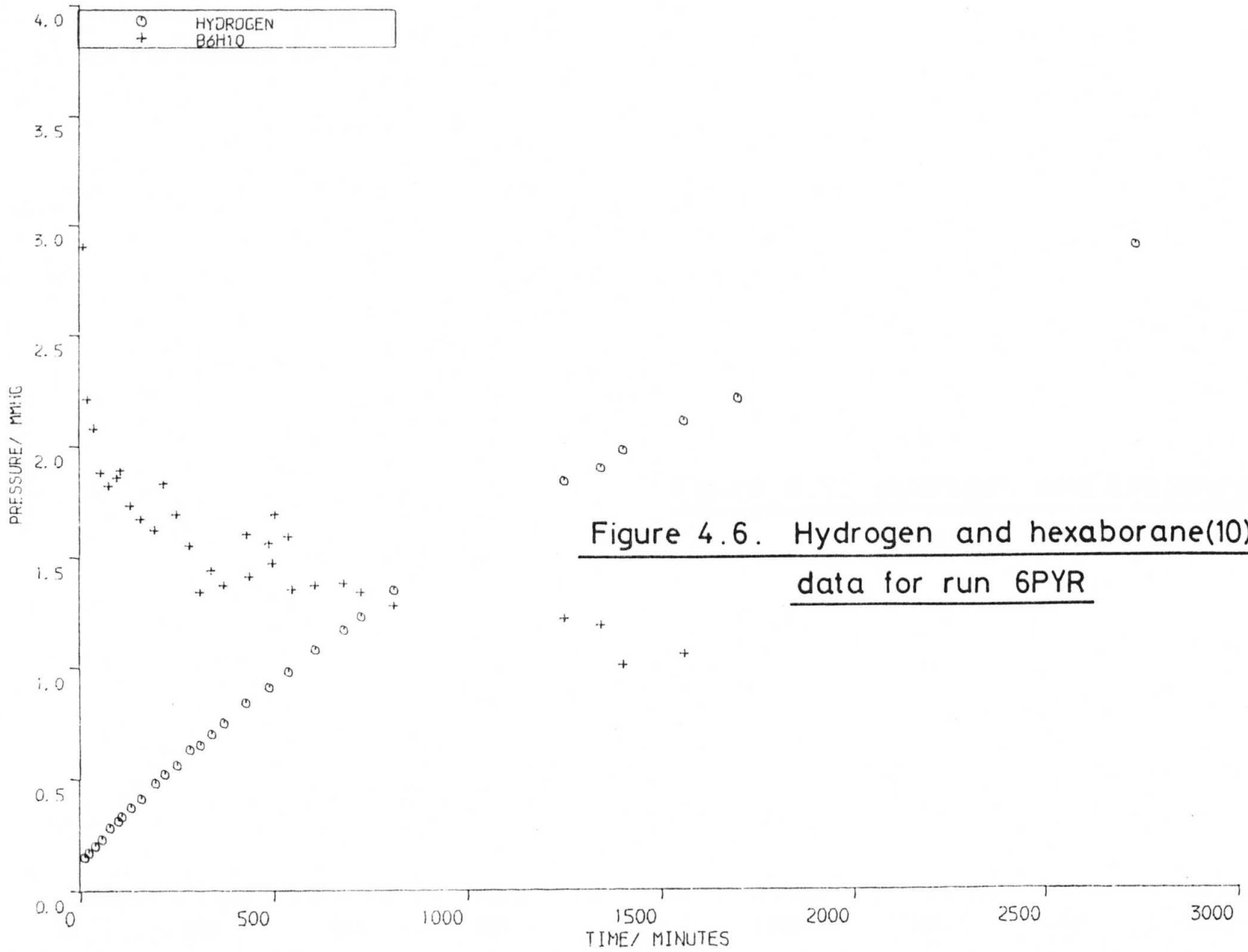

Figure 4.6. Hydrogen and hexaborane(10) data for run 6PYR

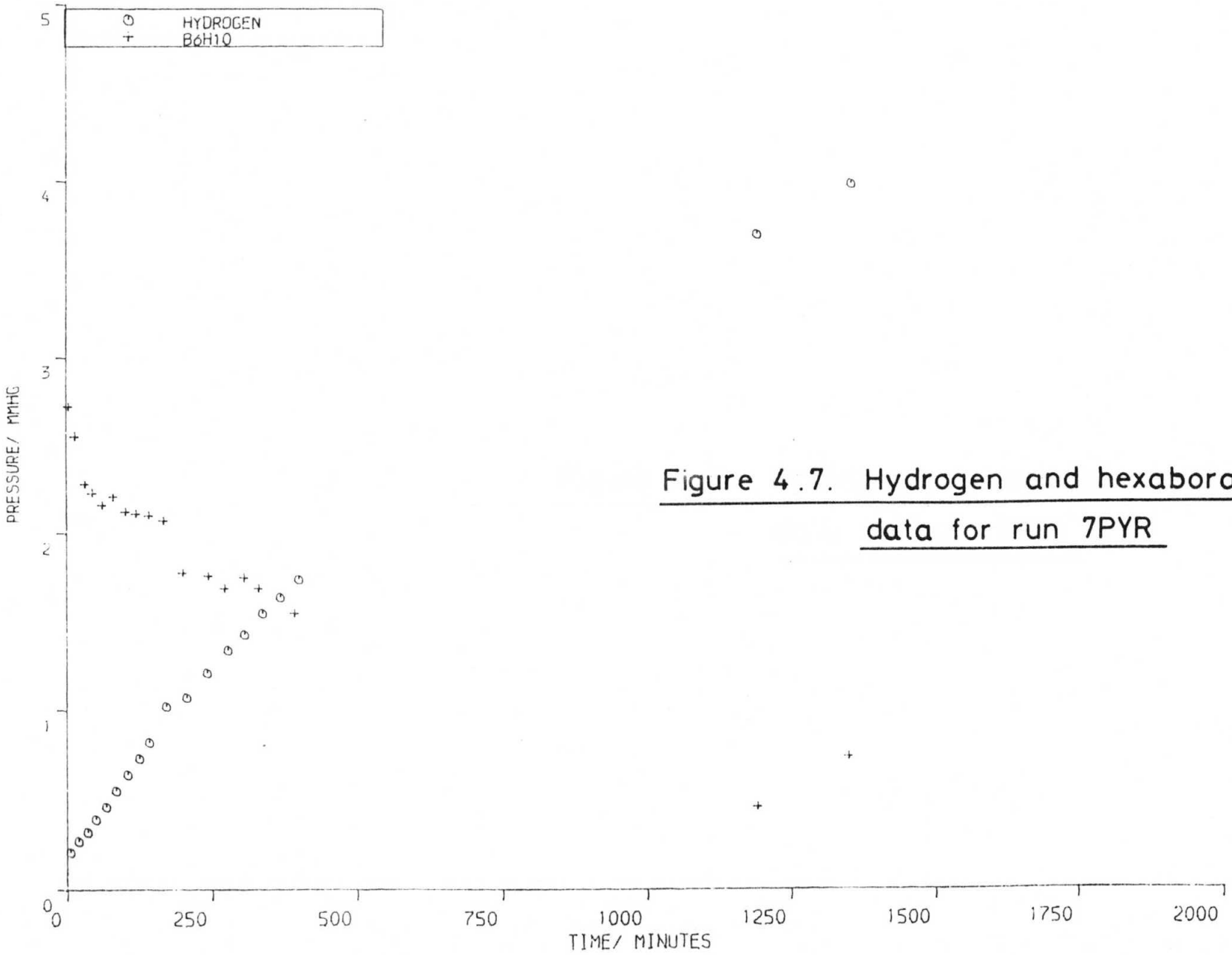

Figure 4.7. Hydrogen and hexaborane(10) data for run 7PYR

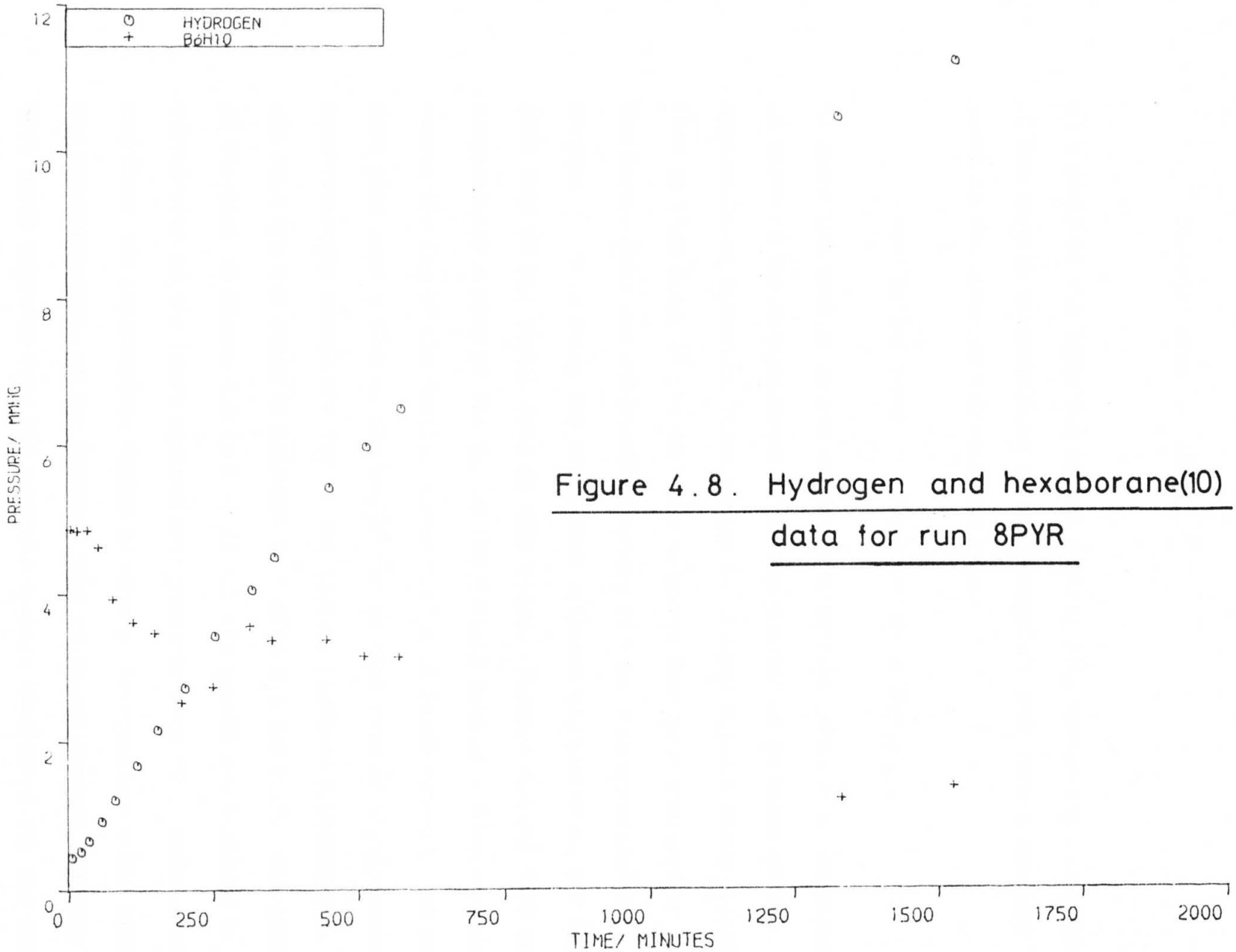

Figure 4.8. Hydrogen and hexaborane(10) data for run 8PYR

$$\text{initial rate} = k[B_6H_{10}]_o^x$$

so a graph of the logarithm of the initial rate versus the logarithm of the initial concentration of hexaborane(10) will have a gradient equal to the order of the reaction thus

$$\log(\text{initial rate}) = \log k + x \log[B_6H_{10}]_o \quad .$$

As mentioned earlier in the chapter the initial rate can be measured in terms of the disappearance of hexaborane(10) or in terms of the appearance of hydrogen. Examination of Figures 4.1-4.8 shows clearly that at this stage of the work the hydrogen data were much better than the borane data and the possible causes of this were discussed in Chapter 3. This being the case, more reliance was placed on the hydrogen data than on the borane data at this stage. Figures 4.9 and 4.10 show respectively a plot of the log of the initial rate of hydrogen production versus the log of the initial concentration of hexaborane(10) and the same plot with a plot of the log of the initial rate of disappearance of hexaborane(10) versus the log of its initial pressure superimposed. The data are tabulated in Appendix B, Tables B.9 and B.10. The gradient of the plot in Figure 4.9 is 1.71 if all the points are included in a calculation of the least squares best straight line fit. However after the first six experiments, during an attempt to recalibrate the system for hexaborane(10), it was observed that while calibration mixtures were being expanded into the reaction vessel, hexaborane(10) was seen to be condensing, both as a brief mist in the reaction vessel and as droplets, especially at the opening of the tap which sealed the mixing vessel. This was probably due to the fast (and therefore adiabatic) expansion against the resistance of the vacuum line causing cooling. Such condensation

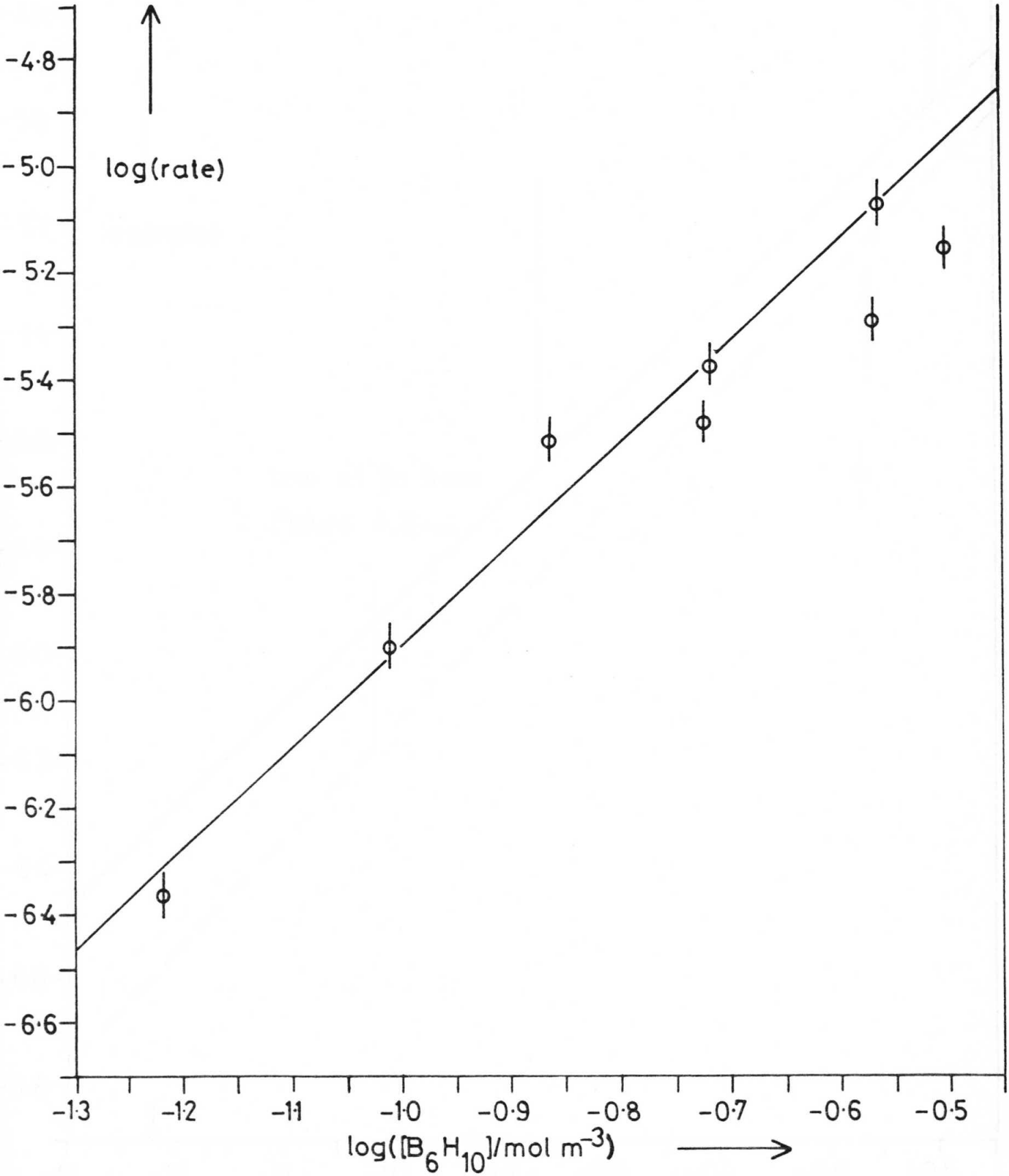

Figure 4.9. Order plot from hydrogen data, runs PYR - 8PYR

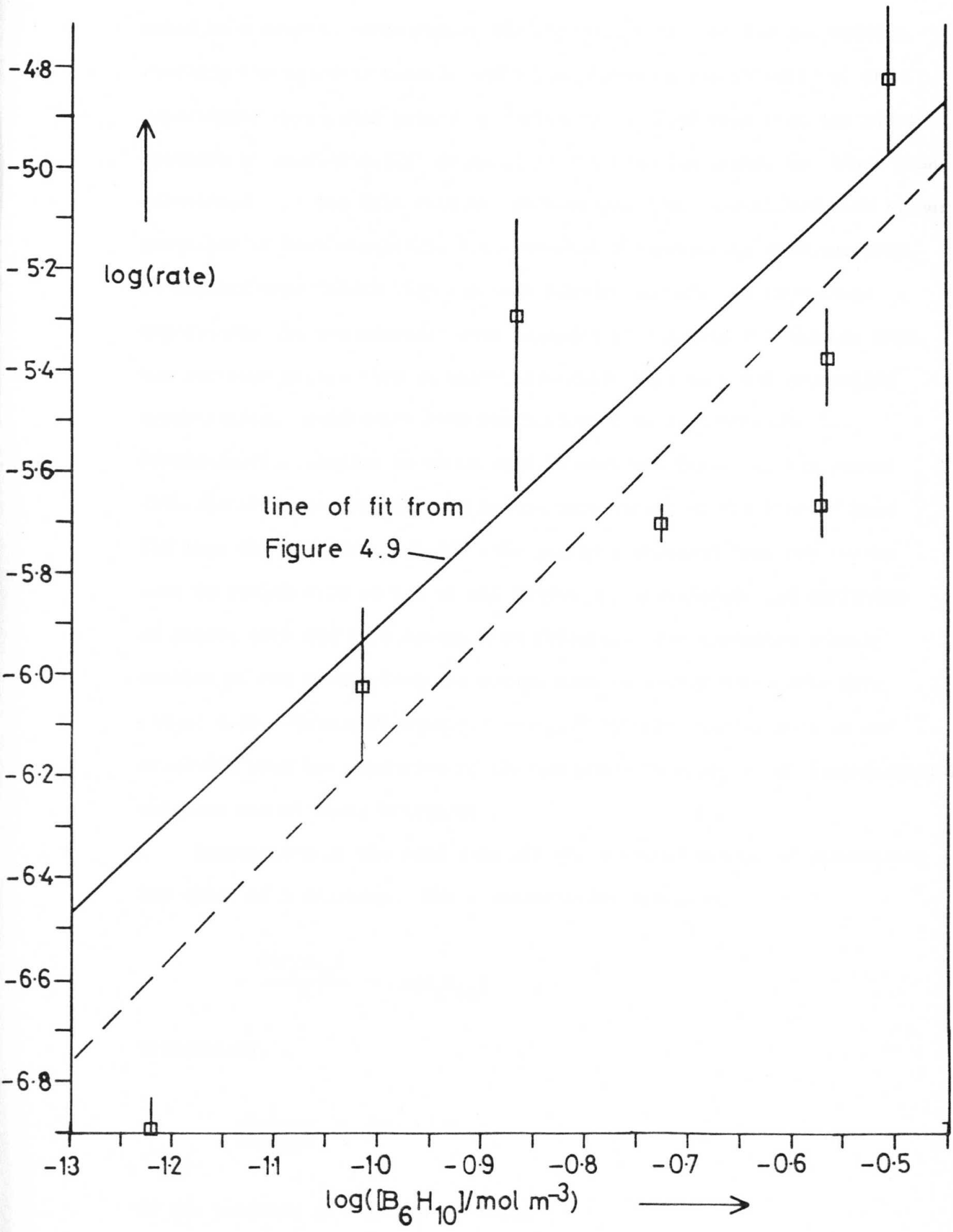

Figure 4.10. Order plot from hexaborane(10) data, runs PYR - 8PYR

would have drastic consequences for the homogeneity of the gas mixture reaching the reaction vessel, and throw doubts on the validity of the experiments up to that point; specifically it might mean that the final pressure of hexaborane(10) obtained in the reaction vessel was lower than calculated. It was felt that the problem would be exacerbated with higher pressures of hexaborane(10), i.e. especially experiments 4PYR and 5PYR, so further experiments 7PYR and 8PYR were performed. In both these experiments the gas mixtures were expanded very slowly (∿1 minute) into the reaction vessel thus allowing isothermal expansion and preventing condensation. Experiment 8PYR was performed using a pressure of hexaborane(10) similar to those used in 4PYR and 5PYR. If the points 4PYR and 5PYR are not included in the calculation of the line of best fit then the gradient is 1.89. The gradient obtained from the borane data in Figure 4.10 is 2.1 if all points are considered, and exclusion of points 4PYR and 5PYR raises this slightly. The generally greater scatter of the points from the borane data is easily noticeable from Figure 4.10. Taking Figures 4.9 and 4.10 jointly into account it was concluded that the mechanism of the gas phase thermolysis of hexaborane(10) exhibits second order kinetics.

Integration of the rate laws affords a second method of determining the order of a reaction. For a second order reaction:

$$-\frac{d[B_6H_{10}]}{dt} = k[B_6H_{10}]^2 \quad .$$

Integrating,

$$\frac{1}{[B_6H_{10}]} = kt + c \quad .$$

If the reaction is first order then:

$$-\frac{d[B_6H_{10}]}{dt} = k[B_6H_{10}]$$

and integrating gives

$$- \ln[B_6H_{10}] = kt + c \quad .$$

So a plot of the inverse of the reactant concentration versus time should be linear for a second order reaction, whereas a plot of the log of the reactant concentration versus time should be linear for a first order reaction. Product concentrations can be used if the stoichiometry is known. Plots of the inverse and logarithmic functions of the hexaborane(10) concentrations versus time are presented for experiments 2PYR, 4PYR and 5PYR in Figures 4.11-4.13 (and tabulated in Appendix B, Tables B.11-B.13). It must be borne in mind when using this type of plot that if a *first* order plot is made using data from a reaction which is actually *second* order then the amount of curvature obtained would not be severe and so this method works best when the data are very accurate. The three graphs presented demonstrate that the difference in curvature between first and second order plots for this data was very small, and so while not positively confirming second order kinetics, the data are consistent with that conclusion.

4.3 Activation energy

Before a molecule can react it must have a certain minimum amount of energy. In the absence of other forms of energy, such as electromagnetic radiation, it acquires this from the thermal energy of the surrounding molecules, during collisions. In a simple but powerful model, the rate of a reaction is thus determined by two factors; the number of collisions per second and the amount of energy required for reaction. In the simplest form of the model, the energy required for reaction can be measured as an overall activation energy by measuring the rate of a reaction at fixed reactant concentration over a range of temperatures and

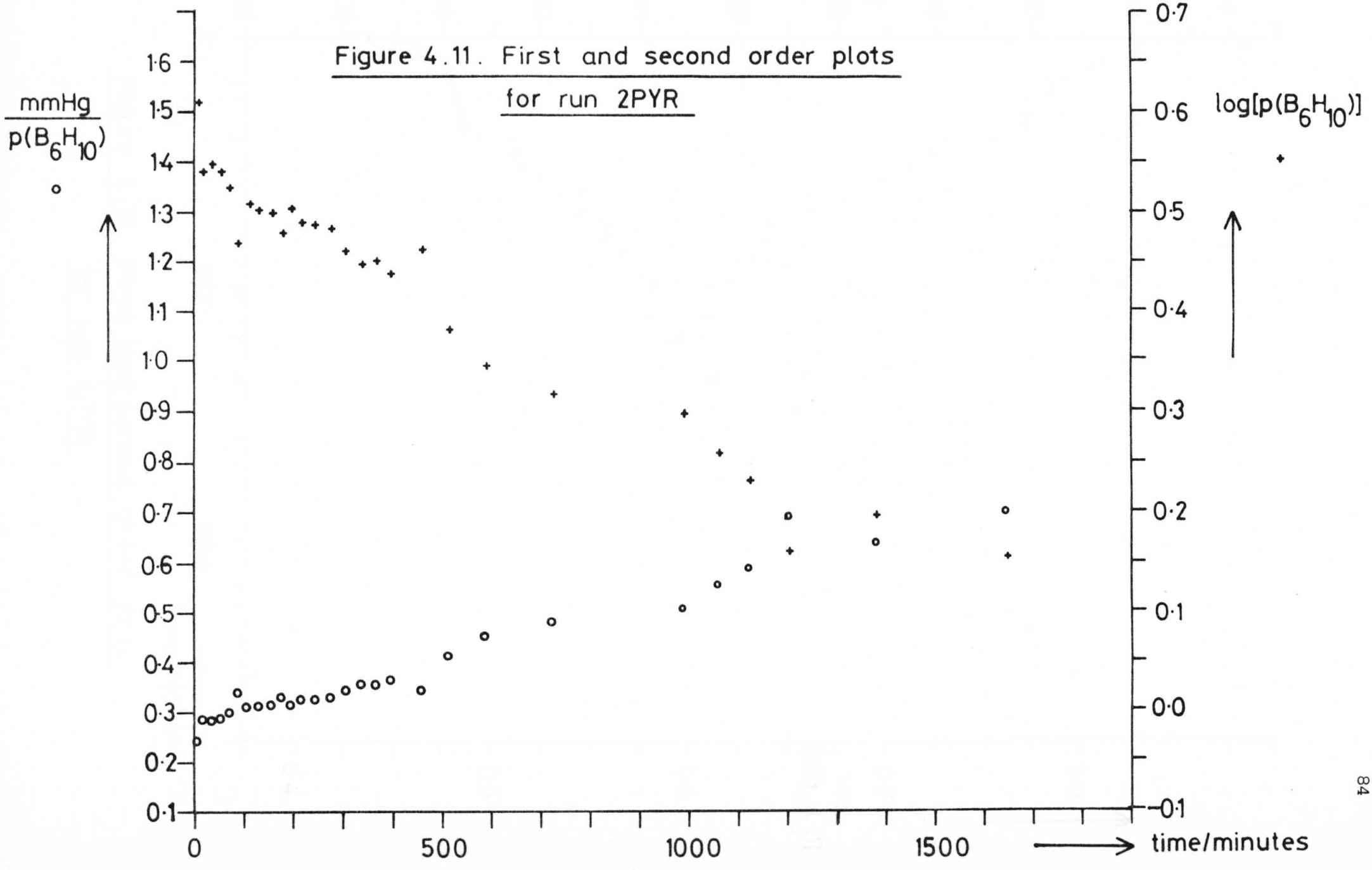

Figure 4.11. First and second order plots for run 2PYR

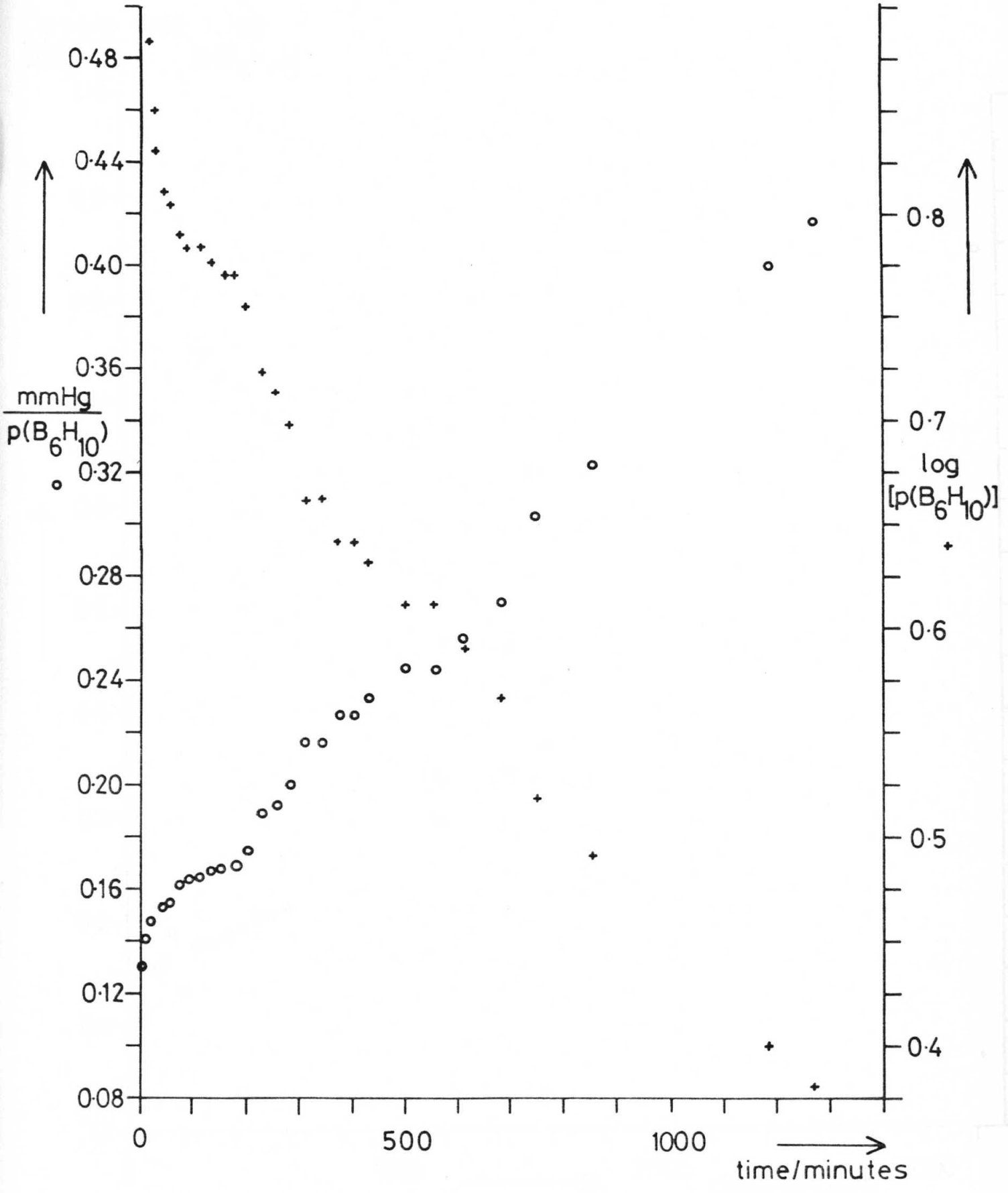

Figure 4.12. First and second order plots for run 4PYR

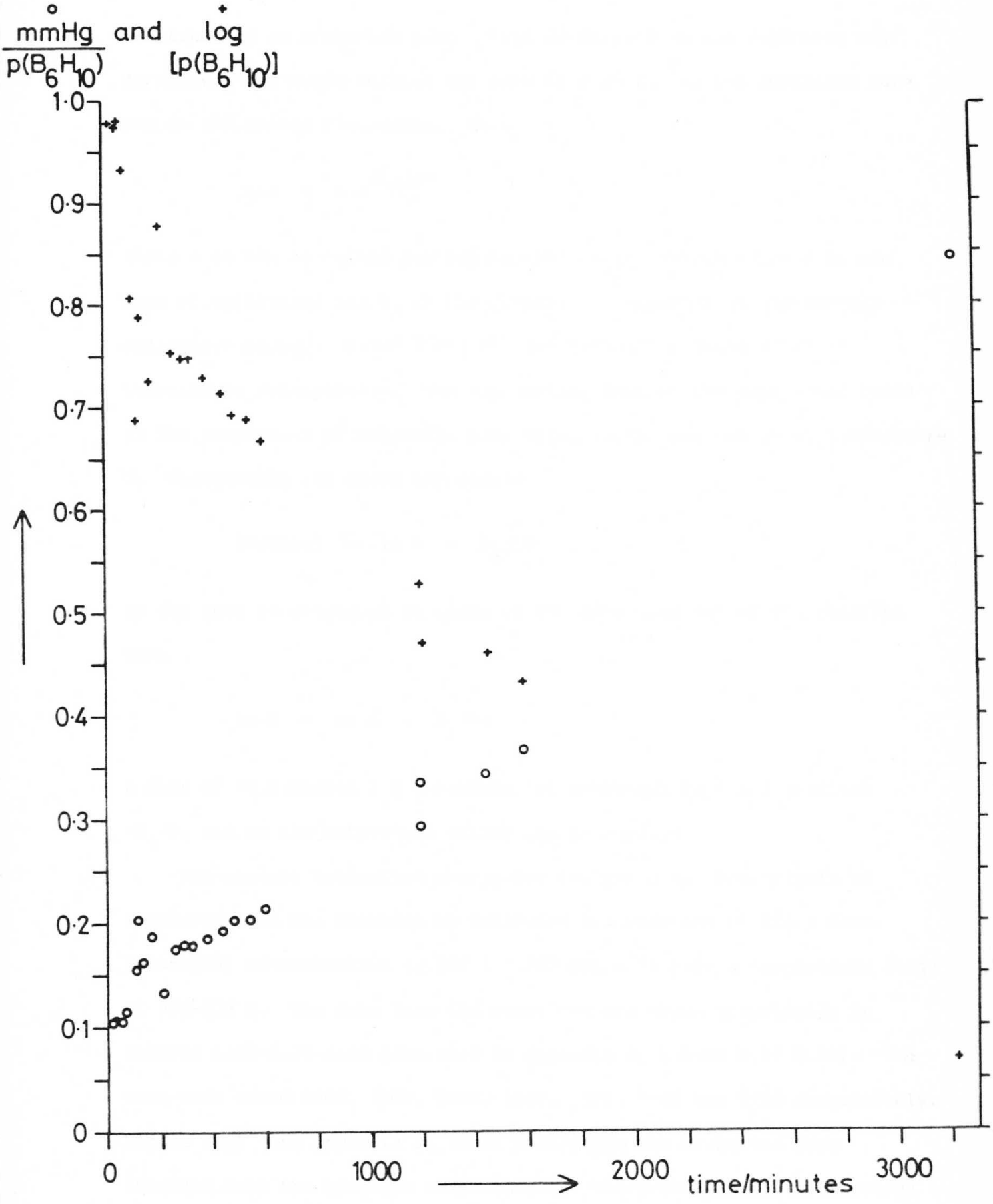

Figure 4.13. First and second order plots for run 5PYR

constructing an Arrhenius plot. This is derived in the following way. As stated, the model relates the rate of reaction to the collision rate and to the energy requirement, thus

$$\text{rate} = A\, e^{-E_a/RT}$$

where A is the so-called pre-exponential factor (which relates to the rate of collision) and E_a is the overall (or apparent, or Arrhenius) activation energy. R and T are the gas constant and the absolute temperature respectively. The exponential form of the expression leads to the proportion of molecules possessing sufficient energy at temperature T. Rearranging the above expression

$$\ln(\text{rate}) = \ln A - E_a/RT \quad .$$

If the rate is expressed in terms of the rate constant of the reaction then

$$\ln k = \ln A - E_a/RT \quad .$$

A plot of ln k versus 1/T therefore has intercept ln A and gradient $-E_a/R$, and so the activation energy can be derived.

The overall activation energy for the gas phase thermolysis of hexaborane(10) was measured by following the reaction at fixed hexaborane(10) concentration (0.134 ± 0.002 mol m^{-3}) over a temperature range of 373-438 K. The data from the reactions are shown graphically in Figures 4.14-4.20 (and tabulated in Appendix B, Tables B.14-B.20). The runs were named 4ACT, 3ACT, 9PYR, 1ACT, 2ACT, 1RB6 and 2RB6 respectively. Figure 4.21 (and Appendix B, Table B.21) shows the Arrhenius data obtained with the hydrogen measurements. The overall activation energy measured from the gradient of the curve is 78.7 ± 5 kJ mol^{-1}, and the pre-exponential factor is $e^{15.1 \pm 1.4}$ (3.5×10^6 M^3 mol^{-1} s^{-1}, best

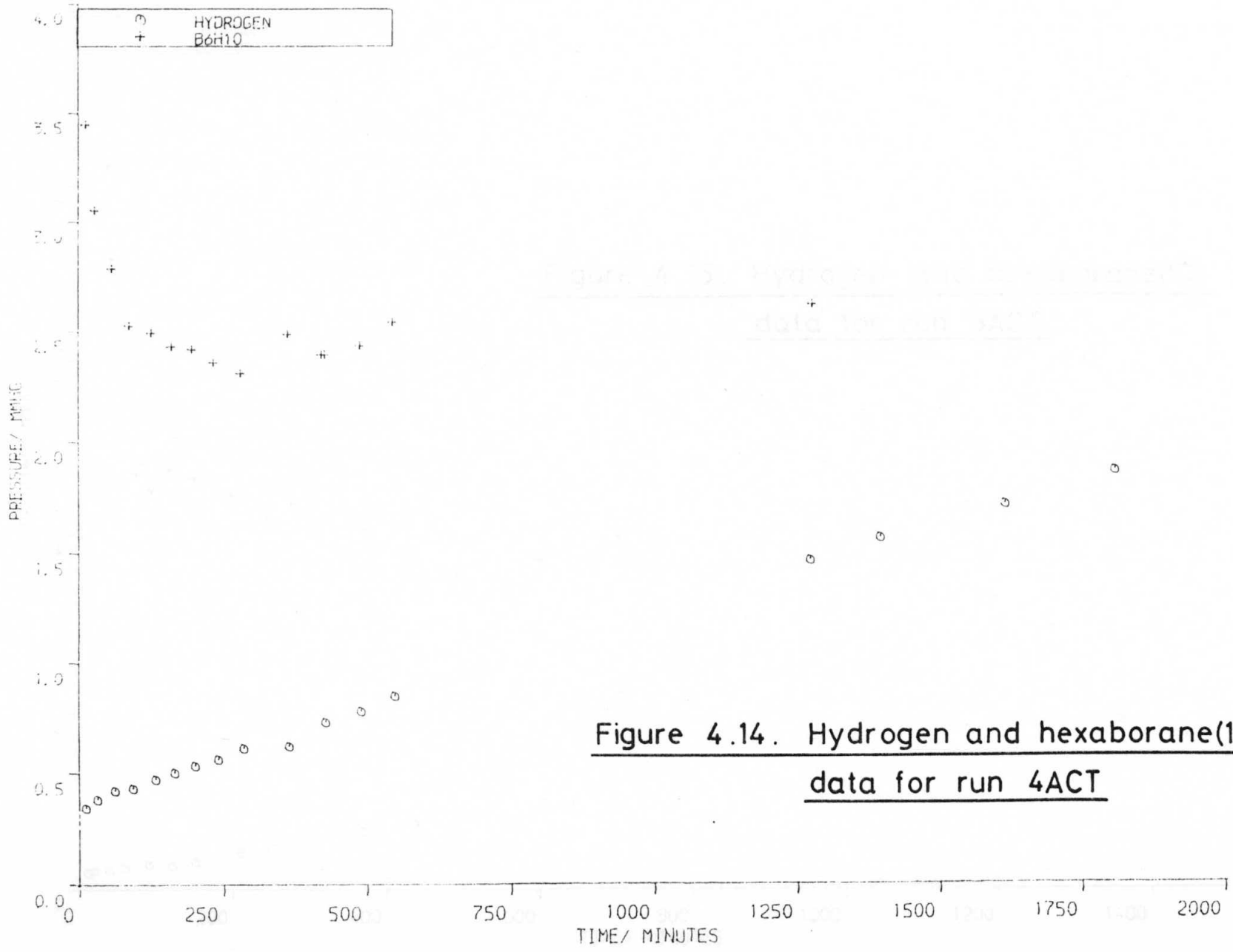

Figure 4.14. Hydrogen and hexaborane(10) data for run 4ACT

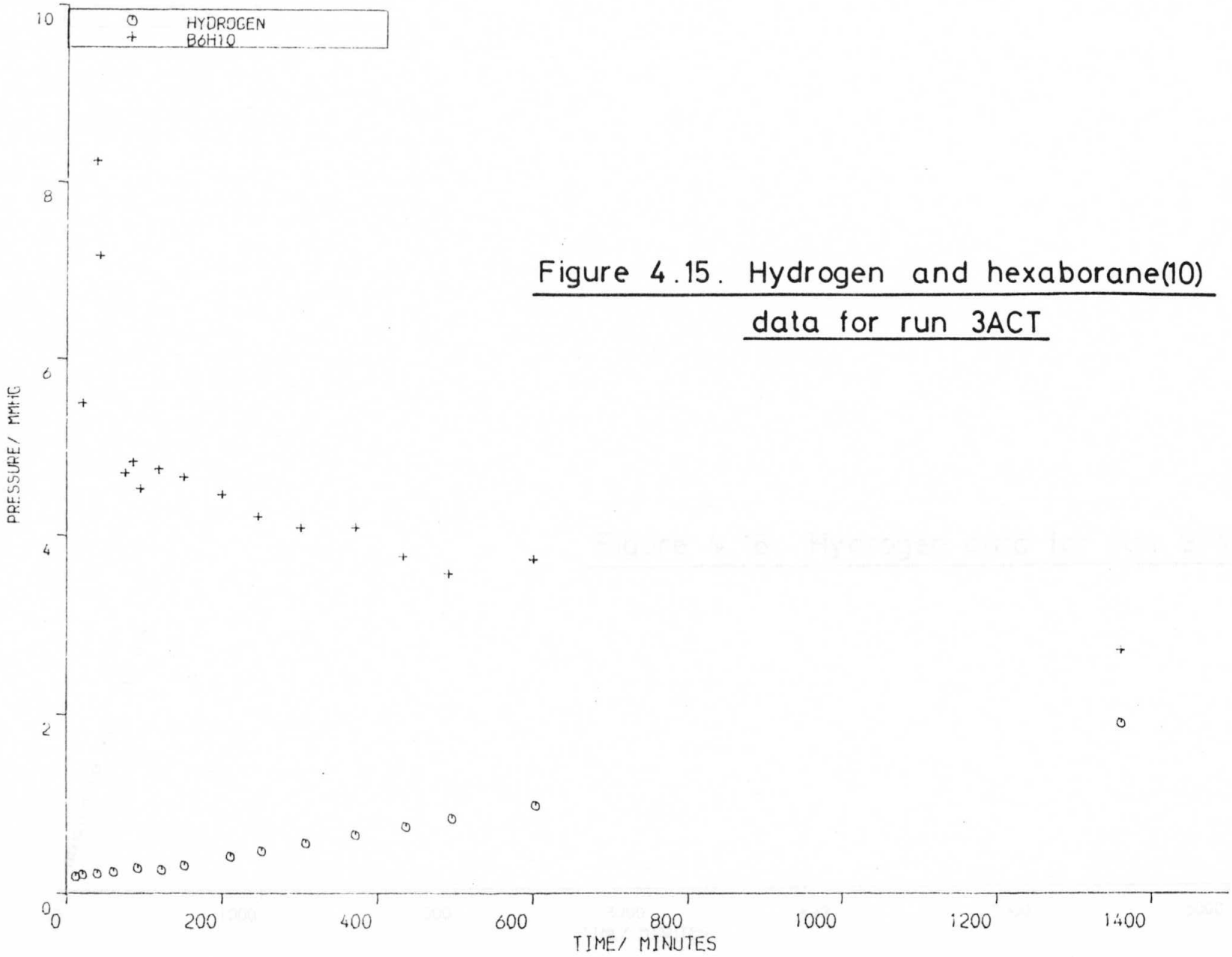

Figure 4.15. Hydrogen and hexaborane(10) data for run 3ACT

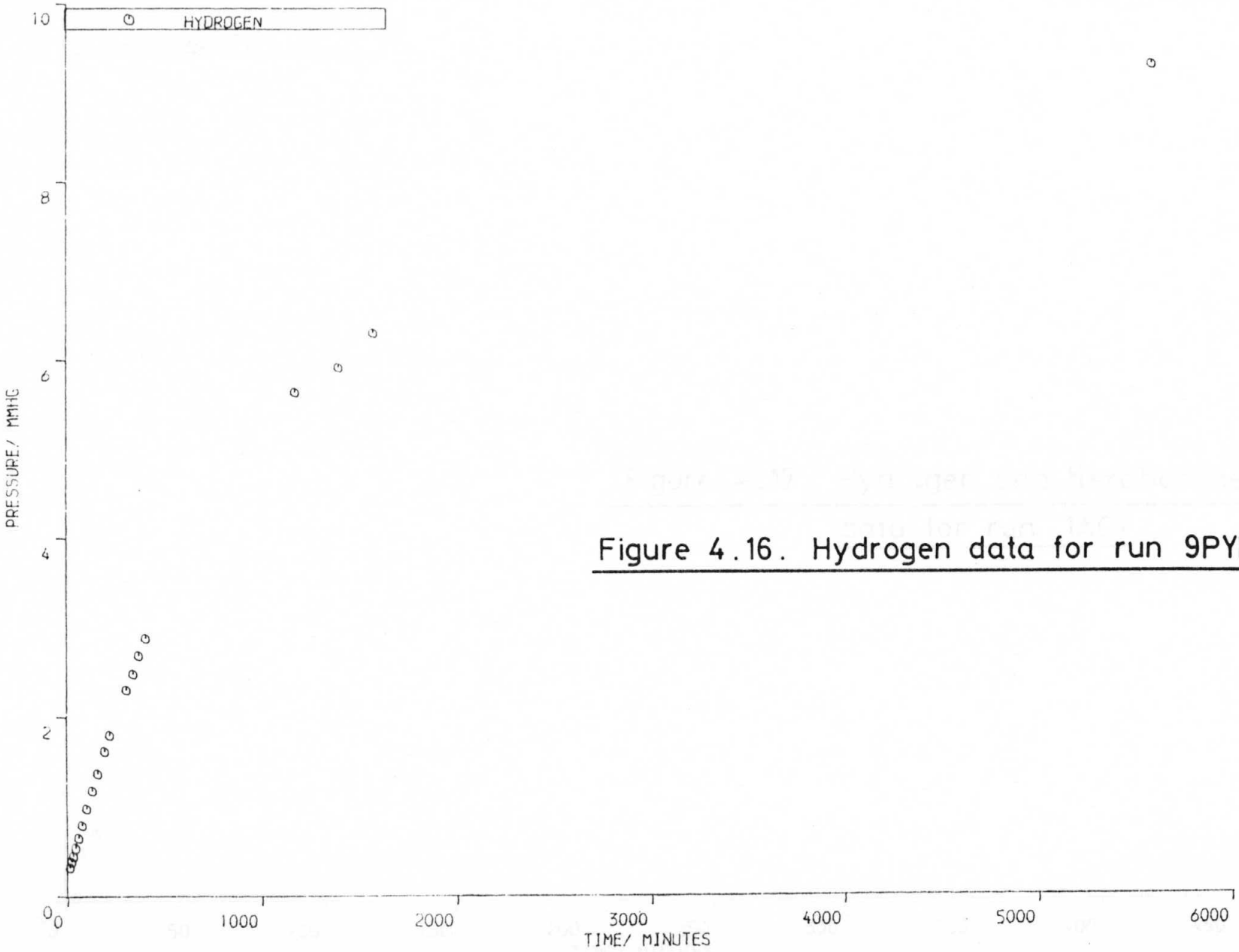

Figure 4.16. Hydrogen data for run 9PYR

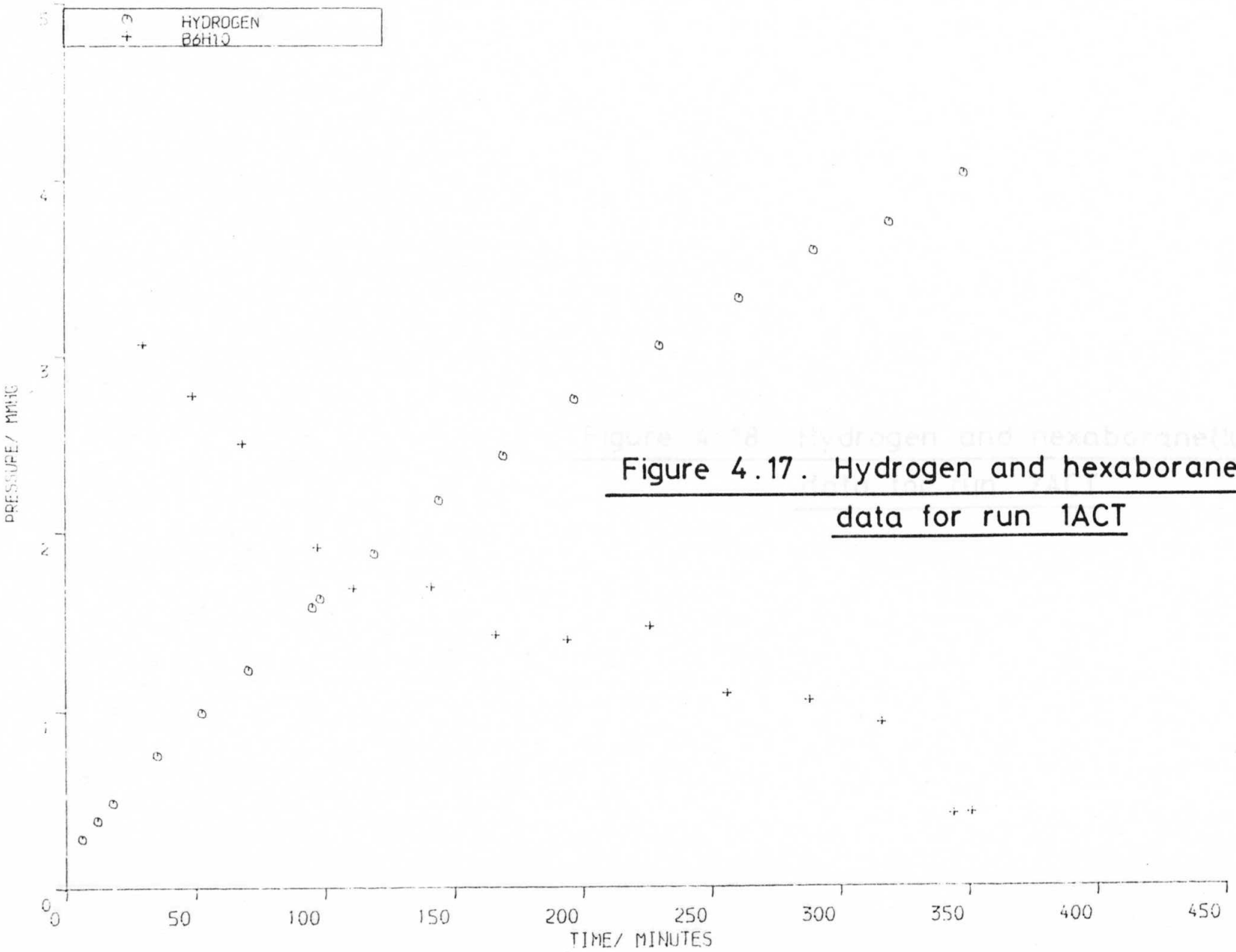

Figure 4.17. Hydrogen and hexaborane(10) data for run 1ACT

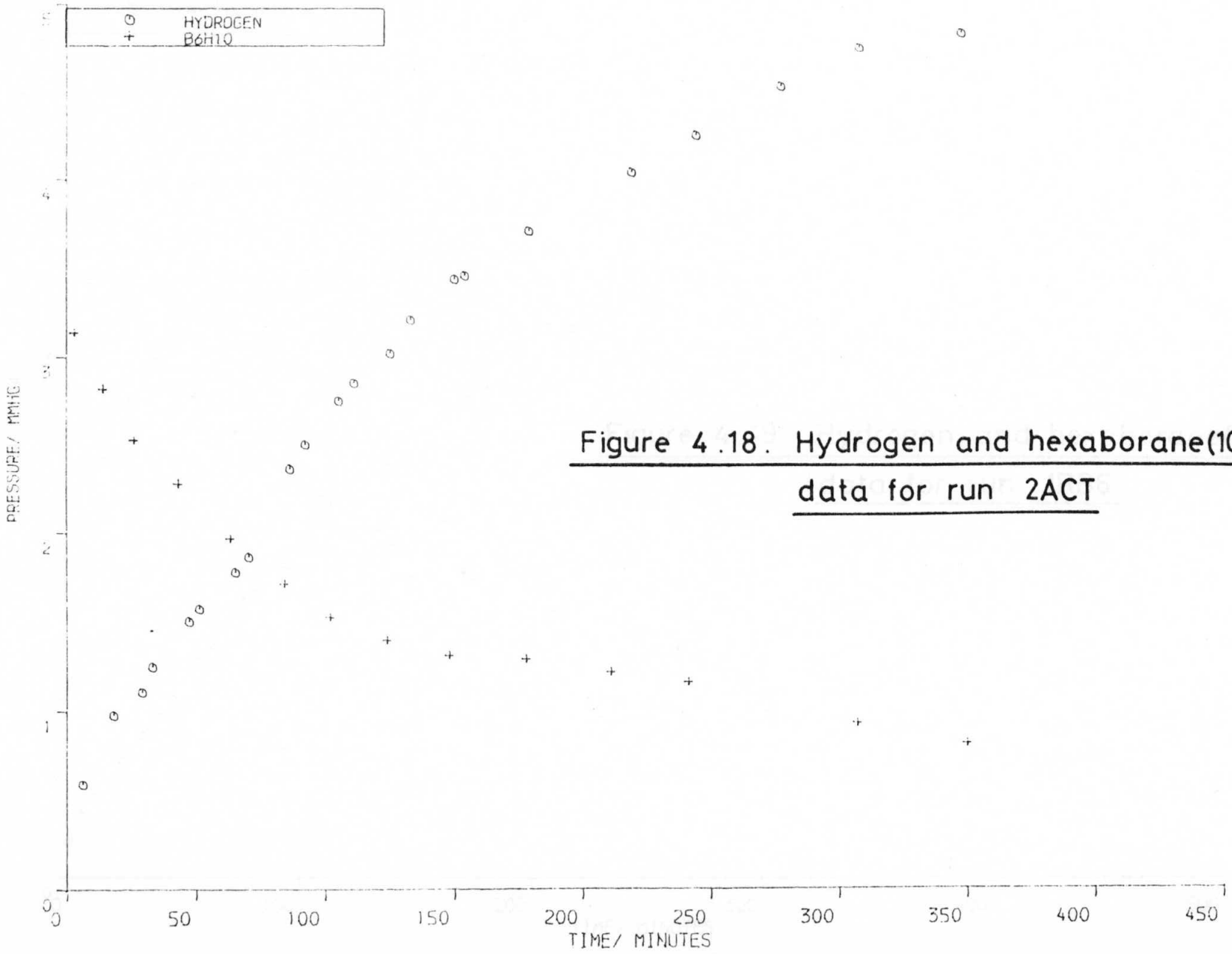

Figure 4.18. Hydrogen and hexaborane(10) data for run 2ACT

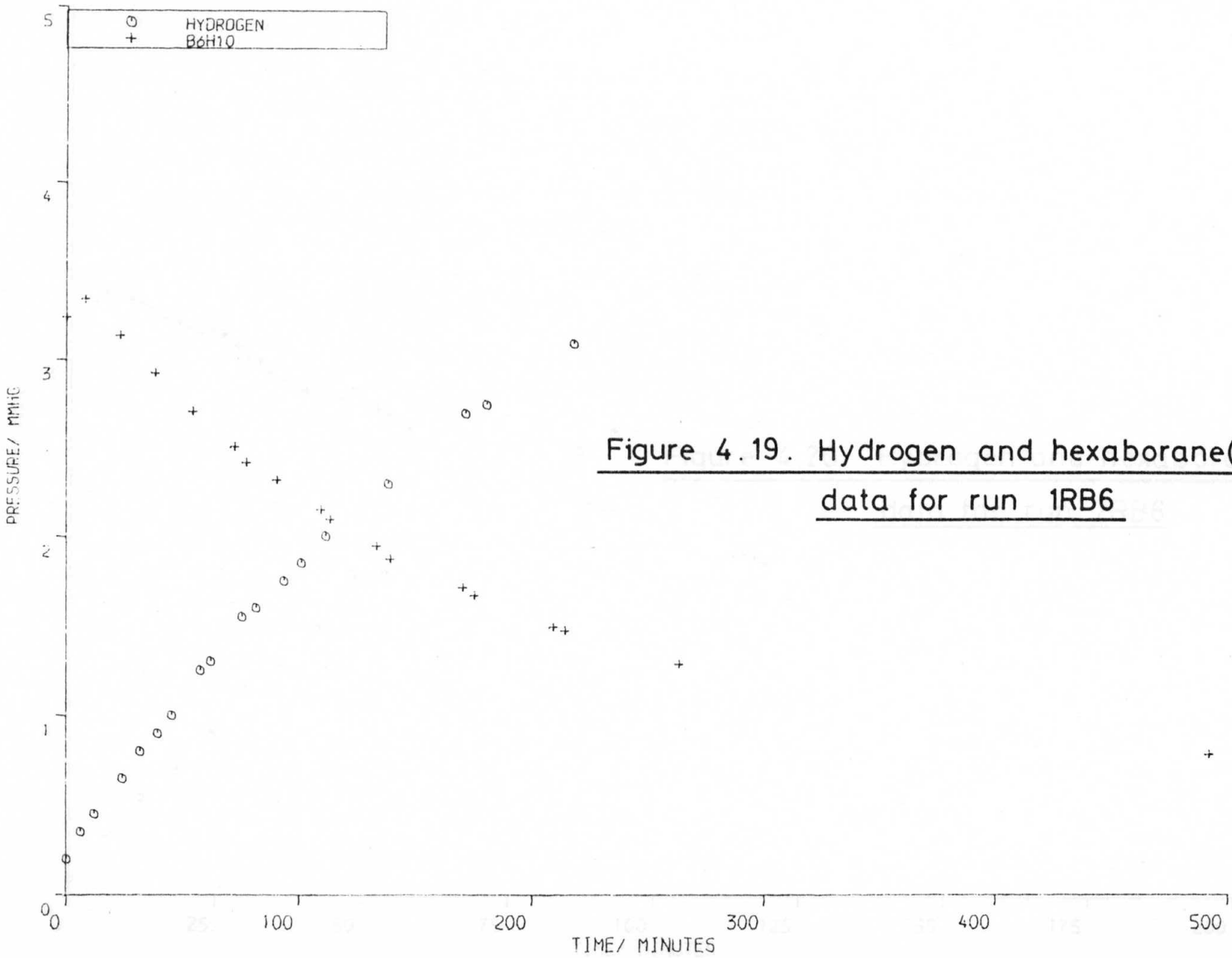

Figure 4.19. Hydrogen and hexaborane(10) data for run 1RB6

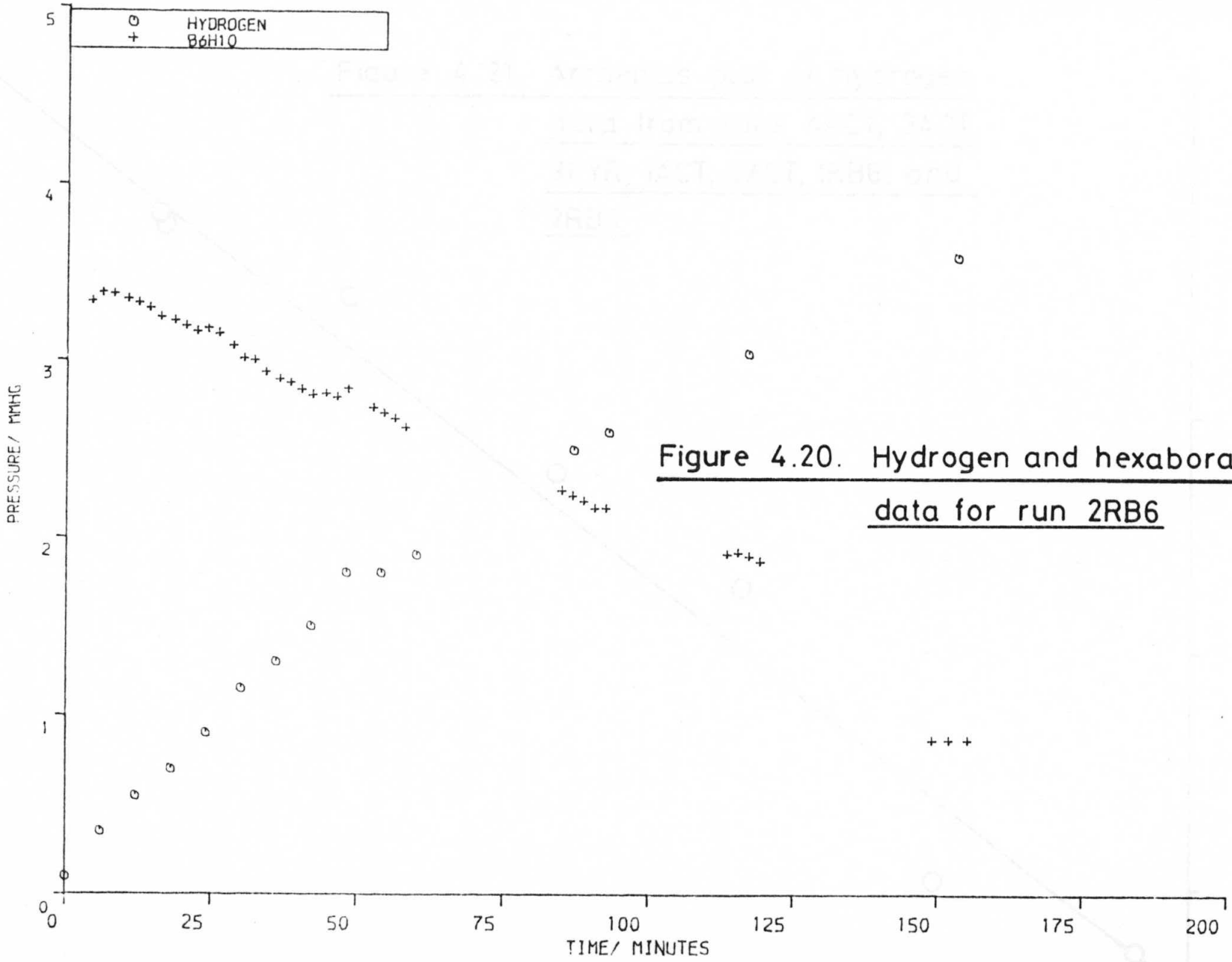

Figure 4.20. Hydrogen and hexaborane(10) data for run 2RB6

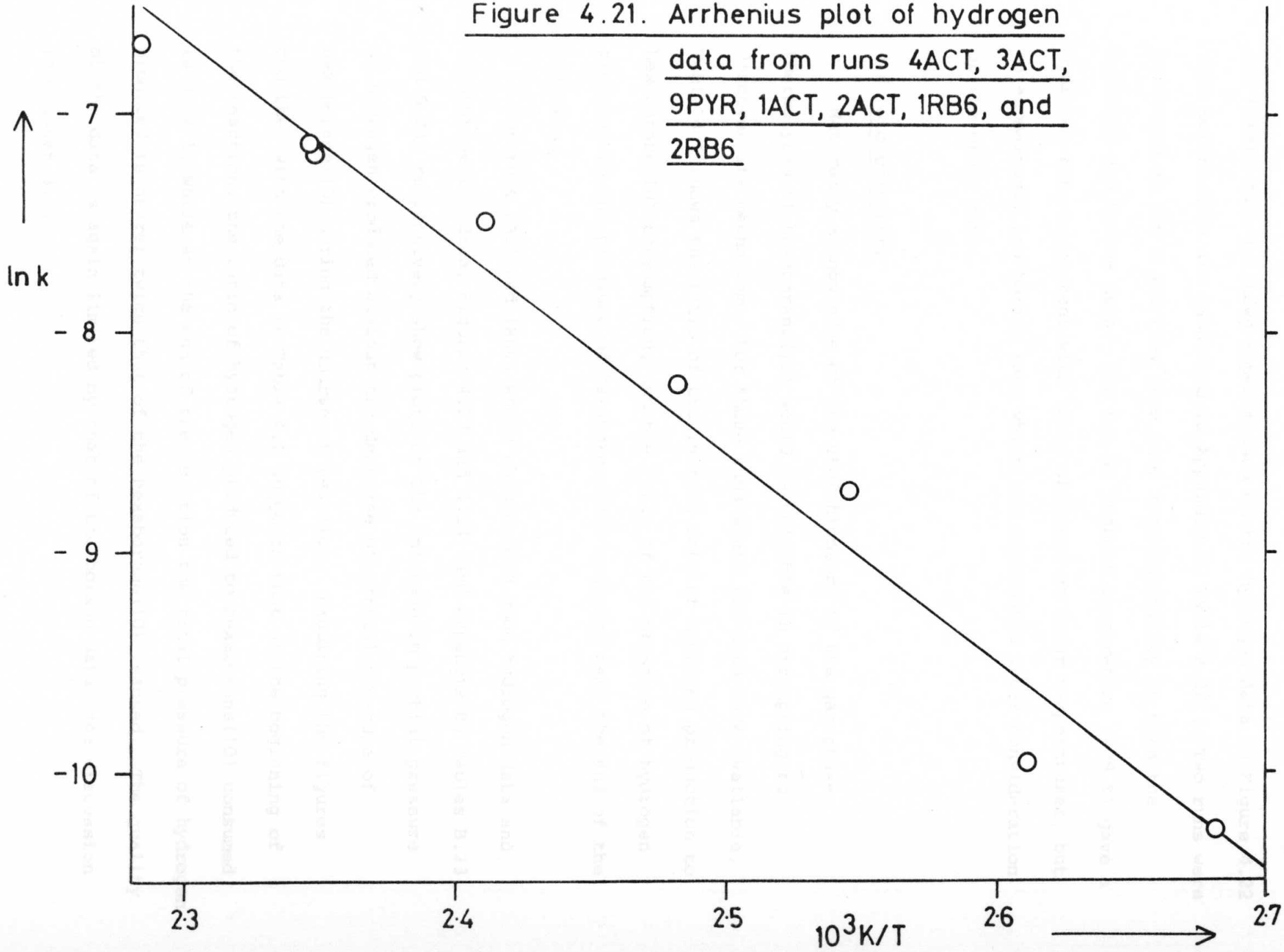

Figure 4.21. Arrhenius plot of hydrogen data from runs 4ACT, 3ACT, 9PYR, 1ACT, 2ACT, 1RB6, and 2RB6

treated as an order of magnitude). The Arrhenius plot obtained using the borane data is shown superimposed on the hydrogen data in Figure 4.22 (the borane data are tabulated in Appendix B, Table B.22). Two runs were performed at 426 K and they gave good reproducibility in both the hydrogen and borane data. The run at highest temperature (438 K) gave a hydrogen rate consistent with those obtained at lower temperatures, but an anomalously low borane rate which was discounted after consideration of the other data.

4.4 Stoichiometry

Naturally a knowledge of the stoichiometry of the gas-phase thermolysis of hexaborane(10) would be valuable in attempting to discover its mechanism. For those runs where the data were available, Table 4.1 shows the ratio of the initial rate of hydrogen production to hexaborane(10) consumption, and the ratio of the pressure of hydrogen produced to the pressure of hexaborane(10) consumed near the end of the reaction.

For runs 2ACT and 1RB6, which showed both good hydrogen data and hexaborane(10) data, Figures 4.23 and 4.24 (and Appendix B, Tables B.23 and B.24) respectively show plots of the increase in partial pressure of hydrogen produced against the decrease of partial pressure of hexaborane(10) during the course of reaction. Examining the figures together with the data in Table 4.1 suggests that at the beginning of the reaction, the ratio of hydrogen produced to hexaborane(10) consumed is near 1, while at the end of the reaction the final pressure of hydrogen produced is nearer twice that of the hexaborane(10) reacted. The quality of the data is again limited by that of the borane data, see discussion in Chapter 3.3.

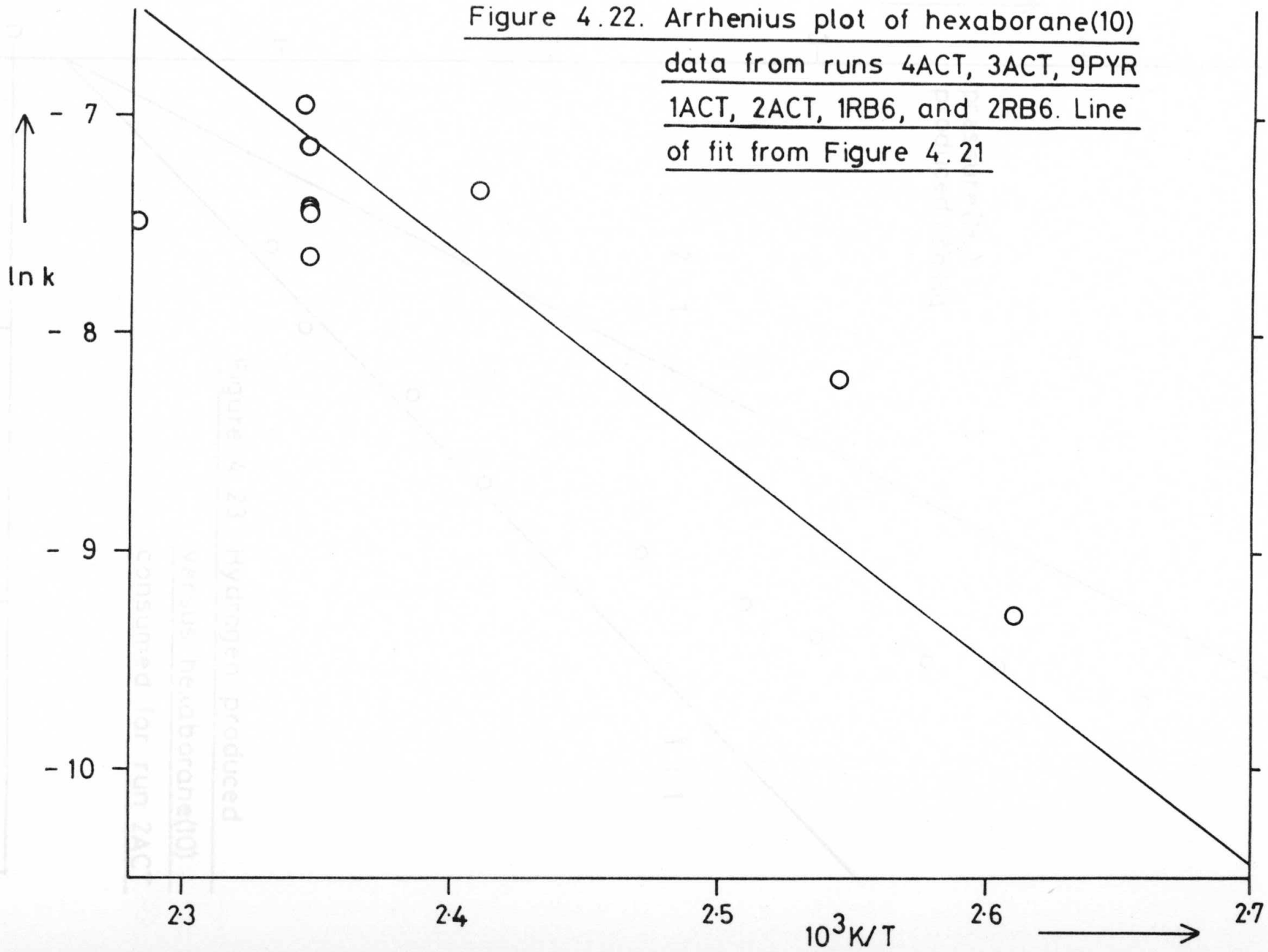

Figure 4.22. Arrhenius plot of hexaborane(10) data from runs 4ACT, 3ACT, 9PYR 1ACT, 2ACT, 1RB6, and 2RB6. Line of fit from Figure 4.21

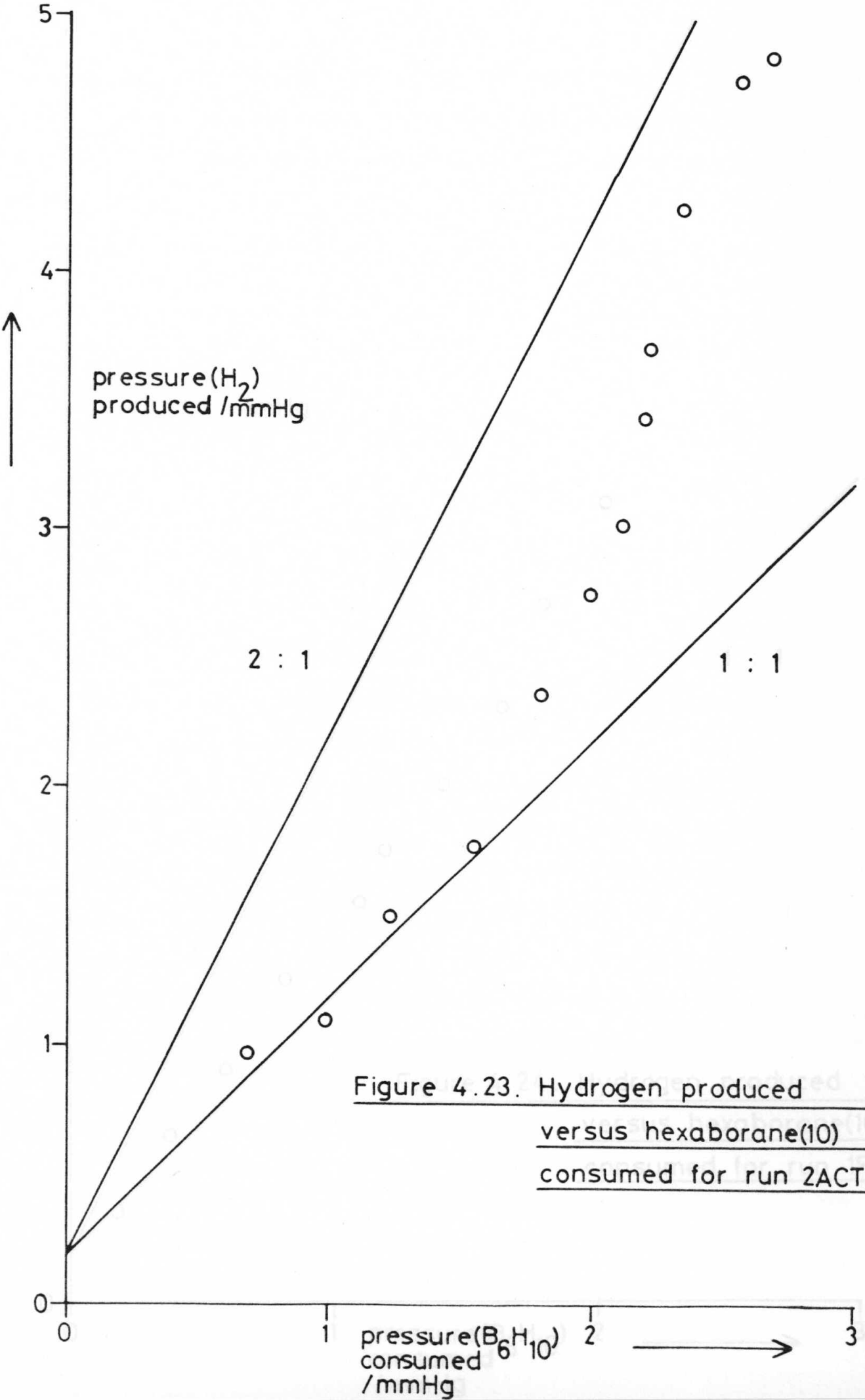

Figure 4.23. Hydrogen produced versus hexaborane(10) consumed for run 2ACT

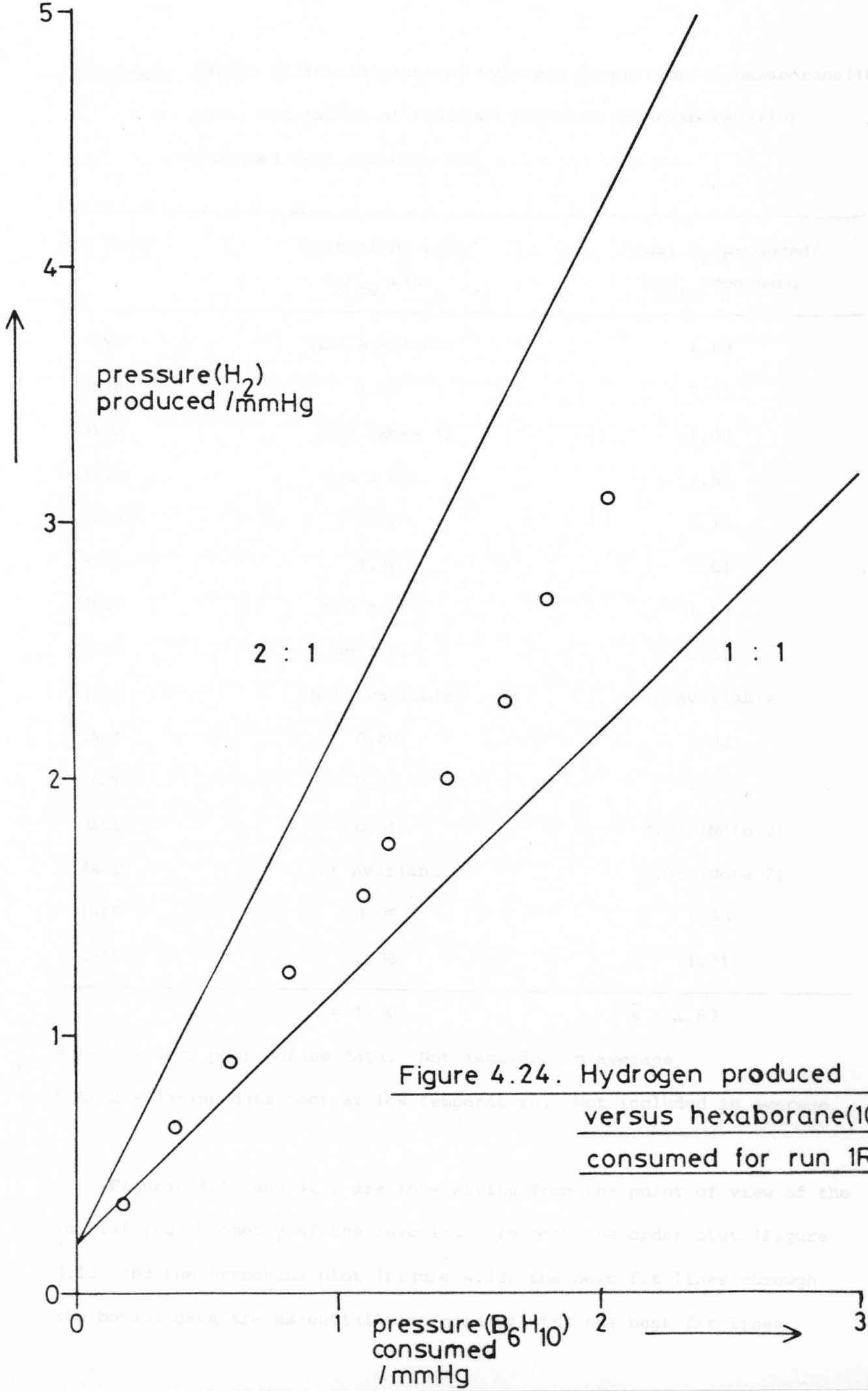

Figure 4.24. Hydrogen produced versus hexaborane(10) consumed for run 1RB6

Table 4.1. Ratios of initial rate of hydrogen production to hexaborane(10) loss, and ratios of hydrogen produced to hexaborane(10) consumed near reaction end.

Run Name	Initial H_2 rate/ B_6H_{10} rate	Final H_2 produced/ B_6H_{10} consumed
1PYR	Not Available	1.88
2PYR	1.64	1.81
3PYR	3.32 (Note 1)	1.03
4PYR	0.6 ± 0.1	1.89
5PYR	2.32	1.76
6PYR	1.32	1.61
7PYR	0.9 ± 0.5	1.53
8PYR	1.96 ± 0.4	2.11
9PYR	Not Available	Not Available
1ACT	0.86	1.32
2ACT	0.84	2.52
3ACT	0.51	3.82 (Note 2)
4ACT	Not Available	2.98 (Note 2)
1RB6	0.96	1.53
2RB6	2.36	1.31
	$\bar{x}$ = 1.30	$\bar{x}$ = 1.69

Note 1 - Very poor borane data. Not included in average

Note 2 - Borane data poor at low temperature. Not included in average.

Figures 4.10 and 4.22 are interesting from the point of view of the initial stoichiometry of the reaction. In both the order plot (Figure 4.10) and the Arrhenius plot (Figure 4.22) the best fit lines through the borane data are essentially coincident with the best fit lines

through the hydrogen data. This implies a value of 1 for the ratio of initial hydrogen formation to hexaborane(10) consumption. A higher ratio is indicated for the overall reaction as measured by final reactant and product pressures.

Further support for an initial stoichiometry of 1:1 came from a separate piece of work in this project in which liquid hexaborane(10) was sealed in a glass vessel for several months. This experiment is discussed in more detail in section 4.8, and the possible meaning of the observations in this section are discussed in Chapter 5.

4.5 Effect of added hydrogen

It was necessary to establish whether the hydrogen released during the thermolysis exercised any retarding effect on the rate. Two experiments were performed in which hydrogen was added to the initial charge of hexaborane(10). The experiments were named 1HYD and 4HYD (unfortunately 2HYD and 3HYD both failed).

1HYD was carried out at 425 K with an initial pressure of hexaborane(10) of 3.36 mmHg and an added pressure of hydrogen of 4.94 mmHg. The data from this reaction are shown in Figure 4.25 and tabulated in Appendix B, Table B.25. The rate constants derived from the initial rate of appearance of hydrogen and the initial rate of disappearance of hexaborane(10) were 101.6 $m^3\ mol^{-1}\ s^{-1}$ and 47.4 $m^3\ mol^{-1}\ s^{-1}$ respectively. These should be compared with 79.6 $m^3\ mol^{-1}\ s^{-1}$ and 95.3 $m^3\ mol^{-1}\ s^{-1}$ for 2ACT, 75.64 $m^3\ mol^{-1}\ s^{-1}$ and 79 $m^3\ mol^{-1}\ s^{-1}$ for 1RB6 and 99.6 $m^3\ mol^{-1}\ s^{-1}$ and 58.3 $m^3\ mol^{-1}\ s^{-1}$ for 4RB6. The data are somewhat self-contradictory in that the hydrogen rate constant has increased in the experiment with added initial hydrogen, while the hexaborane(10) rate constant has decreased. It will be observed that the borane data are extremely poor for 1HYD and that the intercept

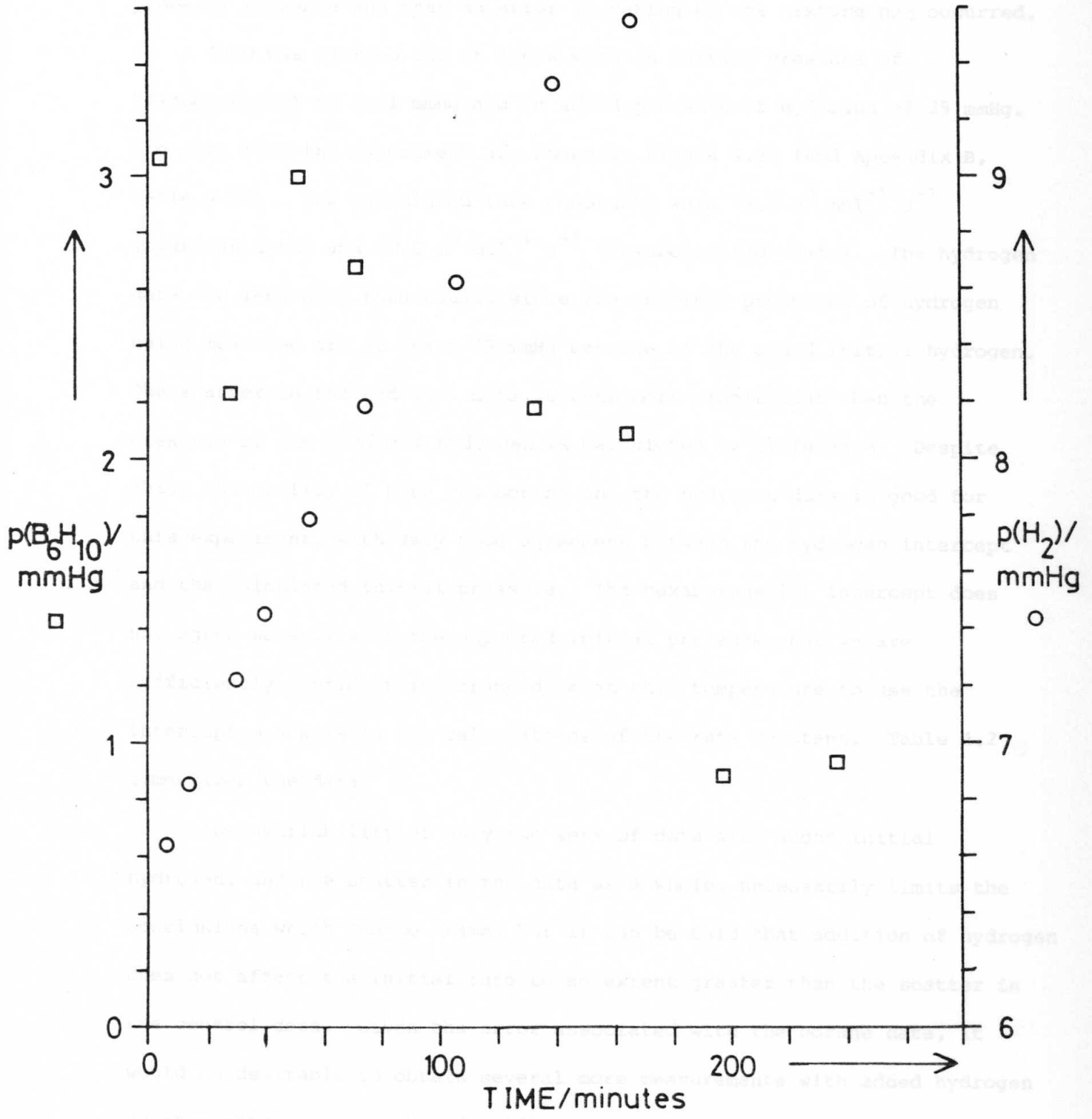

Figure 4.25. Hydrogen and hexaborane(10) data for run 1HYD

of the curve through the hydrogen data on the pressure axis does not agree with the calculated added pressure of 4.9 mmHg. Consideration of the general quality of the hydrogen data suggests that the intercept is probably reliable and that an error in making up the mixture had occurred.

4HYD was carried out at 426 K with an initial pressure of hexaborane(10) of 3.51 mmHg and an added pressure of hydrogen of 25 mmHg. The data from the experiment are shown in Figure 4.26 (and Appendix B, Table B.26). The calculated rate constants were 78.2 $m^3\ mol^{-1}\ s^{-1}$ (hydrogen data) and 59.6 $m^3\ mol^{-1}\ s^{-1}$ (hexaborane(10) data). The hydrogen data are less good than usual, since the absolute pressures of hydrogen being measured are at least 25 mmHg because of the added initial hydrogen. The scatter in the hydrogen data is thus more significant when the pressure of the *produced* hydrogen is calculated by difference. Despite this, the quality of both the borane and the hydrogen data is good for this experiment, with very good agreement between the hydrogen intercept and the calculated initial pressure. The hexaborane(10) intercept does not agree so well with the expected initial pressure, but we are sufficiently confident in borane data at this temperature to use the intercept pressure in the calculations of the rate constant. Table 4.2 summarizes the data.

The availability of only two sets of data with added initial hydrogen, and the scatter in the data as a whole, necessarily limits the conclusions which can be drawn, but it can be said that addition of hydrogen does not affect the initial rate to an extent greater than the scatter in the control data. Given the error associated with the borane data, it would be desirable to obtain several more measurements with added hydrogen so that patterns could be identified in the inevitably scattered data, but unfortunately lack of time prevented this towards the end of the work, and

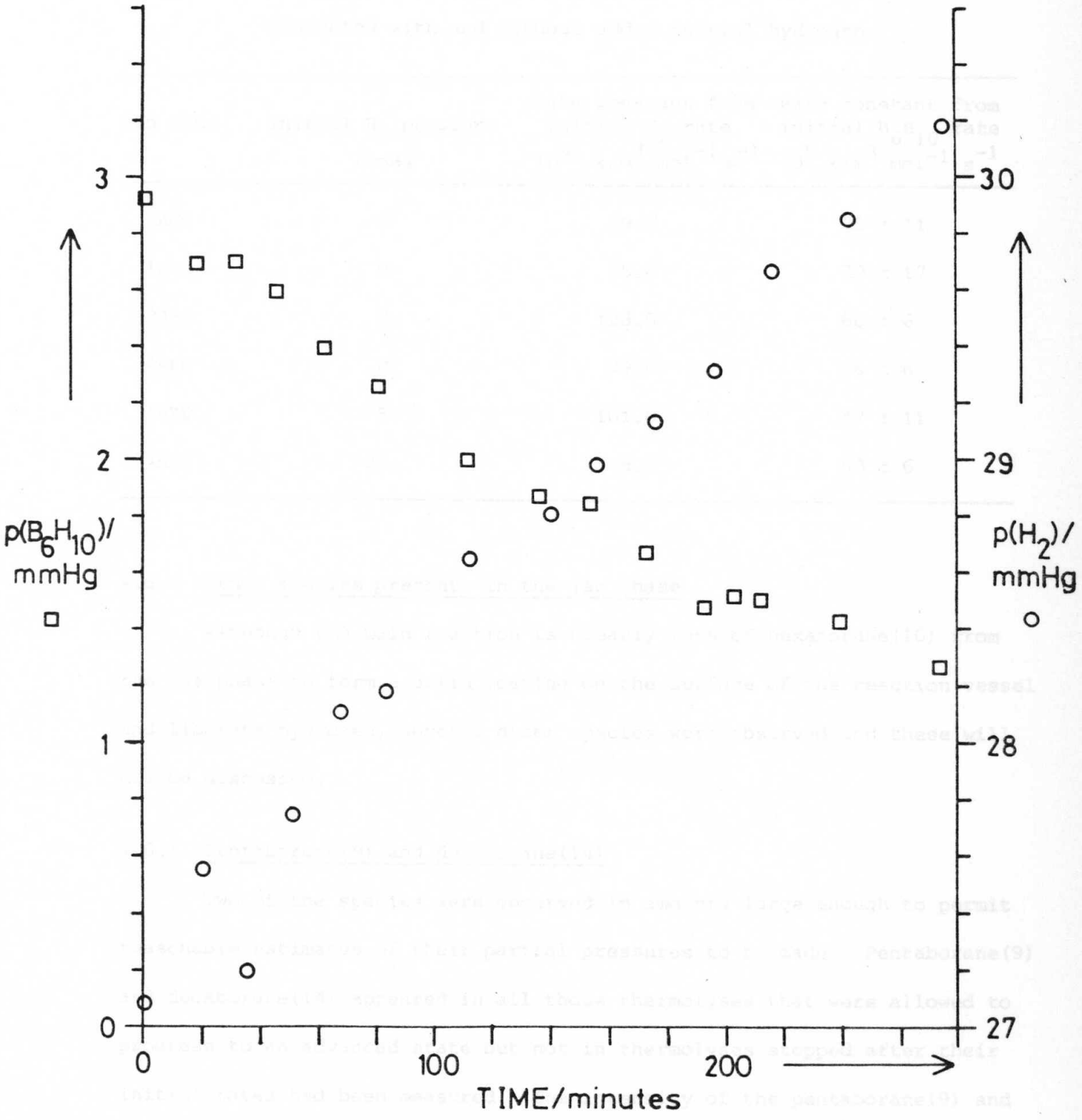

Figure 4.26. Hydrogen and hexaborane(10) data for run 4HYD

to some extent a broad based exploratory approach was adopted after the work on reaction order and activation energy.

Table 4.2: Comparison of initial rates observed in experiments conducted with and without added initial hydrogen

Run Name	Initial H_2 pressure /mmHg	Rate constant from initial H_2 rate 10^5 k/m^3 mol^{-1} s^{-1}	Rate constant from initial B_6H_{10} rate 10^5 k/m^3 mol^{-1} s^{-1}
2ACT	0	79.7	95 ± 11
1RB6	0	75.6	79 ± 17
3RB6	0	128.0	60 ± 6
4RB6	0	99.6	58 ± 6
1HYD	5	101.6	47 ± 11
4HYD	25	78.2	60 ± 6

4.6 Other species present in the gas phase

Although the main reaction is clearly loss of hexaborane(10) from the gas phase to form a solid coating on the surface of the reaction vessel and liberate hydrogen, several other species were observed and these will now be discussed.

4.6.1 Pentaborane(9) and decaborane(14)

Two of the species were observed in amounts large enough to permit reasonable estimates of their partial pressures to be made. Pentaborane(9) and decaborane(14) appeared in all those thermolyses that were allowed to progress to an advanced state but not in thermolyses stopped after their initial rates had been measured. The intensity of the pentaborane(9) and decaborane(14) peaks in the mass spectrum of the mixtures increased slowly during the reaction. Figure 4.27 shows typical mass spectra from the

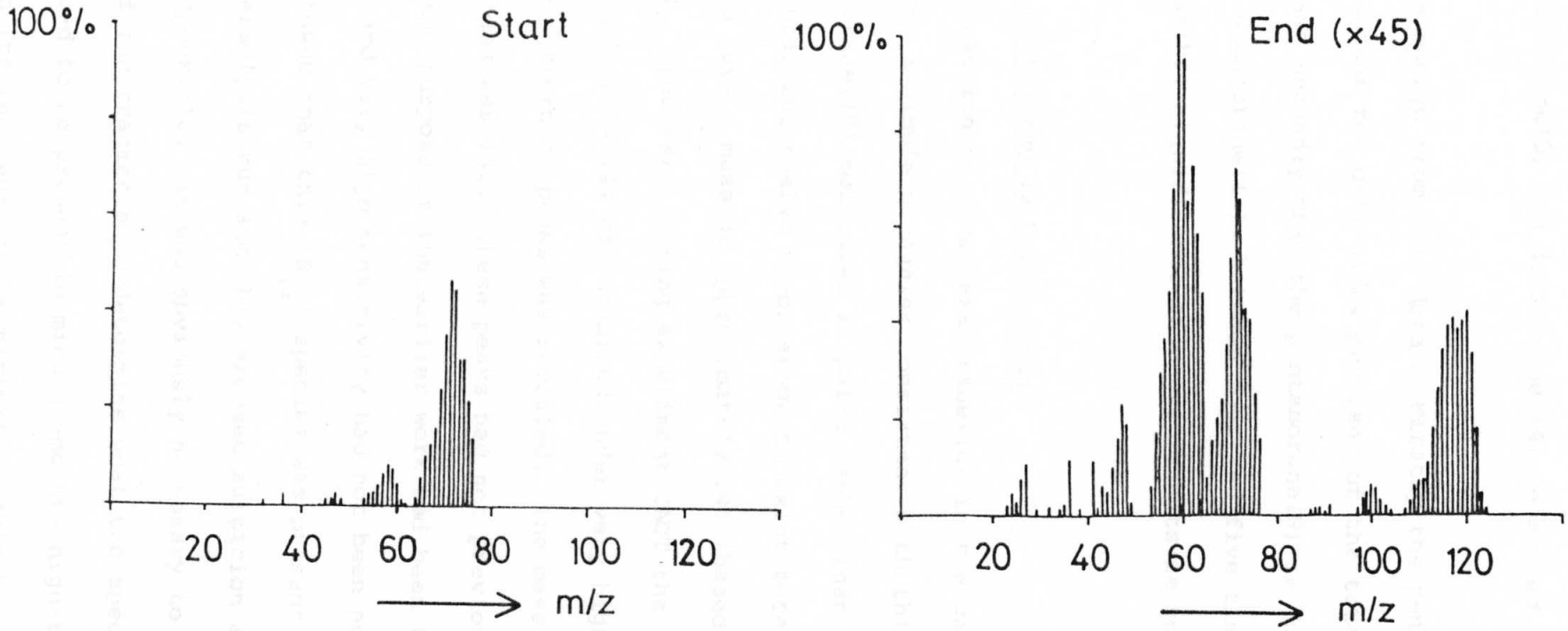

Figure 4.27. Mass spectra from start and end of typical reaction showing appearance of pentaborane(9) and decaborane(14)

beginning and end of a thermolysis run. Table 4.3 shows the final pressures of pentaborane(9) and decaborane(14) generated in some of the thermolyses.

Two points emerge from this data. Firstly the pentaborane(9) and decaborane(14) account for only a few per cent of the total boron present in the reaction and secondly that the pentaborane(9) is formed in greater amounts than the decaborane(14), between four and five times as much on average. The possible significance of these results is considered in Chapter 5.

4.6.2 A species containing 12 boron atoms

Since the reaction of pure hexaborane(10) in the gas phase appeared to be second order, a simple mechanism consistent with this would be the reaction of hexaborane(10) molecules in pairs rather than individually. Were a species containing twelve boron atoms to exist because of this mechanism it would have a mass of approximately 144 (based on a purely hypothetical $B_{12}H_{12}$ species). During experiment 2ACT the region of the mass spectrum around m/z = 144 was examined under very high sensitivity, and a borane-like pattern of peaks was revealed. The mass cut-off was 144 and the base peak was 142. These peaks had not previously been observed because the purpose of the earlier work had been to establish initial rate data and very high sensitivity had not been needed. Subsequent work showed that this 'B_{12}' species was present from the very beginning of a thermolysis run and this aroused suspicion as to the identity of the species responsible. It was obviously necessary to measure the accurate masses of the fragments to determine what the species was. As the species appeared to be present in minute amounts high-resolution mass-spectrometry, with its inherent low sensitivity, would have prevented the detection of the species, so the measurements were made using the spectrometer in low-resolution double-beam mode (see Chapter 2.1.3).

Table 4.3. Comparison of hexaborane(10) consumption and pentaborane(9) and decaborane(14) production from selected thermolyses.

Run name	$p(B_6H_{10})_0$	$p(B_6H_{10})$ near run end	$p(B_6H_{10})$ consumed	$p(B_5H_9)$ produced	$p(B_{10}H_{14})$ produced	$p(B_5H_9)/p(B_{10}H_{14})$	% Boron in B_5H_9 and $B_{10}H_{14}$
2ACT	3.51	0.818	2.692	0.112	0.024	4.7	5
2ACT	3.51	0.362	3.148	0.277	0.046	6.0	10
3ACT	3.24	0.787	2.453	0.197	0.067	2.9	11
3ACT	3.24	0.765	2.475	0.221	0.081	2.7	13
4PYR	7.7	0.346	7.35	0.320	0.127	2.5	7
5PYR	6.6	0.117	6.48	0.122	zero	---	2
5PYR	6.6	0.000	6.6	0.124	zero	---	2
6PYR	2.37	0.633	1.74	0.052	zero	---	3
6PYR	2.37	0.305	2.07	0.078	0.008	9.8	4
						$\bar{x} = 4.76$	$\bar{x} = 6.33$

The masses of the fragments were not consistent with a species containing boron and hydrogen only. However, other peaks were observed, differing in mass from the major peaks sufficiently to be resolved at low resolution, i.e. by 1 part in 1000, and having masses consistent with a species containing only boron and hydrogen. Figure 4.28 shows the appearance of the spectrum in this region under low-resolution double-beam conditions.

Fortuitously then, the 'rogue B_{12}' species led to the observation of what is considered to be a real 'B_{12}' species containing twelve boron atoms and an undetermined number of hydrogen atoms. Before further discussion of the real B_{12} species, the puzzle of the rogue B_{12} will be dealt with.

Decaborane oxide, $B_{10}H_{14}O$, which is a well established species [62] would have a mass cut-off of 140, so it could not be responsible for the rogue peaks, besides which the possibility of oxidation occurring in the reaction vessel was too horrific to contemplate, both from the point of view of the integrity of the data in the earlier runs and from the safety aspect. Oxidation was also unlikely as the vacuum line and the reaction vessel were very reliable and the oxygen peak in the spectrometer was always very low.

It was realized, with both relief and surprise, that the species being observed was 1-bromopentaborane, which is an intermediate in the preparation of hexaborane(10) (see Appendix C). 1-bromopentaborane has a mass cut-off of 144, and the accurate masses of the fragments observed were consistent with bromopentaborane. However it was surprising that 1-bromopentaborane was present in the hexaborane(10) as it is a fairly involatile solid at room temperature. In the preparation of hexaborane(10), 1-bromopentaborane is isolated as a pure intermediate by pumping the reaction products through a U-trap held at -35°C, and in the final

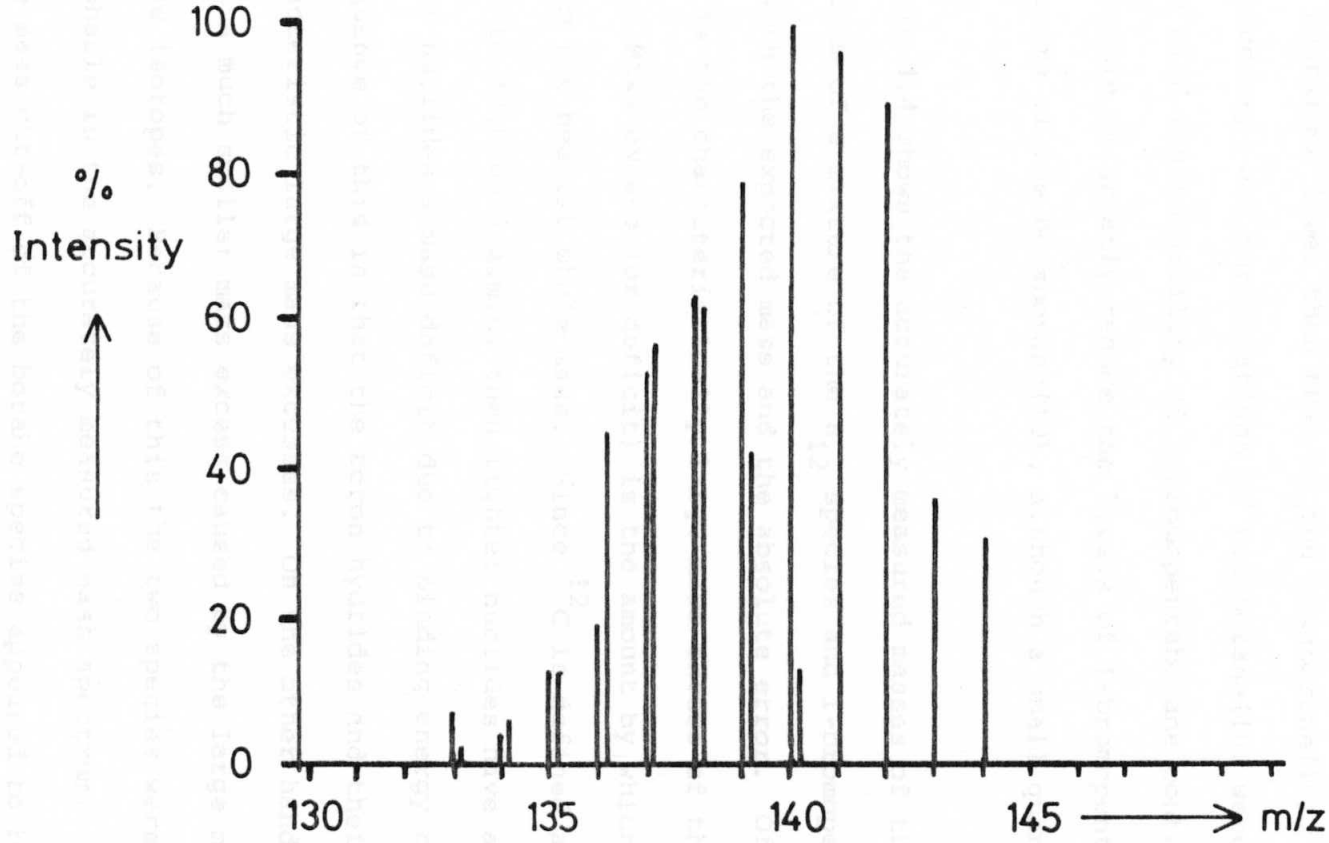

Figure 4.28. Double-beam low resolution mass spectrum showing 'B_{12}' and BrB_5H_8 peaks

purification of the hexaborane(10) the reaction products are held at -35°C to hold back any residual 1-bromopentaborane. But although 1-bromopentaborane moves exceedingly slowly under dynamic vacuum even at room temperature, some of it still managed to be included in the final 'pure' samples of hexaborane(10). Accurate estimation of the bromopentaborane pressure was not possible but the intensity of its spectrum was three orders of magnitude lower than that of the hexaborane(10). Subsequently to this discovery, all purifications of hexaborane(10) were carried out bearing in mind the possibility of 1-bromopentaborane contamination, and it was possible to greatly reduce the levels of 1-bromopentaborane seen in the spectra of the hexaborane(10), although a small quantity always persisted.

Table 4.4 shows the accurately measured masses of the peaks in a mass spectrum of a mixture of the B_{12} species and 1-bromopentaborane, together with the expected mass and the absolute error. Of interest in Table 4.4 is the characteristically large mass excess of the borane fragments. Mass excess (or deficit) is the amount by which the masses differ from the nearest whole mass. Since ^{12}C is defined as having a mass equal to 12.000000 a.m.u. then lighter nuclides have a mass excess and heavier nuclides a mass deficit due to binding energy considerations. The consequence of this is that the boron hydrides and their fragments have characteristic large mass excesses. On the other hand, 1-bromopentaborane has a much smaller mass excess caused by the large mass deficit of the bromine isotopes. Because of this the two species were easily distinguishable in the accurately measured mass spectrum.

The mass cut-off of the borane species appeared to be 140, but it may be possible that because of the low abundance of the species not all the fragments were appearing. The base peak was at 138. The most probable distribution of the two boron isotopes (^{10}B and ^{11}B) for a species

Table 4.4. Accurate mass spectrum of mixture of $B_{12}H_x$ and 1-BrB_5H_8

Measured Mass	Fragment	Calculated Mass	Error (CALC-MEAS)
144.0130	$^{10}B_0\,^{11}B_5\,^{81}BrH_8$	144.0254	0.0124
143.0157	$^{10}B_0\,^{11}B_5\,^{81}BrH_7$	143.0176	0.0019
142.0183	$^{10}B_1\,^{11}B_4\,^{81}BrH_7$	142.0212	0.0029
141.1859	$^{10}B_0\,^{11}B_{12}H_9$	141.18209	-0.0038
141.0245	$^{10}B_0\,^{11}B_5\,^{79}BrH_7$	141.0249	0.0004
140.1758	$^{10}B_0\,^{11}B_{12}H_8$	140.17427	-0.0015
140.0167	$^{10}B_0\,^{11}B_5\,^{79}BrH_6$	140.0170	0.0003
139.1785	$^{10}B_1\,^{11}B_{11}H_8$	139.17790	-0.0006
139.0104	$^{10}B_2\,^{11}B_3\,^{81}BrH_5$	139.0092	-0.0012
138.1812	$^{10}B_2\,^{11}B_{10}H_8$	138.18153	0.0003
138.0031	$^{10}B_1\,^{11}B_5\,^{79}BrH_5$	138.0076	0.0045
137.1835	$^{10}B_3\,^{11}B_9H_8$	137.18516	0.0017
136.9931	$^{10}B_0\,^{11}B_5\,^{79}BrH_3$	136.9883	-0.0048
136.1794	$^{10}B_3\,^{11}B_9H_7$	136.17734	-0.0021
135.9798	$^{10}B_0\,^{11}B_5\,^{79}BrH_2$	135.9805	0.0007
135.1798	$^{10}B_4\,^{11}B_8H_7$	135.18097	0.0012
134.9814	$^{10}B_1\,^{11}B_4\,^{79}BrH_2$	134.9841	0.0027
134.1767	$^{10}B_4\,^{11}B_8H_6$	134.17315	0.0035
133.9880	$^{10}B_2\,^{11}B_3\,^{79}BrH_2$	133.9878	-0.0002
133.1619	$^{10}B_4\,^{11}B_8H_5$	133.16532	0.0034
132.9868	$^{10}B_3\,^{11}B_2\,^{79}BrH_2$	132.9914	0.0046
132.2224	unresolved multiplet		
132.1526	$^{10}B_4\,^{11}B_8H_4$	132.15750	0.0049

continued/....

Table 4.4 (continued)

Measured Mass	Fragment	Calculated Mass	Error (CALC-MEAS)
131.1884	$^{10}B_7\,^{11}B_5H_6$	131.18405	-0.0043
131.1312	$^{10}B\,^{11}B\,H$		
130.9963	PFK reference peak	130.9960	-0.003

Isotope Masses Used

^{10}B = 10.0129

^{11}B = 11.00931

^{79}Br = 78.9183

^{81}Br = 80.9163

^{1}H = 1.007825

containing twelve boron atoms lies between $^{10}B_2{}^{11}B_{10}$ and $^{10}B_3{}^{11}B_9$. These would have masses of 130 and 129 respectively, implying that the fragment giving rise to the base peak contains 8 or 9 hydrogen atoms. If the spectra of the other boranes are considered in relation to their masses then the closeness of base peak and cut-off for the B_{12} species appears anomalous. For example decaborane(14) has base peak 120 and cut-off 124, hexaborane(10) has base peak 71 and cut-off 76 and pentaborane(9) has base peak 59 and cut-off 64, so perhaps some of the B_{12} fragments failed to appear due to its low abundance. The identity of the B_{12} species and the possible implications of its existence in terms of the mechanism of thermolysis of hexaborane(10) are discussed in Chapter 5.

4.6.3 An octaborane species

In the early stages of the lower temperature thermolyses, borane peaks were seen in the mass spectrum in the region 90-100, with base peak at 93. The intensity of these peaks rapidly decreased as the reaction proceeded and they were eventually lost under the B_8 and B_9 envelopes of the decaborane(14) formed in the thermolysis. The base peak of B_8H_{12} is given as 93 in the literature [5] and so the mass spectral evidence is interpreted as being due to the presence of B_8H_{12}. The spectrum in this region is shown in Figure 4.29.

4.7 The solid residue

It has been mentioned several times that apart from hydrogen the major product of the gas-phase thermolysis of hexaborane(10) was a solid film on the wall of the reaction vessel. The solid coating always appeared to be thicker in the bottom half of the vessel, perhaps suggesting its formation in the gas phase rather than on the walls of the vessel. Such residues are common in borane chemistry and are often loosely

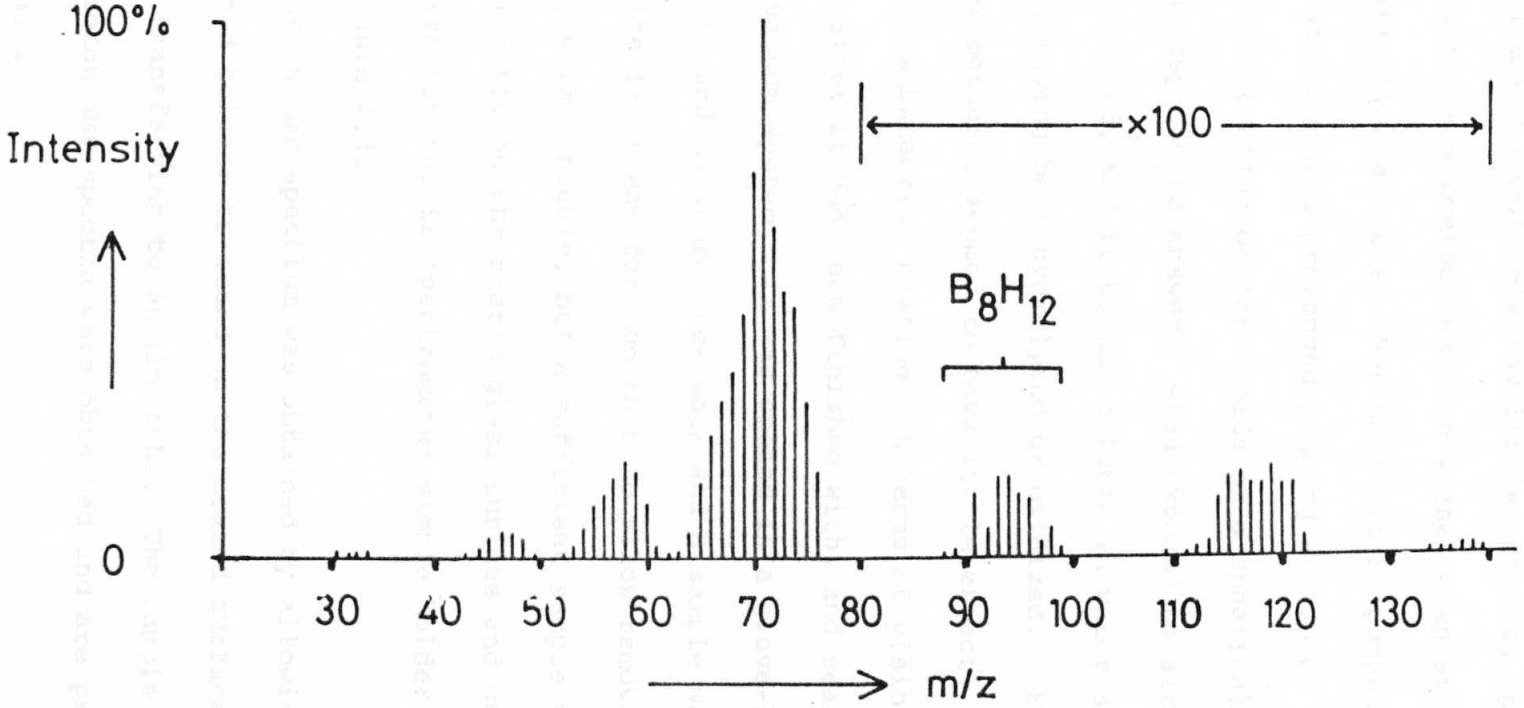

Figure 4.29. Mass spectrum of early stage of thermolysis showing presence of octaborane(12)

referred to as polymers. In the course of this work the films, which built up in thickness over a series of runs, had colourful tinges when thin but were milky white to yellow when thicker. Obviously the solid was composed of boron and hydrogen and any information about it would be of value. The solid was completely involatile; no mass spectrum could be obtained from a thickly coated reaction vessel even at 150°C and using the highest sensitivity available. Nor could it be pumped out of the reaction vessel, withstanding prolonged pumping at 120°C. The question of how to examine the coating on the inside of a spherical glass reaction vessel was not an easy one to answer. When exposed to air, the nature of the solid was changed, and it became soluble in water soon after exposure, probably having been hydrolyzed or oxidized. Solvents, e.g. toluene or dichloromethane, seemed to have little effect. One reaction vessel with a quite substantial coating (in terms of visibility) was filled with argon after it had been finished with, and sealed and removed from the vacuum system. It was opened in a glove-box which was equipped for oxygen- and moisture-free work and a sample was taken for an ir spectrum. The layer was far too thin to allow removal of the sample by scraping with a needle, but a sufficient sample was obtained by grinding KBr directly on the coated glass surface and compressing that KBr into a disc for the ir spectrometer sample holder. The spectrum is presented in Figure 4.30.

A sample for an nmr spectrum was obtained by allowing a small amount of deuterated toluene to stand on the coated surface for a few minutes, and then transferring to an nmr tube. The sample was very weak but the ^{11}B and proton nmr spectra were obtained and are presented in Figures 4.31 and 4.32.

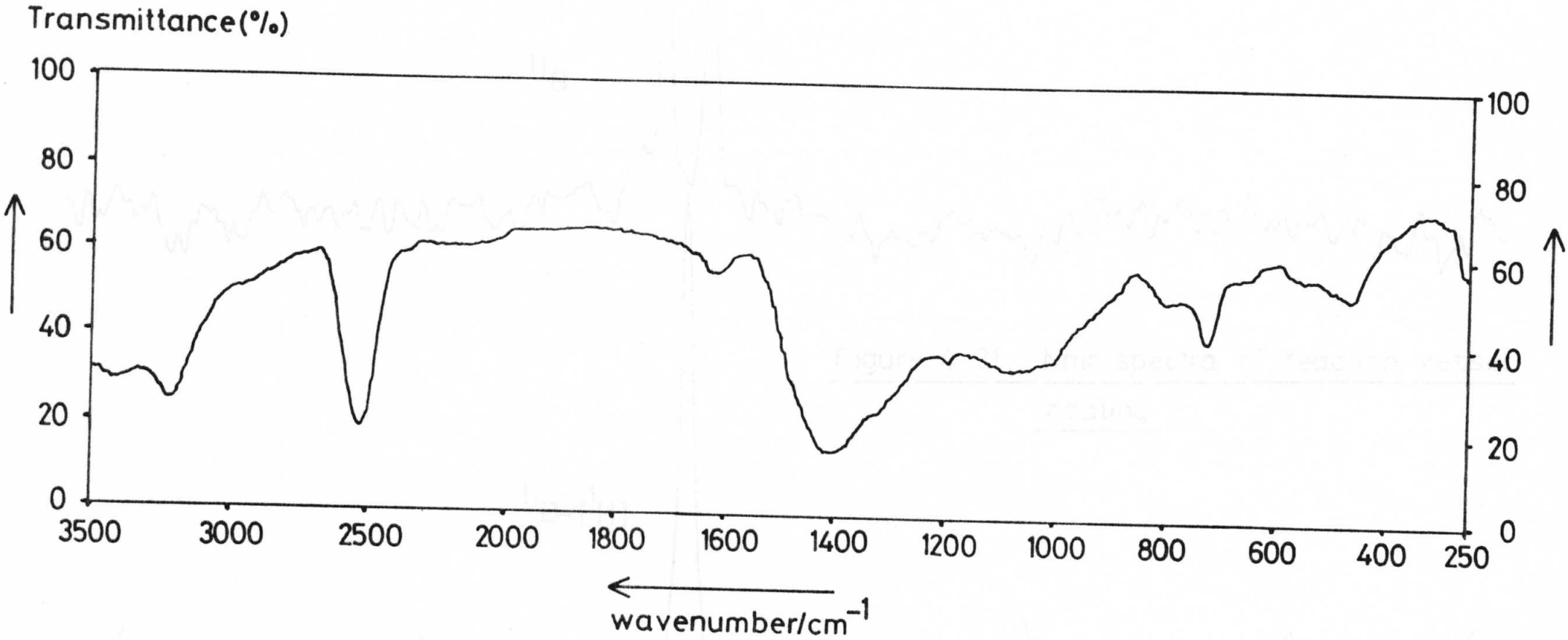

Figure 4.30. Infrared spectrum of reaction vessel coating

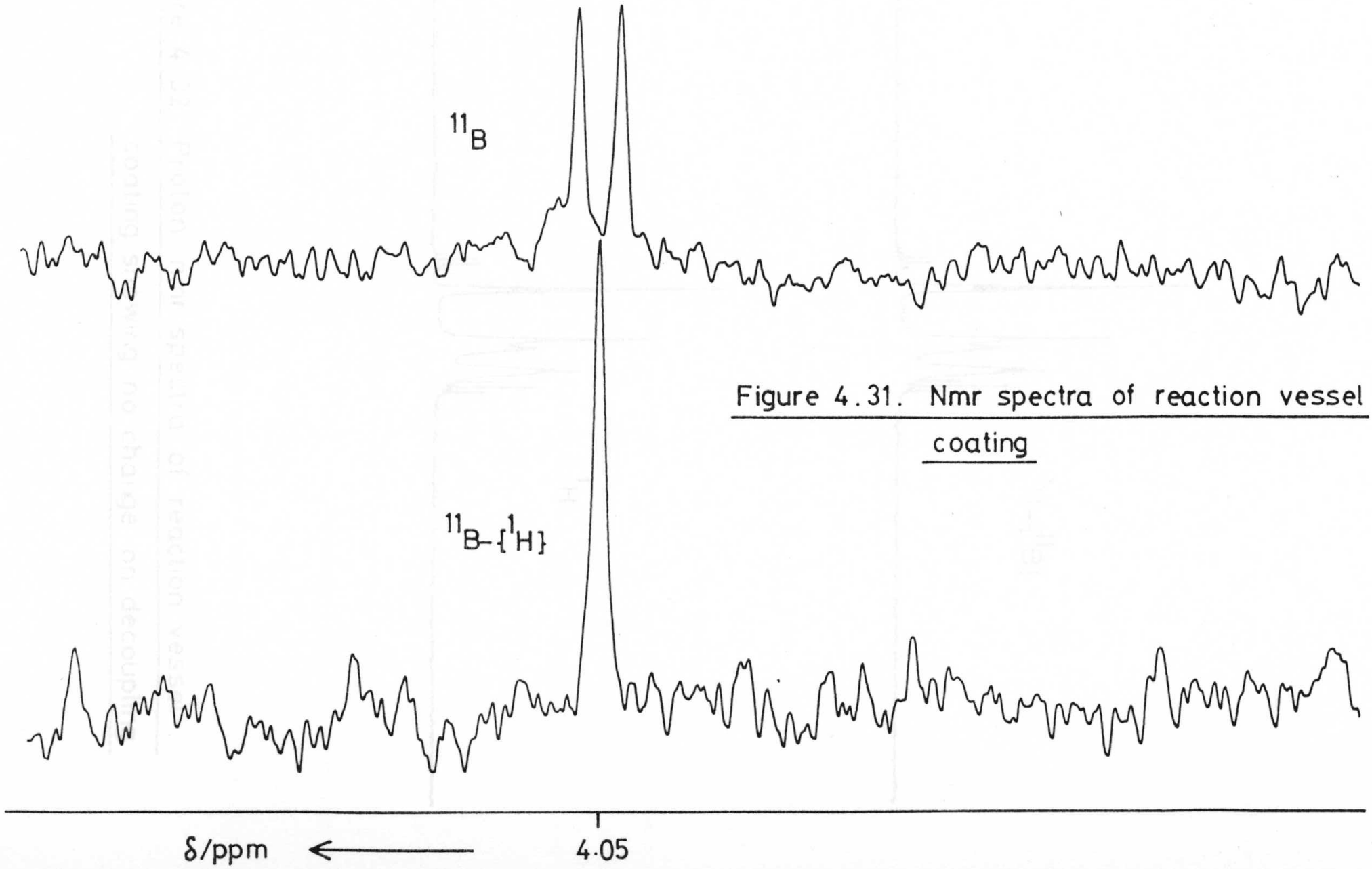

Figure 4.31. Nmr spectra of reaction vessel coating

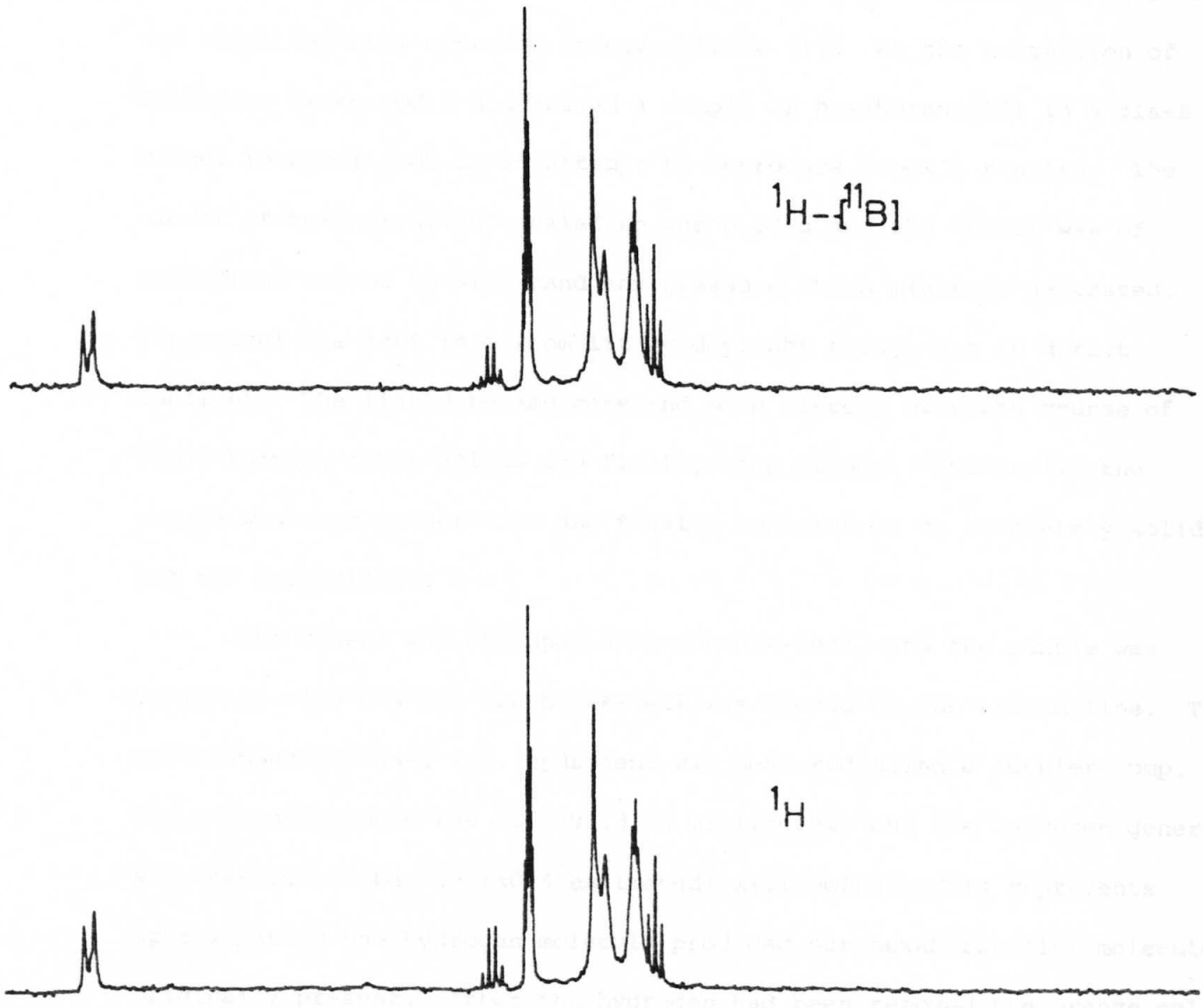

Figure 4.32. Proton nmr spectra of reaction vessel coating showing no change on decoupling

4.8 Room temperature "polymerization" of hexaborane(10)

A related solid was available. There were reports in the literature of samples of hexaborane(10) which had been sealed off and left to stand, and which had been observed to crystallize [1]. At the suggestion of Professor Greenwood I had sealed a sample of hexaborane(10) in a glass vessel in April 1980 in an attempt to reproduce Stock's results. The amount of hexaborane(10) sealed up was 0.27 g and the vessel was of sufficient volume to withstand any pressure which might be generated. The vessel was kept in a room lit by daylight though not in direct sunlight. The liquid became more and more viscous over the course of time, turning first yellow and finally deep orange. Eventually the sample would no longer flow and finally appeared to be completely solid, but not crystalline.

The vessel was equipped with a break-seal, and the sample was cooled to -196°C while the break-seal was opened on the vacuum line. The non-condensable gas, i.e. hydrogen, was measured using a Toepler pump. The original sample was 0.27 g (3.55 millimoles) and the hydrogen generated was measured to be 3.9 (±0.4 estimated) millimoles. This represents approximately one hydrogen molecule produced per hexaborane(10) molecule originally present. After the hydrogen had been removed the orange solid was allowed to warm to room temperature and was pumped dynamically over a weekend through a trap held at -196°C. No volatiles were released from the solid, and its surface appearance did not change, in other words it was completely involatile. It therefore seems reasonable to conclude that all the original hexaborane(10) had reacted, notwithstanding small amounts that might be occluded in the solid matrix. The vessel was resealed and taken into the glove-box. After opening, the solid was confirmed to be extremely hard and glass-like when tested with a sharpened steel needle.

Elemental analysis of a sample of the glassy solid gave (by weight) 10.7% hydrogen and 83.9% boron. If the empirical formula were B_6H_8 (recalling that approximately one molecule of hydrogen was released per hexaborane(10) molecule consumed) this would require an analysis of 11.0% hydrogen and 89.0% boron, so obviously there is very bad agreement between the measured boron figure and the calculated figure. Whatever was responsible for the missing 5% in the boron figure must have become incorporated into the sample after opening the vessel as the original hexaborane(10) was pure, both mass spectrometrically and by vapour pressure measurement. Attack by moisture prior to analysis may have been responsible, since water is also 11% hydrogen by weight and so would affect the boron figure but not the hydrogen figure.

The mass spectrum was obtained and is presented in Figure 4.33. The mass spectrum indicated the presence of pentaborane(9), hexaborane(10) and decaborane(14) and also some peaks heavier than decaborane; a profile in the m/z 190 region was similar to that of $B_{16}H_{20}$ given by Plesek *et al.* [76]. All the peaks in the mass spectrum disappeared very quickly, but on removal of the solid probe sufficient residue remained to account (by visual estimate) for the entire original sample, i.e. the spectrum observed was not due to the bulk components of the sample, but probably to occluded volatiles which comprised a very small fraction of the whole. The bulk was involatile, or had decomposed to an involatile substance (possibly losing hydrogen). This involatility was maintained under the severely testing conditions of the mass spectrometer inlet source (~250°C, 10^{-7} torr). This was consistent with the observed involatility of the substance on the vacuum line.

The ir spectrum of the glassy solid was recorded using a KBr disc, and is presented in Figure 4.34. An ir spectrum of $B_{10}H_{14}$ is presented for comparison in Figure 4.35.

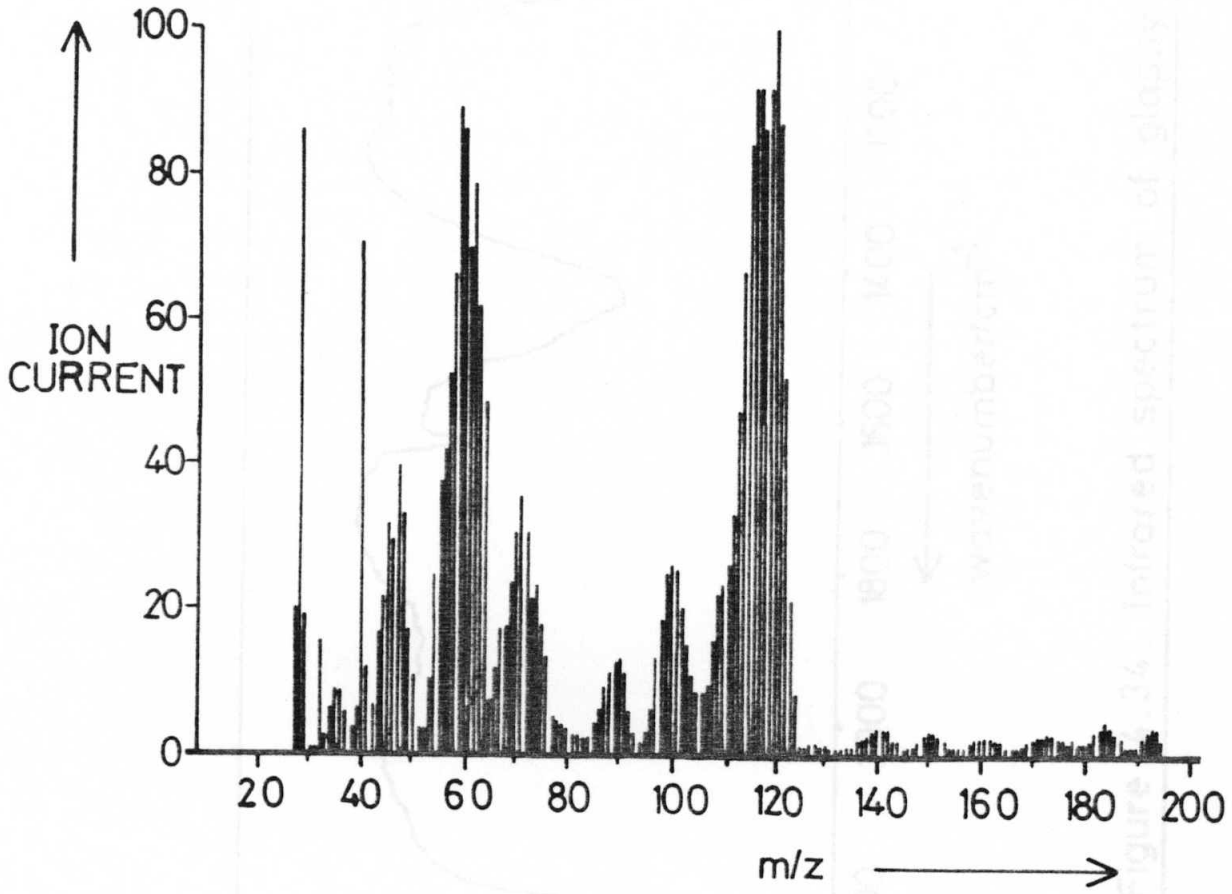

Figure 4.33. Mass spectrum of glassy solid

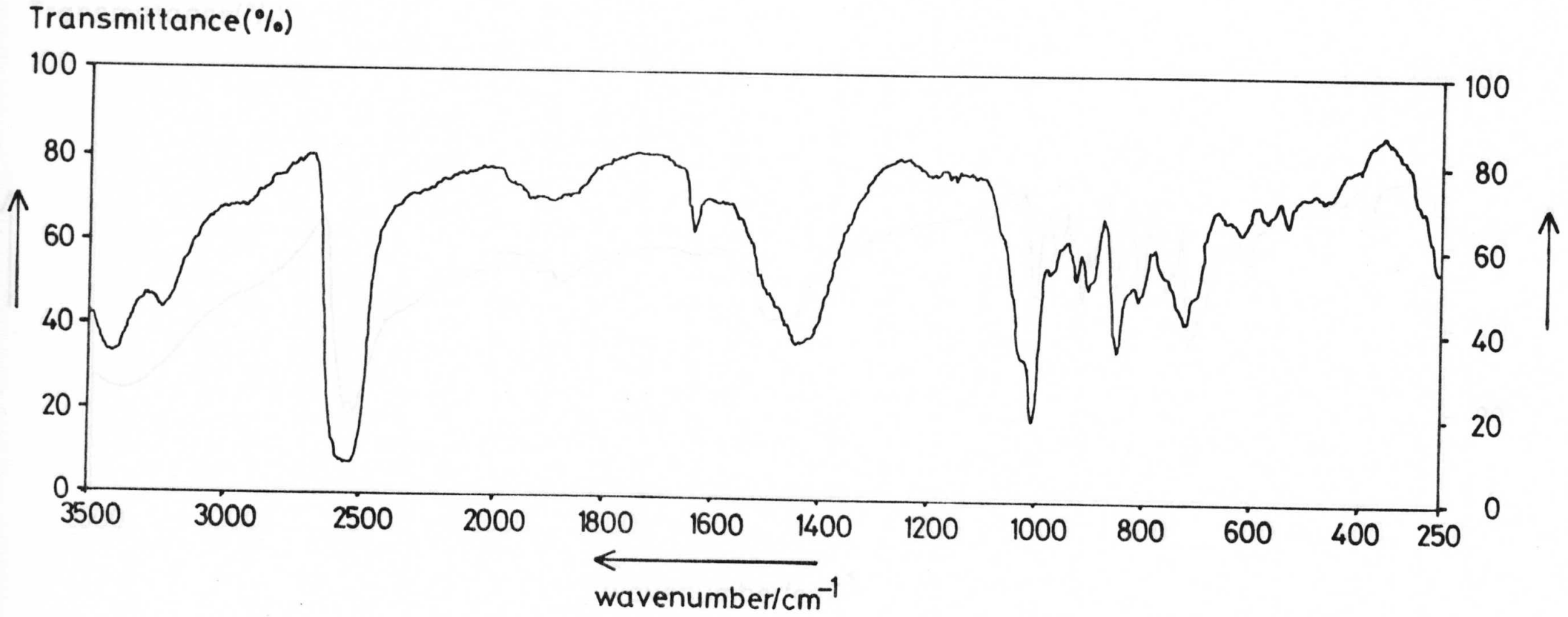

Figure 4.34. Infrared spectrum of glassy solid

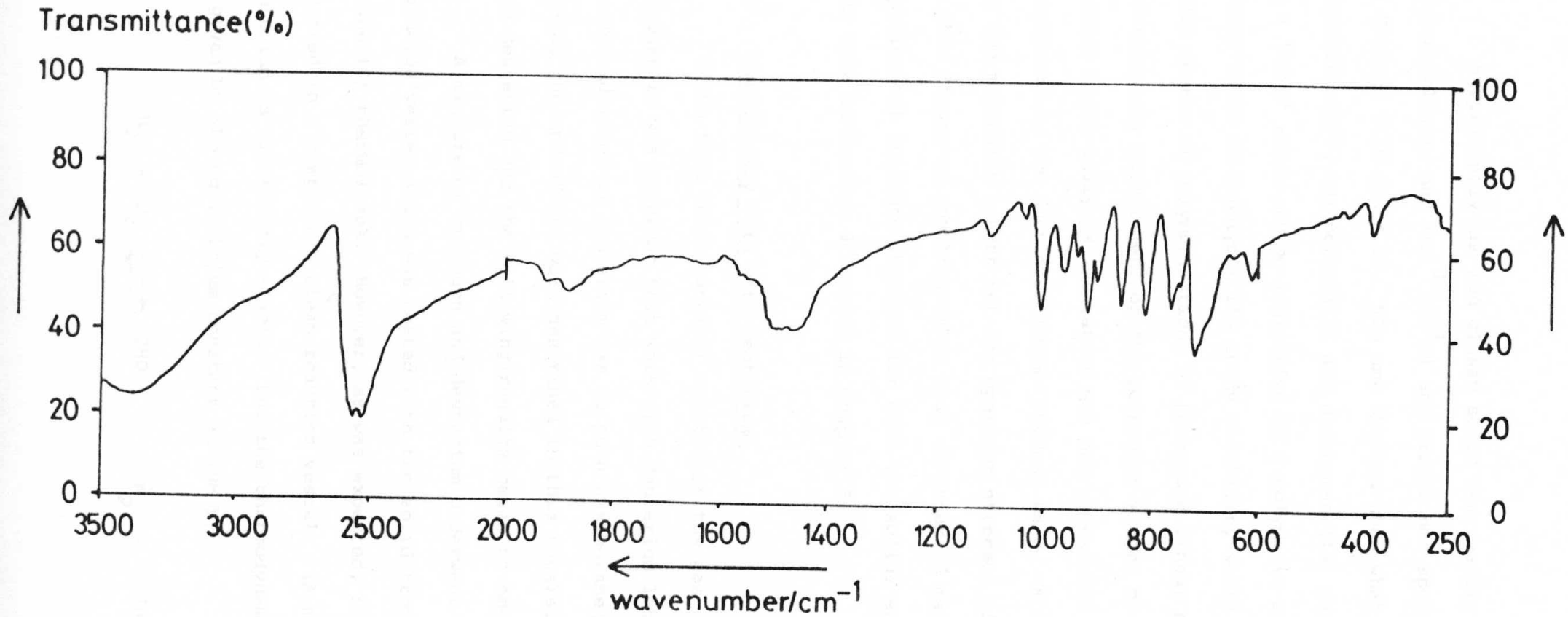

Figure 4.35. Infrared spectrum of decaborane(14)

Surprisingly the red glassy solid was readily soluble in deuterotoluene, and its $^{11}B-\{^{1}H\}$ and proton nmr spectra are presented in Figures 4.36 and 4.37. The nmr spectra show what are probably pentaborane(9), hexaborane(10) and decaborane(14) peaks superimposed on a 'hump' which may be indicative of a polymeric species. If the red glassy solid is a polymer its ready solubility would suggest a fairly small degree of polymerization, or perhaps a linear polymer. Unfortunately measurement of the molecular weight of the solid in the service micro-analysis laboratory was not successful as the substance was decomposed by the dichloromethane solvent used. A figure of 178 was obtained for the molecular weight but the operator stressed his lack of confidence in this figure as anything other than an order of magnitude. The experimental evidence obtained for both the solids encountered during this work is further discussed in Chapter 5.

4.9 Preliminary work with deuterium

Given that hexaborane(10) reacted in the gas phase with loss of hydrogen it was apparent that work with deuterium labelled hexaborane(10), or even addition of deuterium gas to pure hexaborane(10), merited attention. Towards the end of the work described in this thesis, some work was done with deuterium and the following results began to emerge.

A mixture of hydrogen and deuterium underwent exchange in an evacuated vessel which was coated with the solid from previous hexaborane(10) thermolyses. However, as was expected, no such exchange occurred in a completely clean reaction vessel. (A mixture of hydrogen and deuterium is kinetically stable, but the thermodynamically stable state is given by the equilibrium constant at 298 K;

$$H_2 + D_2 \rightleftharpoons 2HD \qquad K_p = 3.28$$

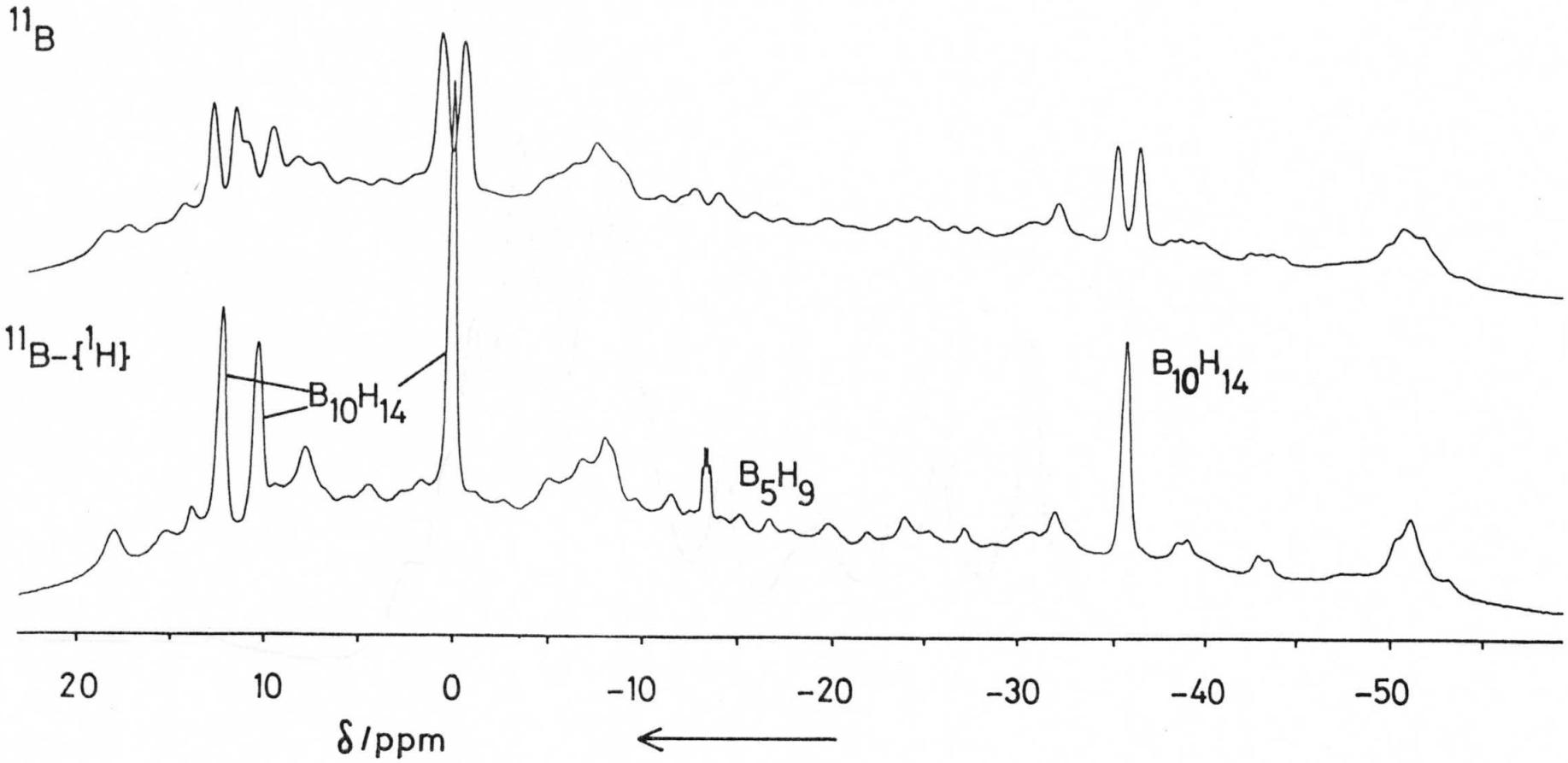

Figure 4.36. High field nmr spectra of glassy solid

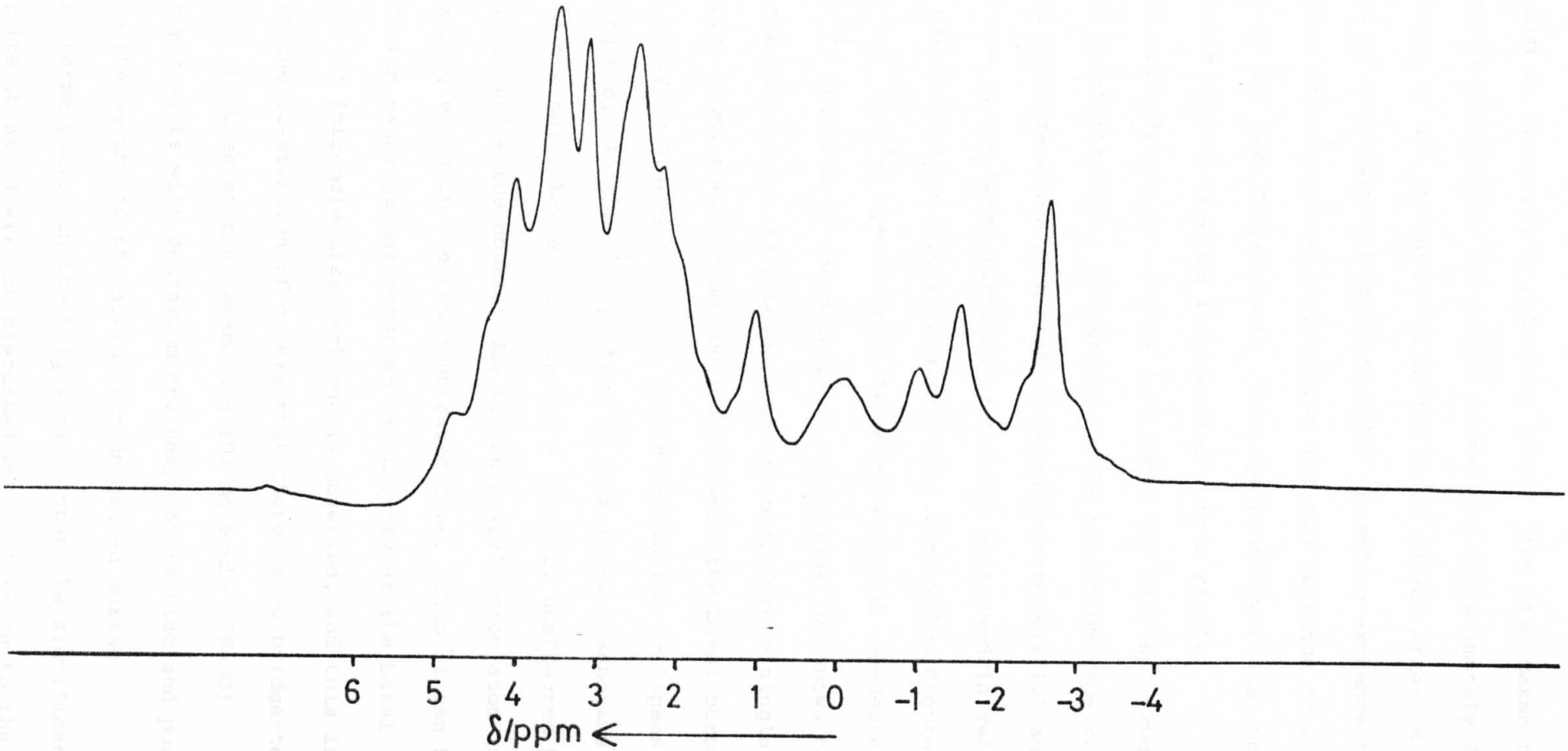

Figure 4.37. Proton nmr spectrum of glassy solid

This equilibrium is discussed in McLelland [77].) The time taken for equilibrium to be attained in the coated vessel was approximately 3 hours, while no exchange at all was observed in the clean vessel after 24 hours.

A mixture of deuterium and hexaborane(10) showed no exchange in a clean reaction vessel at room temperature, but did exchange in a coated vessel at the same temperature. Mass spectrometry showed that the maximum number of deuterium atoms incorporated into a single hexaborane(10) molecule was 5. Figure 4.38 shows the mass spectrum of the deuterated hexaborane(10). Comparison of the proton nmr spectrum of the deuterated hexaborane(10) with that of normal hexaborane(10) shows that the peak due to the basal terminal proton has decreased in relative intensity in the deuterated sample, Figure 4.39. Similarly, Figure 4.40 shows the ^{11}B and $^{11}B-\{^{1}H\}$ spectra for the deuterated and non-deuterated samples. The ^{11}B spectrum of non-deuterated hexaborane(10) shows two doublets, in the ratio 1:5. Each boron atom is coupled to a single terminal hydrogen atom, there is no coupling between the basal boron atoms and the bridging hydrogen atoms. Proton decoupling collapses both doublets to singlets. In the ^{11}B spectrum of deuterated hexaborane(10) the peak due to the basal boron atoms is now a singlet, unaffected by proton decoupling, while the doublet due to the apical boron atom is collapsed to a singlet as in the non-deuterated case. Thus it can be seen that deuterium exchange has occurred exclusively at the basal terminal sites. No intramolecular exchange is observed, and this is consistent with the observation of others that there is no bridge-terminal fluctionality in the base of the hexaborane(10) molecule [78-80].

These early results with deuterium are very interesting and pose questions as to the nature of the solid film deposited during hexaborane(10) thermolysis. In the following chapter the significance of all the results obtained will be discussed with reference to the

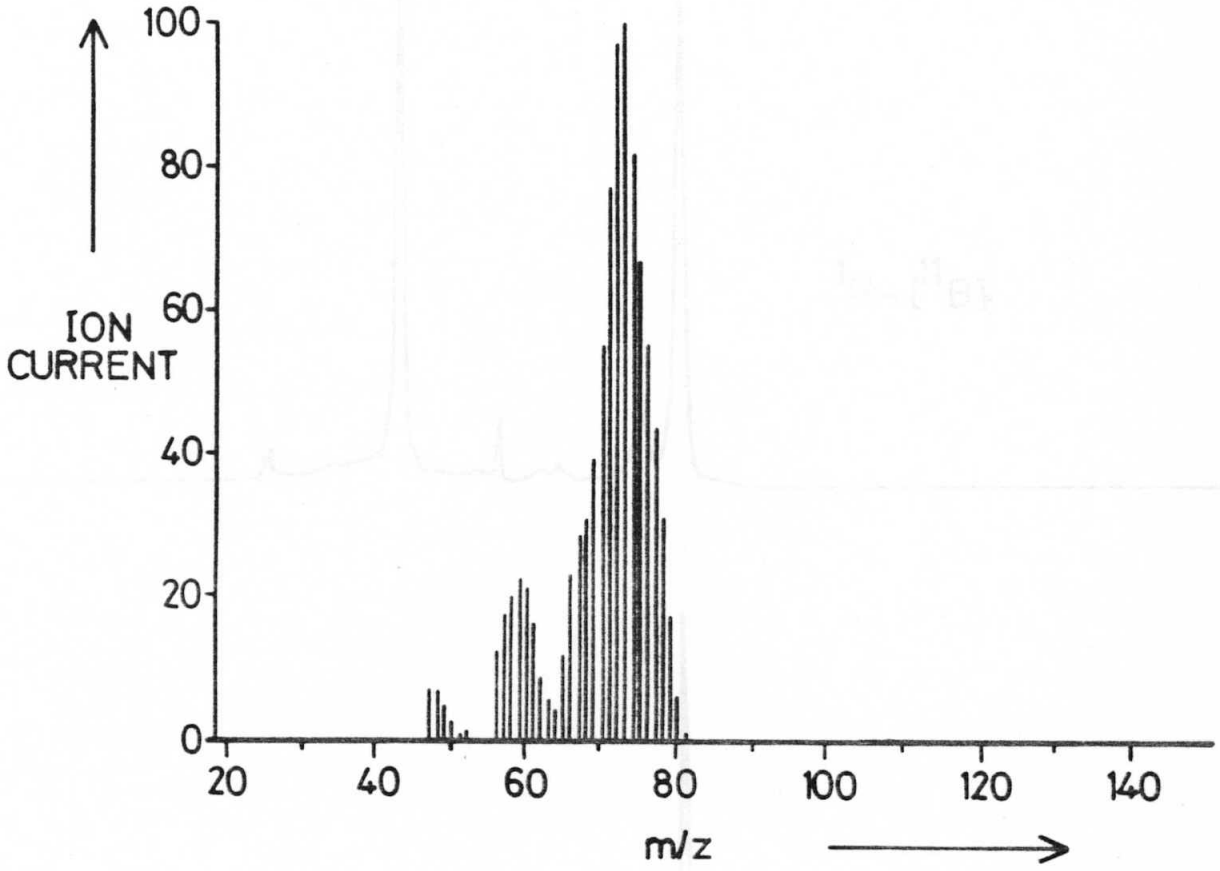

Figure 4.38. Mass spectrum of deuterated hexaborane(10)

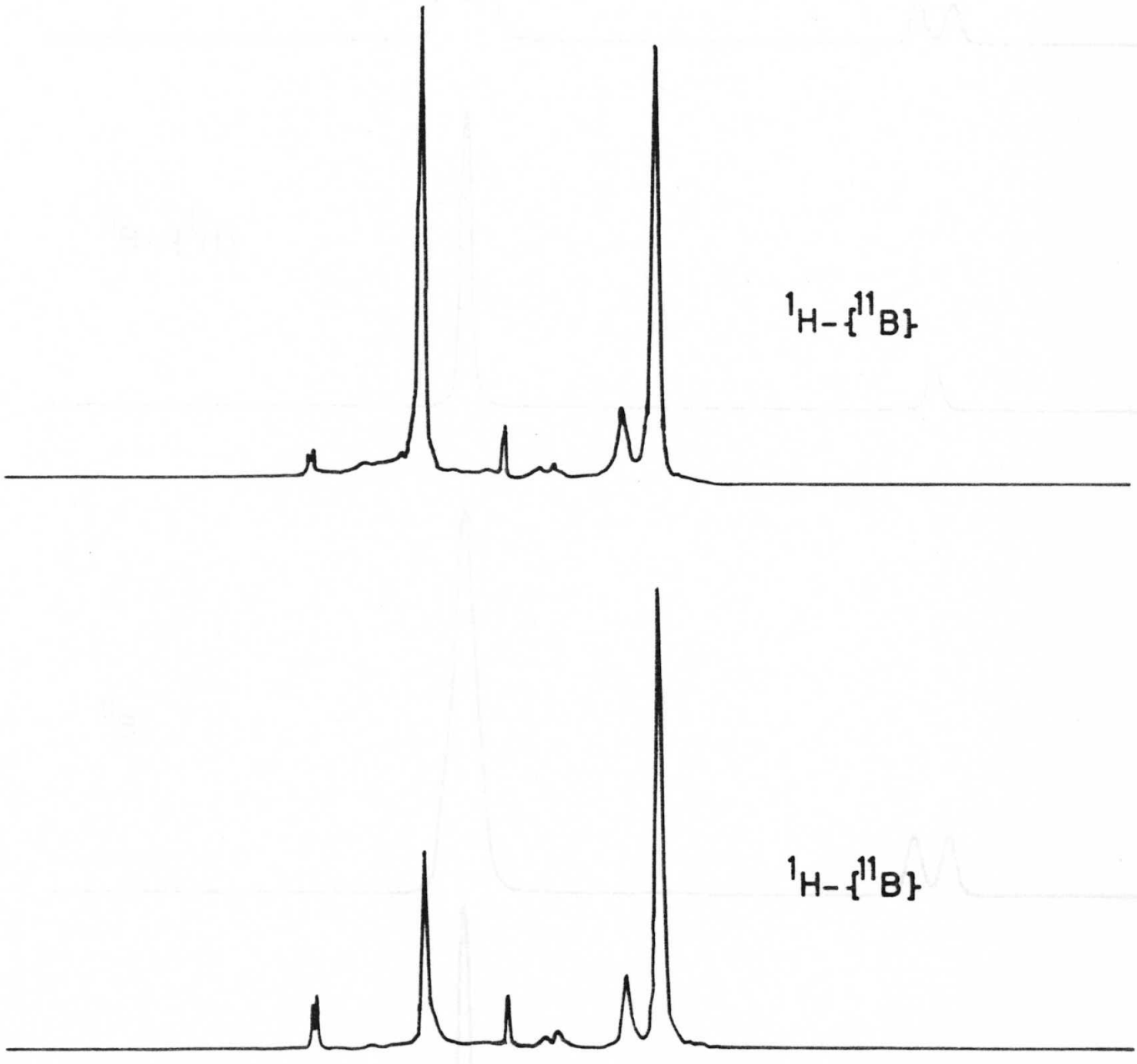

Figure 4.39. Proton nmr spectra of pure hexaborane(10) (top) and deuterated hexaborane(10)(bottom)

Figure 4.40. Nmr spectra of pure hexaborane(10)(top) and deuterated hexaborane(10)(bottom)

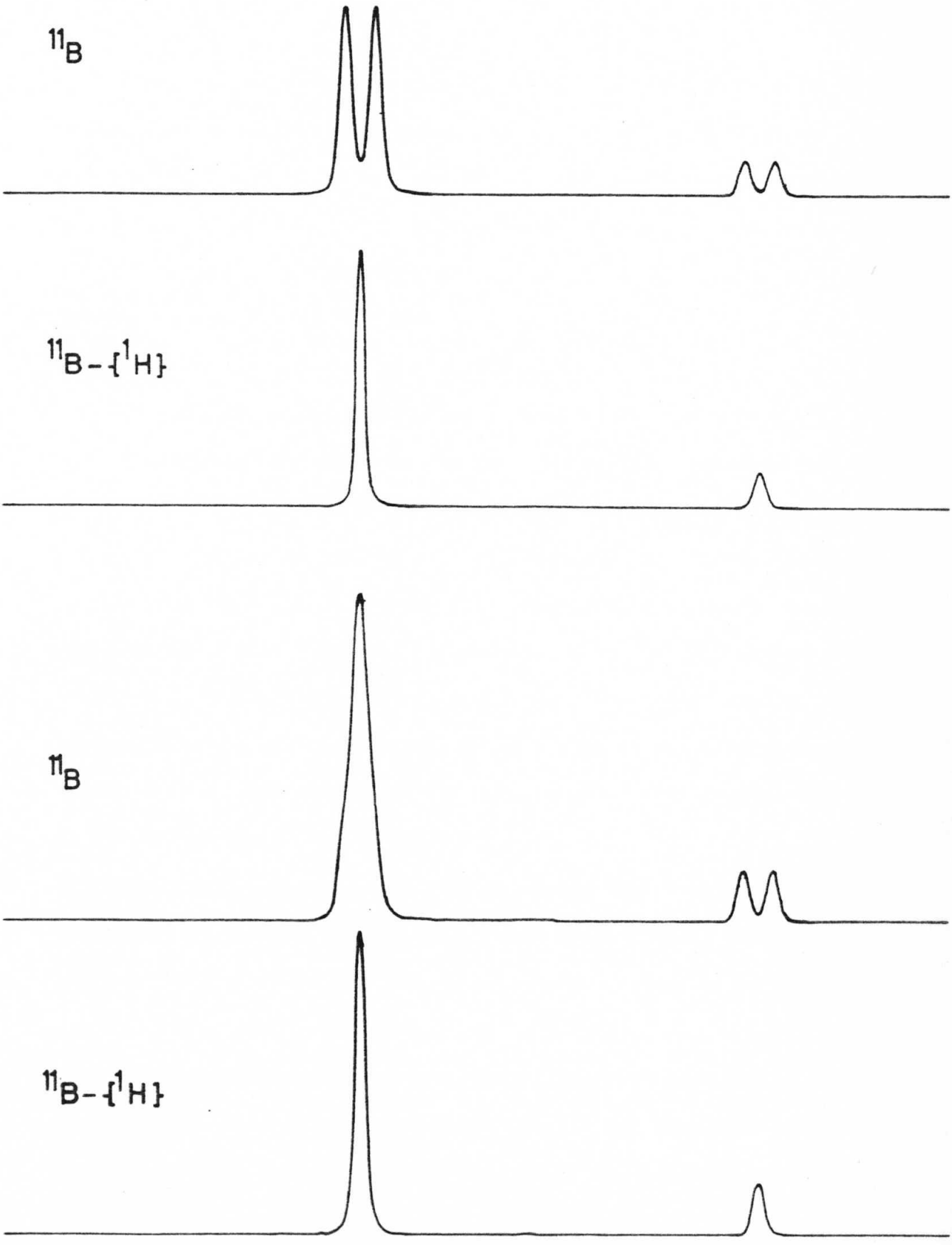

literature and an attempt will be made to interpret all the results in a self-consistent way and to suggest additional work which might be undertaken to further the investigation of the chemistry of hexaborane(10).

CHAPTER 5

Discussion

5.1 Background

There has been very little previous work concerned directly with the study of hexaborane(10) apart from that of Schaeffer's group [46-49] and Shore's group [45,53,54], and this has not specifically concerned mechanisms. Chapter 1 reviewed the different types of mechanistic step which have been postulated to occur in the gas phase thermolysis of boranes in general and the references in that chapter provide a comprehensive introduction to the literature.

The work described in this thesis adds to the large body of knowledge already possessed in the field of borane chemistry.

The project was started in the late seventies by Professor N.N. Greenwood, and his co-workers at that time were Dr. T. Spalding and Mr. D. Taylorson (now Dr. Taylorson). They designed and set up the original experimental system, i.e. a reaction vessel the contents of which could be sampled and analyzed by a mass spectrometer. The work was continued by Dr. R. Greatrex, notably the gas phase thermolysis of hexaborane(10). He also added the parallel MS10 spectrometer for use in hydrogen analysis (see Chapter 2).

The evidence up till this time suggested that hexaborane(10) decomposed to yield B_2H_6, B_5H_9, B_5H_{11} and small amounts of $B_{10}H_{14}$ and B_8H_{12} [81,82]. The rate of decomposition was thought to be appreciable (though not measured) at 348 K.

The initial measurements made by Dr. Greatrex cast doubts on the observations concerning hexaborane(10) in the two published papers [81,82]. Most importantly perhaps, he discovered that the hexaborane(10) used in

that early work was not pure, but contained some pentaborane(11). This was a co-product from the method of synthesis used to prepare the hexaborane(10) [83]. The hexaborane(10) was subsequently prepared by a different method [53,54] which produced more easily-handled side products, and was purified more stringently (but see Chapter 4, Section 4.6.2). Repeating some of the early measurements, Dr. Greatrex observed that the hexaborane(10) was much less reactive than previously thought, no reaction being discernible at 348 K. Initial attempts to measure the order of the reaction were not conclusive, with some data indicating first order kinetics while other data indicated second order kinetics (unpublished work).

The work described in this thesis runs essentially from that point, when the author joined the research group. It started with a series of experiments to determine with certainty the order of the gas phase thermolysis of hexaborane(10). The results are presented in Chapter 4 and are discussed further here.

5.2 Experimental method

Use of a mass-spectrometer to follow the changing composition of a complex gaseous reaction is not a common technique. A very important aspect of this work, from the point of view of establishing a firm foundation for the progress of the project in the future, was the development of the viscous flow sampling technique to the point where the results in Chapter 4 could be obtained, along with the supporting rationalization of that method and the explanation of the anomalies and ultimate failure of the original method (see Chapter 2.4.1). It is probably reasonable to claim that quantitative mass spectrometric analysis using viscous flow sampling is not documented in the literature.

5.2.1 Discussion of method; its strengths and limitations

The method in its present state affords a powerful and flexible means of analyzing a mixture of gaseous boranes. Any mixture of gases could be analyzed in fact, one would merely need to replace the standard spectra and calibration curves of the boranes with those of the relevant gases (see Chapter 3). It is also possible therefore to follow the cothermolysis of the boranes with other gases, i.e. carbon monoxide, by the same experimental method. Obviously the method is less effective when the gaseous system under study produces condensed phases, but even then much useful information can be gained, as the results in Chapter 4 show. The timescale of the reacting system under study is also critical. Reactions with half-lives of the order of minutes are too fast to be studied by this method, although the mass spectrometer may still be of use, particularly if a technique such as multipeak monitoring were to be used. In that technique the spectrum is not scanned but measured continuously at selected m/z values.

As a result of the developments described in Chapter 2 the method is now soundly based. In practice it has performed broadly as expected, i.e. calibration curves can be predicted to be nearly linear, in contrast to the use of viscous flow without a background of excess inert gas, which gave quadratic calibration curves. The prediction of near linearity is borne out by the observed facts. Again, any so-called suppression of the spectrometer's response to one gas by another, so troublesome with the original method, is predicted to be negligible, and this is what is found in practice.

Any data which were disregarded as unreliable were usually obtained during periods of spectrometer malfunction. It was found by experience that, just as the MS30 source was about to burn out, ion-current measurements separated by as little as thirty seconds might bear no resemblance to each

other, and at such times frequent retuning of the spectrometer was necessary. Replacement of the source invariably solved the problem until the new source too burnt out, usually after about one week of continuous use. Occasionally a source would be unsatisfactory from the time it was fitted, due perhaps to some misalignment or poor insulation.

5.2.2 Possible development of experimental method

There is some scope for future refinement and development of the experimental method, in all of its aspects.

The gas mixing and metering line can be adapted in a very short space of time to suit any particular job that may be required of it. Some mechanical method of pressure measurement might be added; this would make pressure measurement easier, perhaps more accurate, and eliminate the need for the mercury manometer.

The reaction vessel itself is at present designed so that replacement is a short job for a glassblower, but two possible improvements might be made. If the reaction vessel were suspended in a thermostatted oil bath, then temperature control would be easier and more accurate. The oil bath would need to be on a jack so that it could be raised and lowered for reaction vessel inspection and replacement. Perhaps more beneficial would be the incorporation of a mechanical mixing device in the reaction vessel (together perhaps with a similar device in the vacuum line). Such a device might take the form of a glass- or PTFE-enclosed magnetic paddle which could be driven from outside the reaction vessel. With mechanical stirring of the gas reaction mixtures, long periods of waiting to ensure efficient mixing could be eliminated, but the reaction vessels would of course be more complex and expensive to make.

There is much opportunity for fuller use of computers in the

analysis of data. Due only to lack of time for the development of suitable programs, much of the kinetic analysis of the data and many of the plots of mixture composition are presently produced by hand; much of this effort could be removed. The main analysis program at present produces its output in tabular form, consisting of the experimentally observed mass spectrum of the mixture, the calculated spectrum for the mixture, and the difference between the two at each m/z value in the spectrum. By presenting these data additionally in graphical form, assessment of the data would be easier and quicker, and would highlight systematic differences which might be indicative of experimental error or even significant but unexpected reaction features.

5.3 Discussion of experimental results

The salient features of the gas-phase thermolysis of hexaborane(10) are summarized and discussed below, and the author's interpretation of the experimental evidence is presented.

The thermolysis of hexaborane(10) in the gas phase follows second order kinetics over the temperature range 100-165°C (373-438 K) for pressures of hexaborane(10) in the range 1-7 mmHg (in a background of 100 mmHg of helium). The activation energy was found to be 79 ± 5 kJ mol^{-1} with a pre-exponential factor of 3.6×10^{6} m^{3} mol^{-1} s^{-1}. The products of the reaction are hydrogen, a non-volatile solid on the wall of the reaction vessel, pentaborane(9) and decaborane(14). There is also mass spectral evidence for octaborane(12), a nonaborane and a species containing 12 boron atoms.

The pentaborane(9) and decaborane(14) were formed in an approximate ratio of 5:1 (see Table 4.3). Jointly the pentaborane(9) and decaborane(14) accounted for approximately 5-10% of the hexaborane(10) consumed. As no other volatile products were observed in significant

amounts, it follows that the non-volatile solid on the wall of the reaction vessel accounted for the other 90-95% of the hexaborane(10). The pressure of hydrogen formed ranged between one and two times the pressure of hexaborane(10) consumed.

It seems likely therefore that two routes of reaction are open to the thermolysing hexaborane(10); a major route leading to the non-volatile solid and hydrogen, and a minor route producing pentaborane(9) and decaborane(14). Because of the great thermal stability of pentaborane(9) and decaborane(14) at the temperatures used in this work [84,85], it is believed that they are probably the end products of the mechanism which leads to them, and not intermediates in the formation of the solid.

It was initially thought that the heaviest species observable in the gas phase during these experiments was decaborane(14), but as stated above it is unlikely that this could be an intermediate in the formation of the solid. However, as described in Chapter 4.6.2, a dodecaborane species was observed later in the work. It was identified as a true 12 boron species by accurate mass measurement, but at the time of writing the number of hydrogen atoms has not been established. The pressure of the B_{12} species was estimated to be about three orders of magnitude lower than that of the hexaborane(10), i.e. approximately 0.001-0.01 mmHg. It was observable throughout the reactions, and also observable in pure samples of hexaborane(10) at room temperature, but it was not observed in reactions where the hexaborane(10) pressures had fallen to low levels.

5.3.1 $B_{12}H_x$: Product, intermediate or secondary ion?

At the fifth International Meeting of Boron Chemists, IMEBORON V, held at Swansea University in July 1983, it was suggested by Professor T.P. Fehlner, of Notre Dame University, Indiana, that the B_{12}

species may be the result of an ion-molecule reaction in the source of the spectrometer and not in the reaction vessel, i.e.

$$B_6H_x^+ + B_6H_{10} \xrightarrow{\text{source}} B_{12}H_{10+x-n}^+ + nH\bullet$$

where n may be zero or positive. Professor Fehlner suggested that one way of determining whether this was the case would be to observe the dependence of the ion current of the B_{12} species on the pressure of B_6H_{10} in the sample. The literature is clear on this point [86,87], stating that the ion current of a primary ion will vary as the first power of the pressure of the neutral forerunner in the sample, while the ion current of a secondary ion (i.e. one produced in an ion-molecule reaction in the source) will vary as the second power of the pressure of the neutral forerunner, since the reaction in the source is

$$A^+ + A \xrightarrow{\text{source}} B^+ + C$$

where B^+ is the secondary ion. Because the concentrations of A^+ and A in the source are both proportional to the concentration of A in the sample, then the concentration of B^+ is proportional to the square of the concentration of A in the sample.

This reasoning is all very well, but since the pressure of the postulated parent B_{12} species in the sample cannot be measured, and since it is believed to be formed in a mechanism which follows second order kinetics with respect to hexaborane(10), the intensity of the B_{12}^+ ion will vary as the second power of the pressure of hexaborane(10) in the sample irrespective of whether it is a primary or a secondary ion. One way around this problem would be to vary the pressure of hexaborane(10) in the source without varying the pressure of hexaborane(10) in the sample; this can be done by using different capillary lengths between the reaction vessel and the source.

Another method of distinguishing between primary and secondary ions is to vary the repeller voltage in the source. The relative intensity of a secondary ion should decrease as repeller voltage increases [88]. This is because as the primary ions gain kinetic energy, their collision cross-section decreases, hence fewer secondary ions are formed [89]. It is important to measure the *relative* ion currents as alteration of repeller voltage affects the absolute values of all ion currents (hopefully to an equal extent across the mass spectrum, else the test is meaningless). If this test appears to be positive, confirmation can be made by a further test. If a secondary ion is suspected, its ion current relative to that of its precursor should remain constant as the energy of the ionizing electrons is varied [89], unless of course the suspected secondary is in fact a primary and its appearance potential is fortuitously similar to that of the suspected precursor.

Most of the secondary ions mentioned in the literature are formed by transfer of a hydrogen atom from a neutral molecule to an ion [88], and this process is very commonly observed in organic mass spectrometry where peaks at m/z ratios M + 1 (where M is the mass of the parent ion) are often observed.

If no neutral species are released during the formation of a secondary ion, the process is described as *attachment*, e.g.

$$B_6H_x^+ + B_6H_{10} \longrightarrow B_{12}H_{10+x}^+$$

Now the literature talks in terms of "larger groups such as acetyl becoming attached" as being unusual, and no examples were given of secondary ions at m/z values $\sim$2M from parents of m/z values M [87,88], so the expectation of formation of a secondary ion from two species each

containing six boron atoms is by implication low. A further argument against attachment of a large group is that no neutral species is released which can carry away the excess kinetic energy from the collision. In fact attachment reactions often require a third body collision to stabilize the newly formed secondary ion and so secondary ions formed in attachment reactions are often seen to follow a third power dependence on the pressure of the sample [87].

Some initial work has been done on the question of whether or not the B_{12} species is 'real' or formed in a secondary process in the source, but the position is not yet clear.

5.3.2 Observations on the polymeric materials

It is interesting to compare the experimental findings concerning the two solids studied in this work; the involatile solid which formed in the reaction vessels and the red glassy solid obtained from a sample of hexaborane(10) sealed under vacuum at room temperature for several months. Comparing the ir spectra of the two substances (Figures 4.30 and 4.34) it can be seen that they are broadly similar in the region from 4000 cm^{-1} to 1200 cm^{-1}, when the spectra diverge in appearance. There is more detail in the spectrum of the glassy solid below 1000 cm^{-1}. Both samples were prepared by grinding with KBr in a moisture- and oxygen-free glove box, and compressing into a disc suitable for the ir spectrometer sample holder. Comparison of these two spectra with the ir spectrum of a sample of decaborane(14) obtained in the same way (Figure 4.35) also reveals similarities in the region 4000 cm^{-1} to 1200 cm^{-1}, with divergence below 1000 cm^{-1}.

The mass spectrum of the red glassy solid is interesting but perhaps misleading. A large sample of the solid shows in its spectrum pentaborane(9), hexaborane(10), decaborane(14) and hexadecaborane(20),

Figure 4.33. But as stated in Chapter 4.7, these species are believed to be suspended in an involatile matrix. No mass spectrum was obtained from the solid coating the reaction vessels, this may have been partly due to the difficulty of scraping even a small sample from the walls to introduce into the direct probe of the spectrometer.

Both ^{1}H and ^{11}B nmr spectra were obtained from the two solids, Figures 4.31, 4.32, 4.36 and 4.37. The spectra of the red glass were the most informative, showing peaks characteristic of pentaborane(9), hexaborane(10) and decaborane(14), rising from a markedly humped baseline. As the sample was very strong, instrumental causes of the hump in the baseline can be excluded, and the hump is probably due to the presence of polymeric species in the sample.

The nmr spectra obtained from the solid reaction vessel coating are very curious. The sample was in perdeuterotoluene solution, and was extremely weak. The ^{1}H spectrum appears to be essentially that of the proton-containing impurities in the solvent, these peaks remaining unchanged on ^{11}B decoupling. However only one very weak peak was observed in the ^{11}B spectrum. This was a doublet at $\delta 4.5$ which became a singlet when ^{1}H decoupled. It is the only signal in the entire spectrum, and appears to be coupled to only one proton. However it did require the accumulation of 25,000 scans to obtain the spectrum, and may just be due to an interesting but extremely minor and slightly soluble component of the reaction vessel coating.

5.3.3 Deuteration work

It is immediately apparent from the preliminary work with deuterium (see Chapter 4.9) that the solid which forms on the walls of the reaction vessel is not inert, and that it plays a part in the exchange of deuterium and hydrogen, both in the reaction

$$H_2 + D_2 \rightleftharpoons 2HD$$

and

$$B_6H_{10} + D_2(\text{excess}) \rightleftharpoons B_6H_5D_5 + H_2/HD/D_2$$

Carter and Mock showed that there was no intermolecular exchange of hydrogen between molecules of hexaborane(10), but that deuterium is exchanged between deuterated diborane(6) and hexaborane(10) [78]. We have shown that exchange occurs between hexaborane(10) and deuterium in a vessel coated with the solid produced by thermolysis of hexaborane(10). Since no exchange was observed in a clean vessel, the deuterium must be first incorporated into the solid on the wall and then into the hexaborane(10). Since base terminal substitution is the result, it may possibly be via some acid-base reaction between the non-bridged boron-boron bond in the base of the hexaborane(10) and the surface of the solid on the wall.

5.3.4 Possible mechanisms of thermolysis

It is possible that at least two mechanisms are involved in the thermolysis of hexaborane(10); the major mechanism in which 90-95% of the hexaborane(10) consumed gives hydrogen plus the solid on the wall of the reaction vessel, and the minor route which leads to pentaborane(9) and decaborane(14).

Taking the minor route first, the following mechanism is postulated as a result of this work:

$$B_6H_{10} + B_6H_{10} \longrightarrow \{B_7H_{11}\} + B_5H_9$$

$$\{B_7H_{11}\} + B_6H_{10} \longrightarrow B_8H_{12} + B_5H_9$$

$$B_8H_{12} + B_6H_{10} \longrightarrow B_9H_{13} + B_5H_9$$

$$B_9H_{13} + B_6H_{10} \longrightarrow B_{10}H_{14} + B_5H_9$$

i.e. overall $5B_6H_{10} \longrightarrow B_{10}H_{14} + 4B_5H_9$

This mechanism, which involves only {BH} transfers, is satisfyingly simple; it is in accord with experimental evidence and suggests at least one test which could be made to aid in verifying whether the mechanism actually occurs. The mechanism predicts a pentaborane(9): decaborane(14) ratio of 4:1, and the experimental average value of this ratio was found to be 5:1 (see Table 4.3). The fate of all the intermediates in the mechanism is to react further with hexaborane(10), which is the only abundant species present and therefore the most likely molecule to be encountered in a collision. Octaborane(12) is identified (not quantitatively) in small amounts in thermolyzing reaction mixtures. Recently Dr. Greatrex has done some work with hexaborane(10) at about 60-70°C in which he observed a nonaborane species, but this is very new work and has not involved the author. Of course, no heptaborane species is observed in the mass spectra of these reaction mixtures, and it is generally agreed that heptaboranes do not exist as isolable species [13], and are not postulated as unstable intermediates. It may be possible that a heptaborane species may exist very fleetingly in the above mechanism. Alternatively the first two steps may occur in a more concerted fashion so that any heptaborane may not be formed in an independent state.

The mechanism involves the successive transfer of BH groups. Such a transfer is frequently postulated for reactions involving triborane(7) [8], and a similar process is invoked to explain the formation of decaborane in the thermolysis of diborane, see Chapter 1.3 and references [8] and [13]. Hexaborane(10) molecules would have to be capable of donating or accepting BH groups, such a capability would certainly be in keeping with the dual acid/base nature of hexaborane(10). One experiment which might be tried to test this mechanism is to examine the reaction

between one equivalent of octaborane(12) and two equivalents of hexaborane(10). Under the correct temperature conditions one might expect, if the postulated mechanism is correct:

$$B_8H_{12} + 2B_6H_{10} \longrightarrow B_{10}H_{14} + 2B_5H_9$$

Such an experiment would be feasible as octaborane(12) can be prepared from nonaborane(15) [13], which in turn is easily prepared [90]. Although a qualitative experiment, using octaborane(12) prepared *in situ*, would be easier than a quantitative reaction, its interpretation would require more care.

Turning now to the major mechanism, there are several possible ways to disproportionate two hexaborane(10) molecules, i.e.

A $B_6 + B_6 \longrightarrow B_7 + B_5$

B $B_6 + B_6 \longrightarrow B_8 + B_4$

C $B_6 + B_6 \longrightarrow B_9 + B_3$

D $B_6 + B_6 \longrightarrow B_{10} + B_2$

E $B_6 + B_6 \longrightarrow B_{11} + B_1$

F $B_6 + B_6 \longrightarrow B_{12}$

The first of these (A) has already been discussed as the minor reaction route

B $B_6 + B_6 \longrightarrow B_8 + B_4$

An octaborane species is indeed observed, but this can be explained by the mechanism postulated above, (A). Arguing most strongly against B is the fact that tetraborane(10) is not observed in the products. Admittedly, even at the lowest temperatures used in this work,

100°C, tetraborane(10) would be short lived [91], although it is not unreasonable to expect that it would be observed. Were tetraborane(8) produced, it would almost certainly lead to some tetraborane(10) by addition of the H_2 which is in plentiful supply once the reaction is under way.

C $\quad B_6 + B_6 \longrightarrow B_9 + B_3$

Again, any nonaborane might be explicable by the minor reaction mechanism above. The triborane presents a more interesting problem. Only two neutral triborane species are possible, triborane(7) and triborane(9) and these are interconvertible in the presence of hydrogen [8,14,15,23]. As neither of them are isolable species, their chemistry is not well studied, and their reaction with hexaborane(10) has never been studied, although Long postulated the step [8]

$$B_3H_7 + B_6H_{10} \longrightarrow B_9H_{15} + H_2 \ .$$

Were triborane(7) formed, and were it to react by transferring a BH to hexaborane(10), diborane(6) would be expected to be observed, but this is not the case. Were it to accept a BH group, then tetraboranes would be observed, again not the case. Triborane(9) would be expected to lead to diborane(6) or tetraborane similarly.

D $\quad B_6 + B_6 \longrightarrow B_{10} + B_2$

Only one diborane species is possible, diborane(6). It is not observed in this work and so its absence would appear to preclude this mechanism.

E $\quad B_6 + B_6 \longrightarrow B_{11} + B_1$

Undecaborane chemistry is not well documented. If monoborane(3)

were produced, then some diborane(6) might be expected as the product of its dimerization [7,27,28], but this is not the case.

$$F \qquad B_6 + B_6 \longrightarrow B_{12} \ (+ H_2\uparrow?)$$

The fact of second order kinetics, and the observation of a twelve-boron species, together with the absence of otherwise common species such as diborane(6) and tetraborane(10) prompts the postulation of this step as the rate-determining step in the major route of thermolysis of hexaborane(10). An equilibrium step

$$B_6H_{10} + B_6H_{10} \rightleftharpoons B_{12}H_{18} + H_2$$

or similar is unlikely for two reasons. The first is that no exchange is observed between hexaborane(10) and deuterium in a clean reaction vessel, and the second is that in experiments with added hydrogen or deuterium, the B_{12} species was observed in amounts comparable to experiments with no added hydrogen or deuterium. Since the equilibrium constant would be very small if an equilibrium existed, addition of hydrogen in appreciable amounts would cause a very noticeable reduction in the amount of B_{12} present, perhaps even cause its disappearance altogether from the observable spectrum of the reaction mixture, but this does not occur.

Only two fates can be envisaged for the B_{12} species which are consistent with the absence of any heavier species in the observed gas-phase spectra of the reaction mixtures, and which are at all likely. The first entails a rapid but short polymerization reaction where the B_{12} molecule reacts with further hexaborane(10) molecules, releasing hydrogen molecules and attaining a molecular weight high enough to cause condensation and therefore no observation of the heavier intermediates. Polymerization may then continue on the walls of the reaction vessel,

probably with further release of hydrogen.

The alternative is that the B_{12} molecules react with the wall of the reaction vessel, and polymerize on the surface. Experiments with different reaction vessel surfaces or surface areas may help to distinguish between these two scenarios, but may be unhelpful since the rate determining step of two hexaborane(10) molecules coming together seems to occur in the gas phase.

5.3.5 Future work

The project described in this thesis is of course continuing, and so the work presented is by nature open-ended, answering many questions while at the same time raising others. Perhaps the most intriguing of those questions is the structure of the proposed dodecaborane intermediate, and indeed its exact formula, since the number of hydrogen atoms in the species is not yet established. Since the species (if it is formed in the reaction vessel, and not as a secondary ion) is not long-lived, the determination of its molecular weight will probably be achieved most easily by mass spectrometry. Chemical ionization sources tend to produce less fragmentation of sample molecules and may possibly be of use in this problem.

More work on the solid deposited on the walls of the reaction vessel is needed. This would be facilitated by production of the solid in greater amounts, possibly on a vacuum line away from the spectrometer. A layer thick enough to be scraped off the vessel walls would enable a more complete study to be made of its solubility, average molecular weight, nmr spectra etc.

The red glassy solid which is obtained by sealing liquid hexaborane(10) at room temperature is extremely interesting. Its average molecular weight has not been established with any certainty, and its nmr spectra suggest that it is a polymeric material with some boranes

occluded (see Chapter 4.8). If the solid can be purified by recrystallization (it is very soluble in toluene) or chromatography etc., a more accurate elemental analysis could be made, and experiments to confirm or refute a polymeric nature could be performed. Limited hydrolysis, if possible, may allow information to be gained about the basic structural units of the polymer. Another approach would be to seal up more samples of hexaborane(10) under similar conditions and to examine them at regular intervals by techniques such as mass spectrometry, nmr, vapour pressure measurement, refractive index, freezing point measurement etc. Some of this information would be very simple to obtain accurately, and would be most informative as to the nature of the solid.

Surface effects on the rate of thermolysis of hexaborane(10) must also be studied. Although the rate determining step appears to take place in the gas phase (the kinetics are second order with respect to the concentration of hexaborane(10); a reaction involving the wall might be expected to vary between zero and first order as the hexaborane(10) pressure is reduced) it is not clear whether the fate of the postulated B_{12} intermediate is gas phase polymerization or reaction at the walls of the vessel.

Finally, for the time being, the cothermolysis of hexaborane(10) with other boranes would be of interest. Certainly the reaction of a 2:1 mixture of hexaborane(10):octaborane(12) would be informative from the point of view of the proposed minor reaction route. Cothermolysis of hexaborane(10) with pentaborane(9) and/or decaborane(14) would be a confirmative test of the mechanisms proposed, and should not give rise to any species not observed in the thermolysis of hexaborane(10) on its own.

Since diborane(6) and tetraborane(10) are not observed in this

work, their respective cothermolyses with hexaborane(10) may give interesting new results. Although the cothermolysis of tetraborane(10) and hexaborane(10) has already been looked at in a preliminary study in this research group [82], the hexaborane(10) used in that work is now known to have been impure, so the work needs to be repeated.

APPENDIX A

This appendix contains the data used to calibrate the response of the mass spectrometer to sample pressures in the reaction vessel. The hydrogen calibration curve is constructed from the hydrogen ion current relative to that of the background helium in the calibration gas mixture. All calibration gas mixtures contained a background pressure of 100 mmHg of helium. See Chapter 3.1 for a full description of the calibration procedure.

Also given are the standard mass spectra of pentaborane(9), hexaborane(10) and decaborane(14) which were used in the analysis program.

Standard mass spectra used in this work

Pentaborane(9)

m/z range: 55-64

ion current at each m/z value:

264, 297, 317, 717, 1237, 995, 1142, 970, 1203, 939

Hexaborane(10)

m/z range: 35-76

ion current at each m/z value:

72, 34, 0, 0, 0, 0, 0, 0, 54, 183, 346, 459, 473, 277,
55, 0, 0, 48, 309, 881, 1385, 1677, 2027, 2165, 1986,
1047, 158, 94, 95, 591, 1692, 3054, 3672, 4025, 5539,
8028, 10570, 9746, 6318, 6029, 3918, 2532

Decaborane(14)

m/z range: 55-124

ion current at each m/z value:

116, 441, 244, 297, 222, 0, 0, 0, 0, 0, 0, 0, 0, 0, 0, 0,
0, 0, 0, 0, 0, 0, 0, 0, 0, 0, 0, 0, 146, 275, 302, 318,
334, 342, 341, 256, 96, 0, 0, 35, 167, 396, 667, 861, 1000,
996, 772, 510, 313, 197, 187, 317, 591, 838, 950, 1101, 1534,
2354, 3561, 4729, 5440, 5629, 5227, 5637, 6376, 5424, 3171,
1206, 446

Argon calibration data

pressure/mmHg	ion current
2·15	29,000
4·10	55,500
6·10	76,500
8·30	103,000
10·30	125,000
12·30	160,000

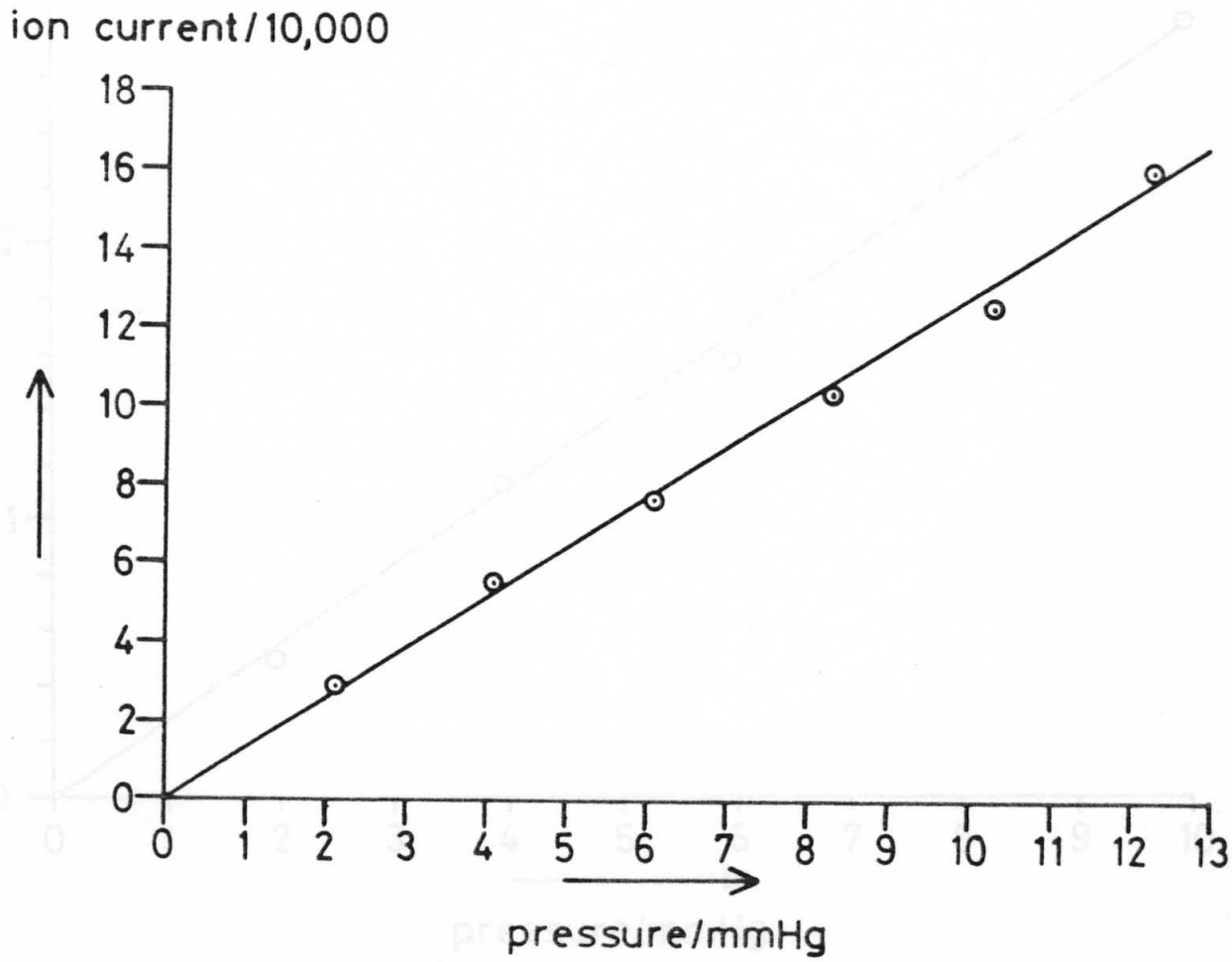

Hydrogen calibration data

pressure/mmHg	H_2/He ion current ratio
1·96	0·049
3·95	0·113
5·96	0·157
7·90	0·221
9·95	0·280

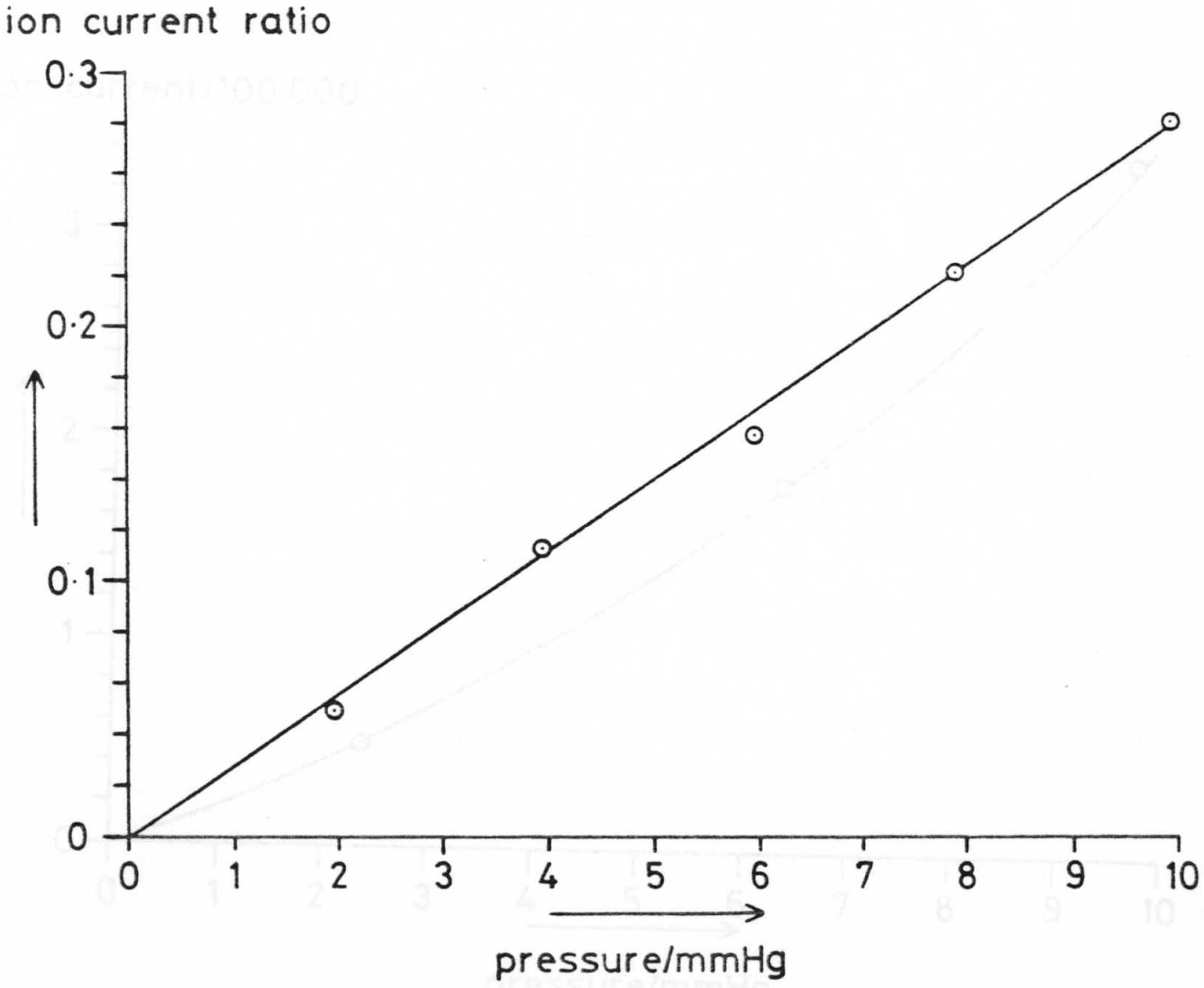

Hexaborane(10) calibration data

pressure/mmHg	ion current
2·4	50,000
6·4	180,000
9·7	340,000

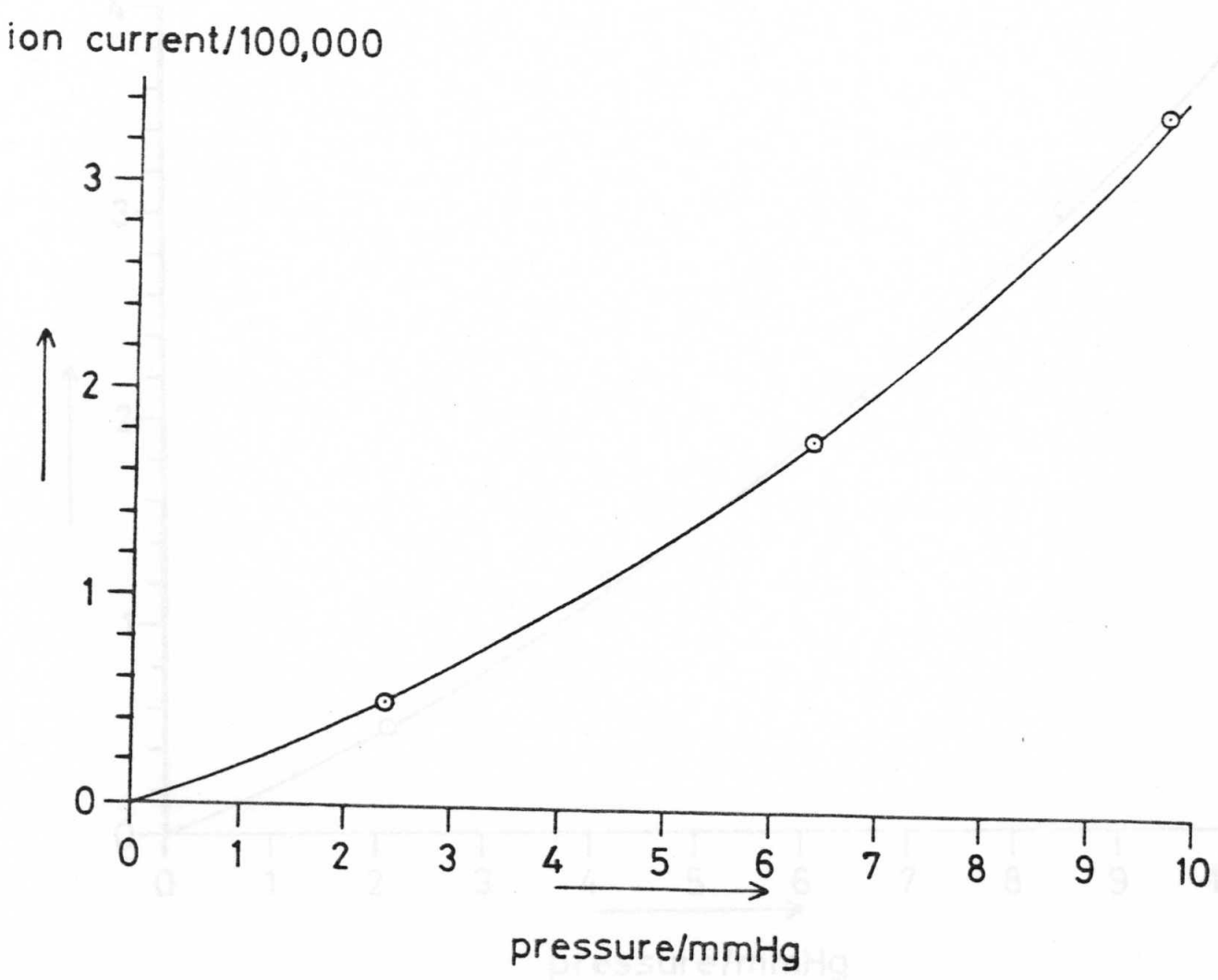

Pentaborane(9) calibration data

pressure/mmHg	ion current
2·1	50,000
4·2	122,500
6·7	210,000
8·5	300,000
10·5	385,000

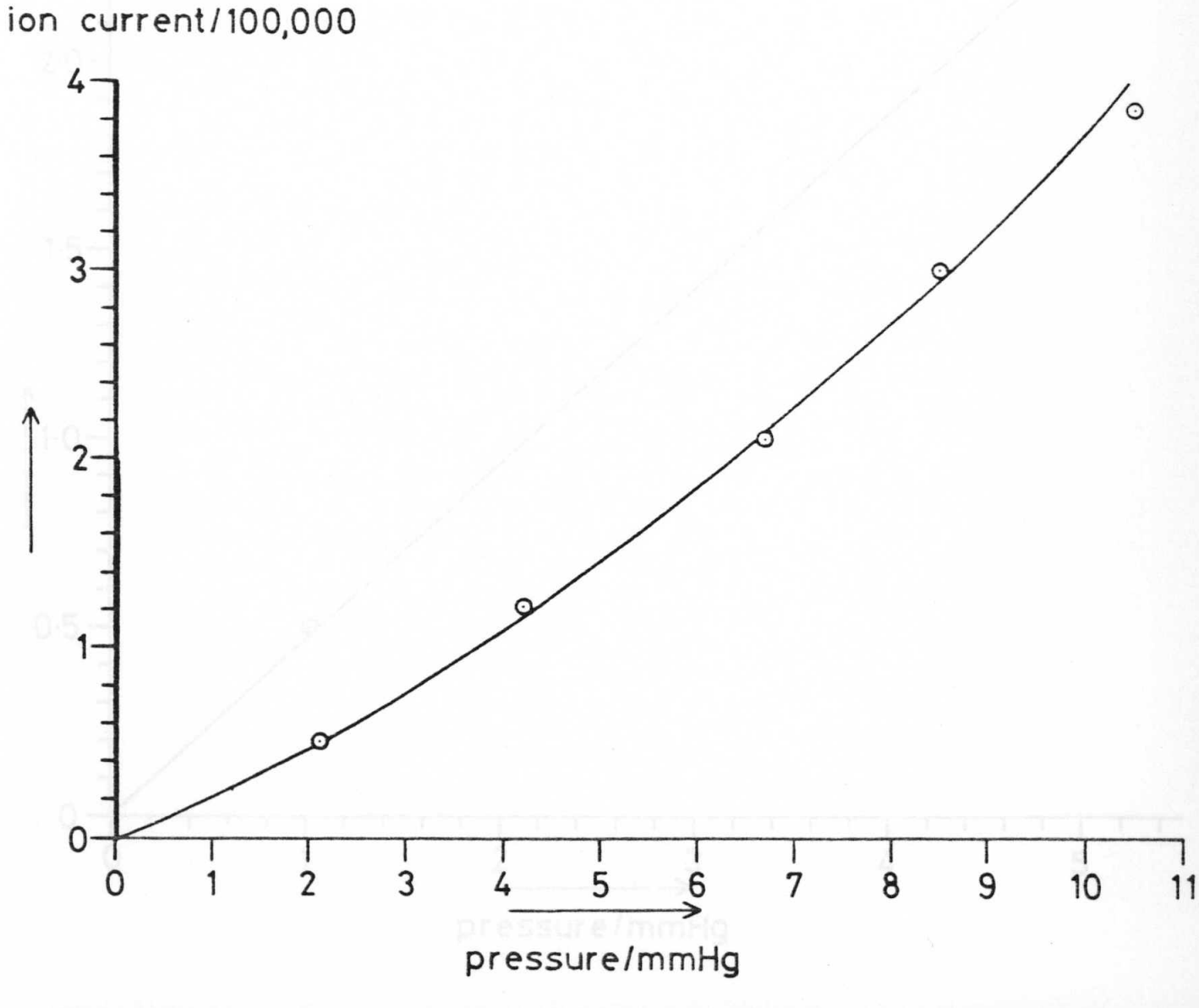

Decaborane(14) calibration data

pressure/mmHg	ion current
1·03	50,000
5·15	237,500

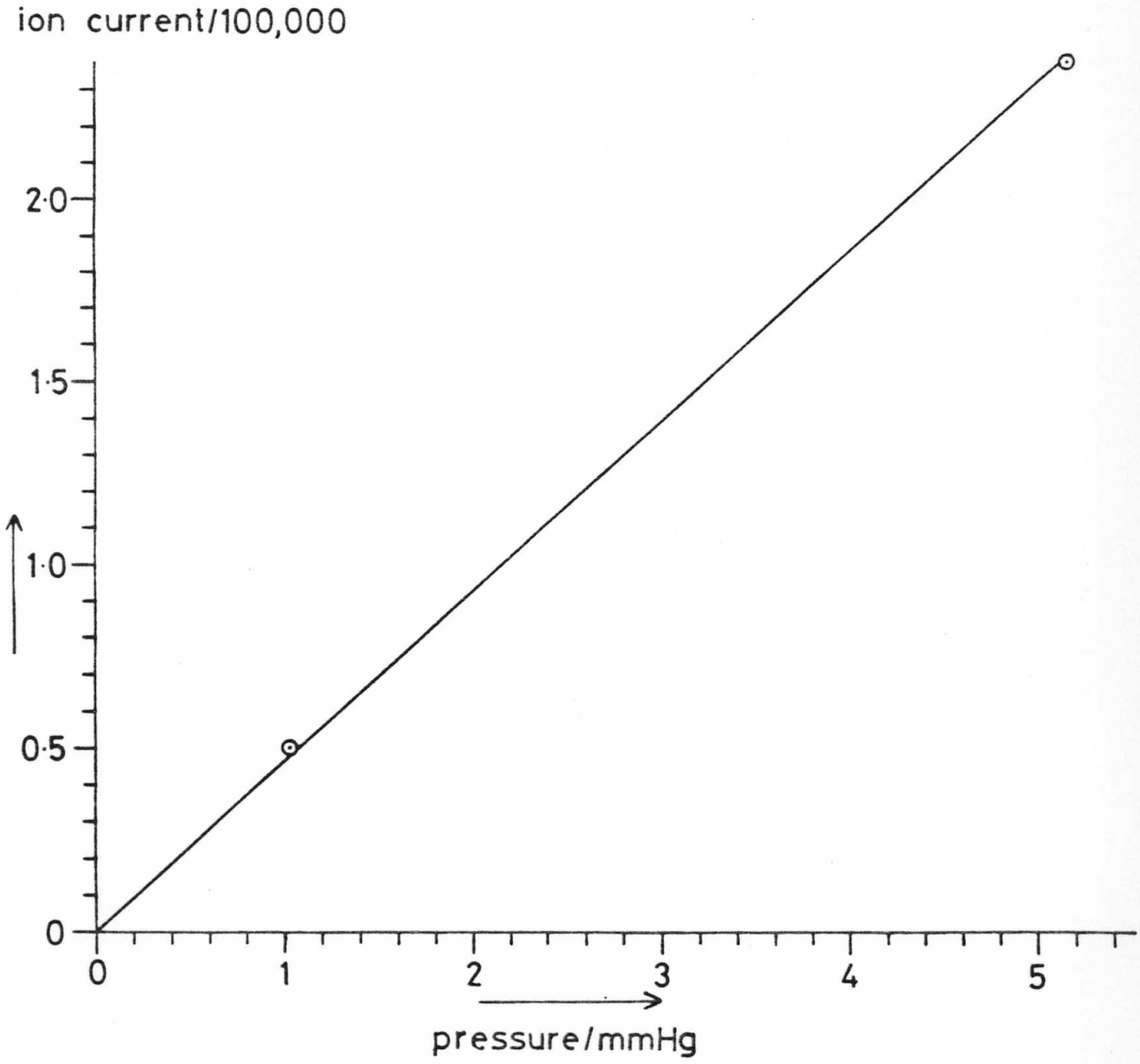

APPENDIX B

This appendix contains tables of experimental data which are presented graphically in Chapter 4.

Table B.1. Hydrogen pressure observed during experiment PYR

Time/minutes	Hydrogen pressure/mmHg
270	1.40
300	1.61
372	1.83
408	1.95
426	2.07
540	2.46
735	3.11
1050	3.72
1620	4.76
2058	5.36
3060	6.28
3840	6.77
4536	7.29
5100	7.59
5868	7.74
6600	7.81
7440	8.16
8808	8.26
9342	8.43
10308	8.61
10740	8.61
11820	8.79

Table B.2. Hydrogen and hexaborane(10) pressures observed during Experiment 2PYR

Time/ minutes	Hexaborane(10) pressure/mmHg	Time/ minutes	Hydrogen pressure/mmHg
5	4.08	5	0.20
15	3.48	15	0.26
35	3.54	41	0.32
53	3.47	56	0.39
72	3.35	76	0.50
88	2.94	93	0.58
107	3.23	112	0.65
130	3.19	136	0.78
155	3.16	161	0.90
176	3.03	183	1.00
196	3.19	200	1.08
216	3.08	221	1.20
243	3.07	248	1.22
274	3.04	281	1.46
305	2.89	308	1.57
336	2.80	339	1.74
366	2.81	369	1.84
395	2.74	399	2.01
457	2.90	458	2.23
513	2.41	515	2.42
588	2.21	591	2.76
723	2.07	725	3.15
988	1.98	991	3.96

continued/.....

Table B.2 (continued)

Time/ minutes	Hexaborane(10) pressure/mmHg	Time/ minutes	Hydrogen pressure/mmHg
1059	1.81	1062	4.14
1123	1.70	1126	4.29
1204	1.45	1207	4.54
1381	1.57	1384	4.99
1644	1.43	1647	5.44
2770	0.81	2749	6.88

Table B.3. Hydrogen and hexaborane(10) pressures observed during Experiment 3PYR

Time/ minutes	Hexaborane(10) pressure/mmHg	Time/ minutes	Hydrogen pressure/mmHg
10	1.80	10	0.00
20	1.87	21	0.04
30	1.61	27	0.04
40	1.73	44	0.04-0.05
65	1.65	64	0.04
100	1.61	97	0.05
125	1.57	126	0.05
175	1.46	182	0.05-0.06
245	1.63	188	0.05-0.06
285	1.49	243	0.05-0.06
360	1.59	285	0.06-0.07
435	1.42	361	0.11
555	1.61	437	0.17
645	1.26	553	0.25
770	1.22	643	0.30
950	1.56	647	0.30
1210	1.24	765	0.38
1295	1.45	772	0.38
1720	1.22	950	0.50
2635	1.21	1212	0.65(0.71)
		1295	0.68
		1722	0.89
		2628	1.26
		2633	1.26

Table B.4. Hydrogen and hexaborane(10) pressures observed during Experiment 4PYR

Time/ minutes	Hexaborane(10) pressure/mmHg	Time/ minutes	Hydrogen pressure/mmHg
6	7.7	8	0.16
17	7.1	24	0.23
23	6.8	39	0.40
38	6.5	54	0.55
53	6.4	74	0.74
69	6.2	91	0.92
88	6.1	109	1.13
109	6.1	129	1.32
129	6.0	151	1.55
151	5.9	172	1.76
172	5.9	196	2.00
196	5.7	221	2.26
221	5.3	250	2.56
250	5.2	275	2.83
275	5.0	305	3.07
305	4.6	335	3.37
335	4.6	365	3.61
365	4.4	395	3.84
395	4.4	425	4.08
425	4.3	485	4.64
492	4.1	550	5.08
550	4.1	603	5.39
603	3.9	665	5.82
674	3.7	743	6.33
743	3.3	845	6.86
845	3.1	1160	8.19
1176	2.5	1260	8.60
1260	2.4	5550	13.53
5550	0.5		

Table B.5. Hydrogen and hexaborane(10) pressures observed during Experiment 5PYR

Time/ minutes	Hexaborane(10) pressure/mmHg	Time/ minutes	Hydrogen pressure/mmHg
21	9.52	10	0.57
38	9.44	21	0.88
53	9.53	38	1.02
70	8.59	53	1.12
103	6.42	70	1.26
117	4.88	103	1.49
136	6.14	117	1.59
170	5.34	136	1.73
210	7.54	169	1.95
258	5.70	210	1.98
295	5.63	258	2.60
325	5.63	295	2.87
380	5.37	325	3.04
441	5.19	380	3.33
485	4.93	441	3.65
545	4.89	485	3.96
600	4.66	545	4.22
1196	3.38	600	4.57
1205	2.97	1196	6.66
1455	2.90	1455	7.39
1592	2.72	1592	7.70
3225	1.18	3225	9.58
		5680	10.95
		6950	11.91
		7251	11.90

Table B.6. Hydrogen and hexaborane(10) pressures observed during experiment 6PYR

Time/ minutes	Hexaborane(10) pressure/mmHg	Time/ minutes	Hydrogen pressure/mmHg
9	2.90	9	0.15
20	2.21	20	0.17
36	2.08	36	0.20
54	1.88	54	0.23
74	1.82	74	0.28
96	1.86	96	0.31
105	1.89	105	0.33
129	1.73	129	0.37
155	1.67	155	0.41
191	1.62	191	0.48
215	1.83	215	0.52
247	1.69	247	0.56
280	1.55	280	0.63
307	1.34	307	0.65
336	1.44	336	0.70
368	1.37	368	0.75
428	1.60	425	0.84
435	1.41	485	0.91
485	1.56	535	0.98
494	1.47	605	1.08
501	1.69	680	1.17
535	1.59	725	1.23
545	1.35	810	1.35
605	1.37	1250	1.84
680	1.38	1345	1.90
725	1.34	1402	1.98
810	1.28	1560	2.11
1250	1.22	1700	2.21
1345	1.19	2734	2.91
1402	1.01	3185	3.10
1560	1.06	4197	3.61
		7063	4.27
		9993	4.68

Table B.7. Hydrogen and hexaborane(10) pressures observed during experiment 7PYR

Time/ minutes	Hexaborane(10) pressure/mmHg	Time/ minutes	Hydrogen pressure/mmHg
3	2.72	5	0.21
14	2.55	19	0.27
31	2.28	35	0.32
44	2.23	49	0.39
61	2.16	67	0.46
80	2.21	84	0.55
101	2.12	104	0.64
119	2.11	124	0.73
141	2.10	141	0.82
166	2.07	170	1.02(0.89)
199	1.78	205	1.07
243	1.76	240	1.21
271	1.69	276	1.34
305	1.75	305	1.43
330	1.69	336	1.55
392	1.55	367	1.64
1191	0.46	399	1.74
1350	0.74	1192	3.70
		1355	3.99

Tables B.8. Hydrogen and hexaborane(10) pressure observed during experiment 8PYR

Time/ minutes	Hexaborane(10) pressure/mmHg	Time/ minutes	Hydrogen pressure/mmHg
4	4.87	5	0.44
16	4.84	21	0.52
34	4.85	35	0.66
53	4.63	57	0.92
78	3.93	80	1.21
113	3.62	118	1.68
149	3.47	153	2.16
195	2.53	200	2.73
250	2.74	252	3.43
313	3.57	316	4.05
351	3.37	355	4.49
445	3.38	449	5.42
509	3.16	513	5.97
569	3.15	573	6.49
1331	1.21	1328	10.46
1526	1.37	1532	11.22

Table B.9. Data showing log of initial rate of hydrogen appearance versus log of initial concentration of hexaborane(10) at 393 K

Experiment	Initial rate/ 10^{-7} mol m^{-3} s^{-1}	log initial rate	Initial conc./ mol m^{-3}	log initial conc.
PYR	42.1 ± 7	-5.38 ± 0.04	0.191	-0.719
2PYR	33.0 ± 3	-5.48 ± 0.04	0.188	-0.725
3PYR	4.32 ± 0.4	-6.37 ± 0.04	0.060	-1.219
4PYR	69.4 ± 7	-5.16 ± 0.04	0.313	-0.505
5PYR	51.0 ± 5	-5.29 ± 0.04	0.270	-0.569
6PYR	12.5 ± 1	-5.90 ± 0.04	0.097	-1.015
7PYR	30.6 ± 3	-5.51 ± 0.04	0.137	-0.864
8PYR	84.1 ± 8	-5.08 ± 0.04	0.273	-0.565

Table B.10. Data showing log of initial rate of hexaborane(10) disappearance versus log of initial concentration of hexaborane(10) at 393 K

Experiment	Initial rate/ 10^{-7} mol m^{-3} s^{-1}	log initial rate	Initial conc./ mol m^{-3}	log initial conc.
PYR	POOR DATA	POOR DATA	POOR DATA	POOR DATA
2PYR	20.1 ± 2	-5.697 ± 0.04	0.188	-0.725
3PYR	1.3 ± 0.2	-6.886 ± 0.06	0.060	-1.219
4PYR	150.3 ± 50	-4.823 ± 0.15	0.313	-0.505
5PYR	22.0 ± 3	-5.658 ± 0.06	0.270	-0.569
6PYR	9.5 ± 3	-6.022 ± 0.15	0.097	-1.015
7PYR	51 ± 28	-5.29 ± 0.27	0.137	-0.864
8PYR	42.9 ± 10	-5.368 ± 0.1	0.273	-0.565

Table B.11. First and second order data for experiment 2PYR

Time/ minutes	Hexaborane(10) pressure/mmHg	1/p	log p
5	4.08	0.245	0.6107
15	3.48	0.287	0.5416
35	3.54	0.282	0.5490
53	3.47	0.288	0.5404
72	3.35	0.299	0.5250
88	2.94	0.340	0.4684
107	3.23	0.310	0.5092
130	3.19	0.313	0.5038
155	3.16	0.316	0.4997
176	3.03	0.330	0.4814
196	3.19	0.313	0.5038
216	3.08	0.325	0.4886
243	3.07	0.326	0.4871
274	3.04	0.329	0.4829
305	2.89	0.346	0.4609
336	2.80	0.357	0.4472
366	2.81	0.356	0.4487
395	2.74	0.365	0.4378
457	2.90	0.345	0.4624
513	2.41	0.415	0.3820
588	2.21	0.452	0.3444
723	2.07	0.483	0.3160
988	1.98	0.505	0.2967
1059	1.81	0.552	0.2577
1123	1.70	0.588	0.2305
1204	1.45	0.690	0.1614
1381	1.57	0.637	0.1959
1644	1.43	0.699	0.1553
2770	0.81	1.235	-0.0915

Table B.12. First and second order data for experiment 4PYR

Time/ minutes	Hexaborane(10) pressure/mmHg	1/p	log p
6	7.7	0.130	0.886
17	7.1	0.141	0.851
23	6.8	0.147	0.833
38	6.5	0.154	0.813
53	6.4	0.156	0.806
69	6.2	0.161	0.792
88	6.1	0.164	0.785
109	6.1	0.164	0.785
129	6.0	0.167	0.778
151	5.9	0.169	0.771
172	5.9	0.169	0.771
196	5.7	0.175	0.756
221	5.3	0.189	0.724
250	5.2	0.192	0.716
275	5.0	0.200	0.699
305	4.6	0.217	0.663
335	4.6	0.217	0.663
365	4.4	0.227	0.643
395	4.4	0.227	0.643
425	4.3	0.233	0.633
492	4.1	0.244	0.613
550	4.1	0.244	0.613
603	3.9	0.256	0.591
674	3.7	0.270	0.568
743	3.3	0.303	0.519
845	3.1	0.323	0.491
1176	2.5	0.400	0.398
1260	2.4	0.417	0.380
5550	0.5	2.000	-0.301

Table B.13. First and second order data for experiment 5PYR

Time/ minutes	Hexaborane(10) pressure/mmHg	1/p	log p
21	9.52	0.105	0.979
38	9.44	0.106	0.975
53	9.53	0.105	0.979
70	8.59	0.116	0.934
103	6.42	0.156	0.808
117	4.88	0.205	0.689
136	6.14	0.163	0.788
170	5.34	0.187	0.728
210	7.54	0.133	0.877
258	5.70	0.175	0.756
295	5.63	0.178	0.751
325	5.63	0.178	0.751
380	5.37	0.186	0.730
441	5.19	0.193	0.715
485	4.93	0.203	0.693
545	4.89	0.204	0.689
600	4.66	0.215	0.668
1196	3.38	0.296	0.529
1205	2.97	0.337	0.473
1455	2.90	0.345	0.462
1592	2.72	0.368	0.435
3225	1.18	0.847	0.072

Table B.14. Hydrogen and hexaborane(10) pressures observed during experiment 4ACT

Time/ minutes	Hexaborane(10) pressure/mmHg	Time/ minutes	Hydrogen pressure/mmHg
12	3.45	11	0.34
28	3.05	31	0.38
58	2.79	62	0.42
88	2.53	93	0.43
126	2.49	132	0.47
161	2.43	165	0.50
196	2.42	200	0.53
233	2.36	240	0.56
280	2.31	285	0.61
362	2.49	364	0.62
421	2.39	428	0.73
427	2.39	490	0.78
488	2.43	549	0.85
545	2.54	1272	1.47
1275	2.63	1395	1.57
		1614	1.72
		1807	1.87
		2678	2.41
		3155	2.68
		3465	2.86
		4490	3.39
		6060	3.93

Table B.15. Hydrogen and hexaborane(10) pressures observed during experiment 3ACT

Time/ minutes	Hexaborane(10) pressure/mmHg	Time/ minutes	Hydrogen pressure/mmHg
20	5.50	11	0.19
38	8.24	20	0.21
42	7.17	39	0.22
75	4.70	60	0.24
85	4.84	91	0.28
94	4.53	122	0.26
118	4.75	151	0.31
150	4.66	210	0.41
199	4.46	250	0.47
245	4.21	307	0.56
300	4.08	371	0.65
371	4.08	436	0.74
432	3.77	495	0.83
490	3.58	603	0.98
600	3.74	1360	1.92
1360	2.74		
1535	2.50		
1832	2.30		
4505	1.13		
5803	1.10		
8844	0.79		
10042	0.77		

Table B.16. Hydrogen pressure observed during experiment 9PYR

Time/minutes	Hydrogen pressure/mmHg
10	0.32
18	0.38
27	0.44
40	0.53
55	0.64
73	0.78
97	0.97
125	1.17
154	1.36
190	1.61
216	1.79
301	2.30
335	2.48
365	2.69
401	2.88
1165	5.62
1389	5.90
1568	6.30
5578	9.32

Table B.17. Hydrogen and hexaborane(10) pressures observed during experiment 1ACT

Time/ minutes	Hexaborane(10) pressure/mmHg	Time/ minutes	Hydrogen pressure/mmHg
30	3.07	6	0.28
49	2.77	12	0.38
68	2.50	18	0.48
97	1.91	35	0.75
111	1.69	52	0.99
141	1.70	70	1.23
166	1.43	95	1.58
194	1.40	98	1.63
226	1.48	119	1.88
256	1.10	144	2.18
288	1.06	169	2.43
316	0.93	197	2.75
344	0.41	230	3.06
351	0.41	261	3.33
		290	3.60
		319	3.76
		348	4.04
		1333	7.66
		1486	7.82
		1746	8.17

Table B.18. Hydrogen and hexaborane(10) pressures observed during experiment 2ACT

Time/ minutes	Hexaborane(10) pressure/mmHg	Time/ minutes	Hydrogen pressure/mmHg
3	3.14	6	0.59
14	2.82	18	0.98
26	2.53	29	1.11
43	2.28	33	1.25
63	1.97	47	1.50
84	1.71	51	1.57
102	1.53	65	1.78
124	1.40	70	1.86
148	1.31	86	2.36
178	1.29	92	2.50
211	1.22	105	2.75
241	1.16	111	2.85
307	0.93	125	3.02
350	0.82	133	3.21
1404	0.36	150	3.44
		154	3.46
		179	3.71
		219	4.04
		244	4.25
		277	4.53
		308	4.75
		347	4.84
		1407	7.93

Table B.19. Hydrogen and hexaborane(10) pressures observed during experiment 1RB6

Time/ minutes	Hexaborane(10) pressure/mmHg	Time/ minutes	Hydrogen pressure/mmHg
0	3.24	0	0.20
8	3.34	6	0.35
23	3.14	12	0.45
38	2.92	24	0.65
54	2.71	32	0.80
72	2.51	39	0.90
77	2.42	45	1.00
90	2.32	57	1.25
109	2.15	62	1.30
113	2.09	75	1.55
133	1.95	81	1.60
139	1.88	93	1.75
170	1.72	101	1.85
175	1.67	111	2.00
209	1.50	138	2.30
214	1.48	171	2.70
263	1.29	180	2.75
492	0.79	218	3.10

Table B.20. Hydrogen and hexaborane(10) pressures observed during experiment 2RB6

Time/ minutes	Hexaborane(10) pressure/mmHg	Time/ minutes	Hydrogen pressure/mmHg
4.3	3.33	0	0.10
6.2	3.38	6	0.35
8.0	3.37	12	0.55
10.4	3.34	18	0.70
12.3	3.32	24	0.95
14.2	3.29	30	1.15
16.1	3.24	36	1.30
18.4	3.22	42	1.50
20.3	3.19	48	1.80
22.2	3.16	54	1.80
24.1	3.18	60	1.90
26.0	3.15	87	2.50
28.4	3.08	93	2.60
30.3	3.01	117	3.05
32.1	3.00	153 *	3.60
34.0	2.93		
36.4	2.89		
38.3	2.87		
40.2	2.83		
42.1	2.80		
44.4	2.81		
46.3	2.79		
48.2	2.84		
52.5	2.73		
54.4	2.70		
56.2	2.67		
58.1	2.62		
85.0	2.27		
86.9	2.24		
88.8	2.21		

continued/...

Table B.20 (continued)

Time/ minutes	Hexaborane(10) pressure/mmHg	Time/ minutes	Hydrogen pressure/mmHg
90.7	2.17		
92.6	2.17		
113.5	1.91		
115.4	1.92		
117.3	1.90		
119.2	1.87		
149.1	0.87		
151.9	0.87		
155.2	0.87		

* Hydrogen pressure not measured after 153 minutes

Table B.21. Arrhenius data showing ln of initial rate constant versus inverse of temperature at constant hexaborane(10) concentration (0.134 mol dm^{-3}). Hydrogen data only.

Experiment	10^5 k/ m^3 mol^{-1} s^{-1}	ln k	T/K	10^3 K/T
4ACT	3.48	-10.265	373	2.681
3ACT	4.76	-9.953	383	2.611
7PYR	16.37	-8.717	393	2.545
9PYR	26.47	-8.237	403	2.481
1ACT	55.54	-7.496	415	2.410
2ACT	79.66	-7.135	426.5	2.345
1RB6	75.64	-7.187	426	2.347
2RB6	132.1	-6.629	438	2.283
3RB6	128.0	-6.661	426	2.347
4RB6	99.6	-6.912	426	2.347
1HYD	101.6	-6.892	426	2.347
4HYD	78.2	-7.154	426	2.347

Table B.22. Arrhenius data showing ln of initial rate constant versus inverse of temperature at constant hexaborane(10) concentration (0.134 mol dm^{-3}). Hexaborane(10) data only.

Experiment	10^5 k/ m^3 mol^{-1} s^{-1}	ln k	T/K	10^3 K/T
4ACT	POOR DATA	POOR DATA	373	2.681
3ACT	9.2 ± 2	-9.294	383	2.611
7PYR	27 ± 15	-8.217	393	2.545
9PYR	POOR DATA	POOR DATA	403	2.481
1ACT	64.5 ± 10	-7.346	415	2.410
2ACT	95.3 ± 11	-6.956	426.5	2.345
1RB6	79 ± 17	-7.144	426	2.347
2RB6	56	-7.488	438	2.283
3RB6	59.9	-7.420	426	2.347
4RB6	58.3	-7.447	426	2.347
1HYD	47.4 ± 12	-7.654	426	2.347
4HYD	59.6	-7.425	426	2.347

Table B.23. Hydrogen production versus hexaborane(10) consumption for experiment 2ACT

Time/ minutes	Hexaborane(10) consumed/mmHg	Hydrogen produced/mmHg
14	0.69	0.98
26	0.98	1.11
43	1.23	1.50
63	1.55	1.78
84	1.80	2.36
102	1.98	2.75
124	2.11	3.02
148	2.20	3.44
178	2.22	3.71
241	2.35	4.25
307	2.58	4.75
350	2.69	4.84

Table B.24. Hydrogen production versus hexaborane(10) consumption for experiment 1RB6

Time/ minutes	Hexaborane(10) consumed/mmHg	Hydrogen produced/mmHg
0	0.00	0.20
8	0.17	0.35
23	0.37	0.65
38	0.59	0.90
54	0.81	1.25
77	1.09	1.55
90	1.19	1.75
113	1.42	2.00
139	1.64	2.30
170	1.79	2.70
214	2.03	3.10

Table B.25. Hydrogen and hexaborane(10) pressures observed during experiment 1HYD

Time/ minutes	Hexaborane(10) pressure/mmHg	Time/ minutes	Hydrogen pressure/mmHg
4	3.06	6	6.64
28	2.23	14	6.85
52	3.00	30	7.22
72	2.68	40	7.45
133	2.18	56	7.79
165	2.09	75	8.19
198	0.88	107	8.63
237	0.94	140	9.33
1731	0.57	167	9.56
2113	0.52	201	10.03
2116	0.49	239	10.12
3185	0.23	1735	14.29
3490	0.21	2115	15.20
4570	0.10	3118	15.47
		3490	15.61

Table B.26. Hydrogen and hexaborane(10) pressures observed during experiment 4HYD

Time/ minutes	Hexaborane(10) pressure/mmHg	Time/ minutes	Hydrogen pressure/mmHg
0	2.92	6	27.09
18	2.69	20	27.56
31	2.70	35	27.20
45	2.59	51	27.75
61	2.39	67	28.11
80	2.26	83	28.18
111	2.00	112	28.65
136	1.87	140	28.80
153	1.84	156	28.98
172	1.67	175	29.13
192	1.48	196	29.31
202	1.51	216	29.67
212	1.50	242	29.85
239	1.42	275	30.18
273	1.27		

APPENDIX C

Preparation of Hexaborane(10)

Hexaborane(10) was prepared by the method of Shore and co-workers [53,54]. The preparation was carried out several times during the course of this work, both by myself and my colleagues, and also by Dr. Ann Woollins who joined the group temporarily and to whom I am most grateful. Successful syntheses were achieved both on a standard ground-glass joint vacuum line (the grease used was Apiezon L) and on a greaseless vacuum line constructed from Young's taps and joints.

As discussed in Chapter 5, it was found that Derek Taylorson and Dr. Trevor Spalding unknowingly used impure hexaborane(10) in their work on its thermolysis. They used a different method of preparation which yielded several boranes, thereby complicating the task of purification [83]. The method used for this work gave hexaborane(10) as the only significant volatile product. The main stages of the reaction are:

$$B_5H_9 + Br_2 \xrightarrow{AlCl_3} 1\text{-}BrB_5H_8 + HBr$$

$$1\text{-}BrB_5H_8 + KH \longrightarrow K[1\text{-}BrB_5H_7] + H_2$$

$$K[1\text{-}BrB_5H_7] + \tfrac{1}{2}B_2H_6 \longrightarrow K[B_6H_{10}Br]$$

$$K[B_6H_{10}Br] \longrightarrow B_6H_{10} + KBr$$

and these are now described briefly in turn.

Synthesis of $1\text{-}BrB_5H_8$

On the vacuum line, bromine (typical scale 16.75 mmol; dried over phosphorus pentoxide) was distilled into a round bottomed flask (100 cm^3)

containing a magnetic stirring bar and a few milligrams of sublimed aluminium trichloride. A small excess of pentaborane(9) (17.2 mmol; measured by volume and pressure) was distilled into the flask at -196°C. The flask was opened to a large volume on the vacuum line to allow for the production of hydrogen bromide, and the manometers were isolated to avoid reaction between the mercury and the bromine. The flask was warmed to -40°C (acetone/solid carbon dioxide) with frequent stirring. Reaction was slow and it was usually observed that the bromine did not finally disappear (judged by colour) until the mixture had been warmed to room temperature. The reaction vessel was then cooled to -40°C while hydrogen bromide and unused pentaborane(9) were pumped into a waste trap maintained at -196°C. The resulting 1-bromopentaborane was then pumped into a U-tube held at -196°C and weighed. Yield was usually approximately 80%.

Deprotonation of $1\text{-}BrB_5H_8$

Potassium hydride (14.25 mmol; previously washed with dry pentane and stored dry in a glove box) was weighed (in the glove box) into a glass reaction tube (approximately 35 x 200 mm) containing a stirring bar. The tube was removed from the glove box and fitted to the vacuum line without delay to minimize exposure of the hydride to moist air. The activity of the hydride was not determined and care had to be taken that it was not present in excess, as this would lead to deprotonation of the products. For this reason the hydride was usually the yield limiting reactant.

The reaction tube was then cooled to -196°C and 1-bromopentaborane (14.0 mmol) and dimethyl ether (15 cm^3, as solvent) were distilled in. The reaction tube was then opened to a large volume on the vacuum line and warmed to -80°C (acetone/solid carbon dioxide). The vigour of the

reaction depended on the activity of the potassium hydride, occasional cooling being sometimes necessary to control the rate. The reaction mixture was intermittently frozen (-196°C) to allow removal of the liberated hydrogen.

Conversion of potassium salt to hexaborane(10)

Diborane(6) (7 mmol; measured by volume and pressure) was condensed at -196°C into a tube adjacent to that containing the products of deprotonation of the 1-bromopentaborane, also held at -196°C (diborane(6) was prepared by the method of Freeguard and Long using iodine and sodium borohydride [92]).

The tube containing the reaction products was warmed to -80°C, with stirring, and the diborane was allowed to warm up so that it distilled into the stirred trap as it was consumed. The last fraction of diborane(6) was condensed into the reaction tube at -196°C which was then rewarmed to -80°C, this operation ensuring complete reaction of the diborane.

The mixture was then warmed to -35°C (dichloroethane slush bath) with stirring. The mixture became a pale sandy colour with a heavy precipitate of potassium bromide, and the reaction was then complete.

Purification

The reaction mixture was cooled to -80°C and the bulk of the solvent and unreacted diborane(6) were pumped into a waste trap at -196°C. The remaining volatile components of the reaction mixture were collected in a phial at -196°C and attached to the fractionating train on the vacuum line. The hexaborane(10) was separated from the unwanted volatiles by trap to trap distillation. The phial was held at -35°C to retain unreacted 1-bromopentaborane and the hexaborane(10) was stopped in a -80°C trap, dimethyl ether and diborane(6) passed through to a waste trap at -196°C.

Several passes (at least ten) were required to completely remove the ether.

Traces of pentaborane(9) were observed mass spectrometrically in some of the hexaborane(10) samples and this was removed by several rapid passes of the hexaborane(10) through a trap held at -63°C (trichloromethane slush bath) which retained the hexaborane(10) and permitted the pentaborane(9) to pass through. Purity was assessed initially by vapour pressure measurement (pure hexaborane(10) has vapour pressure 7.47 mmHg at 0°C [53]) and then mass spectrometrically. Yield, usually limited by the potassium hydride was approximately 40% based on 1-bromopentaborane consumed.

REFERENCES

1. A. Stock, "Hydrides of Boron and Silicon", Cornell University Press, 1933.
2. R.L. Hughes, I.C. Smith, and E.W. Lawless, "Production of the Boranes and Related Research", ed. R.T. Holzmann, Academic Press, New York, 1967.
3. H.C. Longuet-Higgins, *Quart. Rev. Chem. Soc.*, 1957, 11, 121.
4. K. Wade, *J. Chem. Soc., Chem. Commun.*, 1971, 792.
5. "Gmelin Handbuch der Anorganischen Chemie", Band 54, "Borverbindungen", Teil 20.
6. J. Dobson, R. Maruca, and R. Schaeffer, *Inorg. Chem.*, 1970, 9, 2161.
7. "Boron Hydride Chemistry", ed. E.L. Muetterties, Academic Press, New York, 1975.
8. L.H. Long, *J. Inorg. Nucl. Chem.*, 1970, 32, 1097.
9. S.A. Fridmann and T.P. Fehlner, *Inorg. Chem.*, 1972, 11, 936.
10. S.G. Gibbins and I. Shapiro, *J. Am. Chem. Soc.*, 1960, 82, 2968.
11. T.P. Fehlner and W. Koski, *J. Am. Chem. Soc.*, 1964, 86, 1012.
12. R. Schaeffer, K.H. Ludlum, and S.E. Wiberley, *J. Am. Chem. Soc.*, 1959, 81, 3157.
13. J.F. Ditter, J.R. Spielman, and R.E. Williams, *Inorg. Chem.*, 1966, 5, 118.
14. J.K. Bragg, L.V. McCarty, and F.J. Norton, *J. Am. Chem. Soc.*, 1951, 73, 2134.
15. R.P. Clarke and R.N. Pease, *J. Am. Chem. Soc.*, 1951, 73, 2132.
16. P.C. Maybury and W.S. Koski, *J. Chem. Phys.*, 1953, 21, 742.
17. A.J. Owen, *J. Appl. Chem.*, 1960, 10, 483.
18. K. Borer, A.B. Littlewood, and C.S. Phillips, *J. Inorg. Nucl. Chem.*, 1960, 15, 316.

19. T.P. Fehlner and S.A. Fridmann, *Inorg. Chem.*, 1970, 9, 2288.

20. H. Fernandez, J. Grotewold, and C.M. Previtali, *J. Chem. Soc., Dalton Trans.*, 1973, 2090.

21. T.P. Fehlner, *J. Am. Chem. Soc.*, 1965, 87, 4200.

22. T.P. Fehlner and S.A. Fridmann, *Inorg. Chem.*, 1970, 9, 2288 (see reference number 5 at foot of first column).

23. R.E. Enrione and R. Schaeffer, *J. Inorg. Nucl. Chem.*, 1961, 18, 103.

24. A.B. Bayliss, G.A. Pressley, E.J. Sinke, and F.E. Stafford, *J. Am. Chem. Soc.*, 1964, 86, 5358.

25. J.H. Wilson and H.A. McGee, *J. Chem. Phys.*, 1967, 46, 1444.

26. M.F.R. Mulcahy, "Gas Kinetics", Nelson, 1973, Chapter 1.

27. T.P. Fehlner and W.S. Koski, *J. Am. Chem. Soc.*, 1965, 87, 409.

28. T.P. Fehlner and G.W. Mappes, *J. Phys. Chem.*, 1969, 73, 873.

29. M.E. Garabedian and S.W. Benson, *J. Am. Chem. Soc.*, 1964, 86, 176.

30. J. Grotewold, E.A. Lissi, and A.E. Villa, *J. Chem. Soc. A*, 1966, 1038.

31. B.S. Askins and C. Riley, *Inorg. Chem.*, 1977, 16, 481.

32. J.R. Morrey and G.R. Hill, O.A. Technical Report 1, Contract No. AF49(638)-28, 1958.

33. M. Hillman, D.J. Mangold, and J.H. Norman, "Borax to Boranes", Advances in Chemistry Series, Am. Chem. Soc., Washington D.C., 1961, p.151.

34. R.D. Stewart and R.G. Adler, American Potash and Chemical Corp., Report No. WTR-6204, Contract No. AF33(600)-35745, 1962.

35. R. Schaeffer, *J. Inorg. Nucl. Chem.*, 1960, 15, 190.

36. R. Schaeffer and F.N. Tebbe, *J. Am. Chem. Soc.*, 1962, 84, 3974.

37. A.B. Burg and H.I. Schlesinger, *J. Am. Chem. Soc.*, 1933, 55, 4009.

38. R.K. Pearson and L.J. Edwards, Abstracts of Papers presented to the Division of Inorganic Chemistry of the American Chemical Society, New York, September 1957, Abstract No. 39.

39. R. Schaeffer, *J. Chem. Phys.*, 1957, 26, 1349.

40. R. Maruca, J.D. Odom, and R. Schaeffer, *Inorg. Chem.*, 1968, 7, 412.

41. M. Kameda and G. Kodama, *Inorg. Chem.*, 1981, 20, 1072.

42. A. Davison, D.D. Traficante, and S.S. Wreford, *J. Chem. Soc., Chem. Commun.*, 1972, 1155.

43. A. Davison, D.D. Traficante, and S.S. Wreford, *J. Am. Chem. Soc.*, 1974, 96, 2802.

44. J.P. Brennan, R. Schaeffer, A. Davison, and S.S. Wreford, *J. Chem. Soc., Chem. Commun.*, 1973, 354.

45. H.D. Johnson, V.T. Brice, G.L. Brubaker, and S.G. Shore, *J. Am. Chem. Soc.*, 1972, 94, 6711.

46. J. Rathke and R. Schaeffer, *J. Am. Chem. Soc.*, 1973, 95, 3402.

47. J. Rathke, D.C. Moody, and R. Schaeffer, *Inorg. Chem.*, 1974, 13, 3040.

48. J. Rathke and R. Schaeffer, *Inorg. Chem.*, 1974, 13, 3008.

49. P.J. Dolan, D.C. Moody, and R. Schaeffer, *Inorg. Chem.*, 1981, 20, 745.

50. F.L. Hirschfeld, K. Erics, R.E. Dickerson, E.L. Lippert, and W.N. Lipscomb, *J. Chem. Phys.*, 1958, 28, 56.

51. R. Schaeffer, 24th Int. Cong. Pure Appl. Chem., Vol. 4, "Compounds of Non-Metals", Butterworths, 1974, p.1.

52. W. Kotlensky and R. Schaeffer, *J. Am. Chem. Soc.*, 1958, 80, 4517.

53. H.D. Johnson, V.T. Brice, and S.G. Shore, *Inorg. Chem.*, 1973, 12, 689.

54. R.J. Remmel, H.D. Johnson, and S.G. Shore, *Inorg. Synth.*, 1979, 19, 247.

55. B.J. Millard, "Quantitative Mass Spectrometry", Heyden, London, 1978.

56. J.R. Chapman, "Computers in Mass Spectrometry", Academic Press, London, 1978.

57. H.W. Washburn, H.F. Wiley, and S.M. Rock, *Ind. Eng. Chem., Anal. Ed.*, 1943, 15, 541.

58. R.E. Honig, *J. Appl. Phys.*, 1945, 16, 646.

59. A.O. Nier, T.A. Abbot, J.K. Pickard, W.T. Leland, T.I. Taylor, C.M. Stevens, D.L. Dukey, and G. Goertzel, *Anal. Chem.*, 1948, 20, 188.

60. R.E. Halsted and A.O. Nier, *Rev. Sci. Instrum.*, 1950, 21, 1019.

61. P.D. Zemany, *J. Appl. Phys.*, 1952, 23, 924.

62. D. Taylorson, Ph.D. Thesis, Leeds University, 1978.

63. J. Roboz, "Introduction to Mass Spectrometry, Instrumentation and Techniques", Interscience, New York, 1968.

64. "MTP International Review of Science", Volume 5, "Mass Spectrometry", ed. A. Maccoll, Butterworths, London, 1972.

65. L.B. Loeb, "The Kinetic Theory of Gases", Dover Publications Inc., New York, 1961, 3rd Edn.

66. J.H. Beynon, "Mass Spectrometry and its Applications to Organic Chemistry", Elsevier Publishing Co., Amsterdam, 1960.

67. M.L. Lee and B.W. Wright, *J. Chromatogr.*, 1980, 184, 283.

68. R.C. Reid, J.M. Prausnitz, and T.K. Sherwood, "The Properties of Gases and Liquids", McGraw-Hill Book Co., New York, 1977, 3rd Edn.

69. R. Herzog, *Ind. Eng. Chem.*, 1944, 36, 997.

70. H.J. Hrostowski and R.J. Myers, *J. Chem. Phys.*, 1954, 22, 262.

71. G.T. Furukawa and R.P. Park, *J. Res. Nat. Bur. Stand.*, 1955, 55, 255.

72. G.A. Miller, *J. Phys. Chem.*, 1963, 67, 1363.

73. A. John Jr., *Nucl. Sci. Abstr.*, 1956, 10, 1295.

74. "Curve Fitting by Polynomials in One Variable, Numerical Approximation to Functions and Data", ed. J.G. Hayes, Athlone Press, London, 1970.

75. L. Fox, "An Introduction to Numerical Linear Algebra", Clarendon Press, Oxford, 1964.

76. J. Plesek, S. Hermanek, and F. Hanousek, *Collect. Czech. Chem. Commun.*, 1968, 33, 699.

77. B.J. McLelland, "Statistical Thermodynamics", Chapman and Hall, London 1979.

78. J.C. Carter and N.L.H. Mock, *J. Am. Chem. Soc.*, 1969, 91, 5891.

79. J.D. Odom and R. Schaeffer, *Inorg. Chem.*, 1970, 9, 2157.

80. J.B. Leach, T. Onak, J. Spielman, R.R. Rietz, R. Schaeffer, and L.G. Sneddon, *Inorg. Chem.*, 1970, 9, 2170.

81. T.C. Gibb, N.N. Greenwood, T.R. Spalding, and D. Taylorson, *J. Chem. Soc., Dalton Trans.*, 1979, 1392.

82. T.C. Gibb, N.N. Greenwood, T.R. Spalding, and D. Taylorson, *J. Chem. Soc., Dalton Trans.*, 1979,1398.

83. H.A. Beall and W.N. Lipscomb, *Inorg. Chem.*, 1964, 3, 1783.

84. A.C. Bond and G. Hairston, *Inorg. Chem.*, 1970, 9, 2610.

85. H.C. Beachell and J.F. Haugh, *J. Am. Chem. Soc.*, 1958, 80, 2939.

86. C.A. McDonnel, Ed., "Mass Spectrometry", McGraw-Hill, New York, 1963.

87. P.F. Knewstubb, "Mass Spectrometry and Ion-Molecule Reactions", Cambridge University Press, 1969.

88. R.G. Cooks, J.H. Beynon, R.M. Caprioli, and G.R. Lester, "Metastable Ions", Elsevier, Amsterdam, 1973.

89. R.I. Reed, Ed., "Mass Spectrometry", Academic Press, London, 1965.

90. A.B. Burg and R. Kratzer, *Inorg. Chem.*, 1962, 1, 725.

91. A.C. Bond and M.L. Pinsky, *J. Amer. Chem. Soc.*, 1970, 92, 32.

92. G.F. Freeguard and L.H. Long, *Chem. Ind.*, 1965, 471.